LA-3257-MS

LOS ALAMOS SCIENTIFIC LABORATORY
OF THE UNIVERSITY OF CALIFORNIA o LOS ALAMOS NEW MEXICO

OPTIMAL CONTROL OF NUCLEAR REACTOR PROCESSES

LEGAL NOTICE

Printed in USA. Price $5.00. Available from the

Clearinghouse for Federal Scientific
and Technical Information,
National Bureau of Standards,
U. S. Department of Commerce,
Springfield, Virginia

UNIVERSITY OF CALIFORNIA
LOS ALAMOS SCIENTIFIC LABORATORY
(CONTRACT W-7405-ENG-36)
P. O. BOX 1663
LOS ALAMOS, NEW MEXICO

IN REPLY
REFER TO:

April 21, 1965

To: Copyholders of LA-3257-MS

From: Report Library

Subject: Errata to LA-3257-MS

Please make the following changes in LA-3257-MS:

Page 32, line 11 (equation 2.26), $p_{1o}n_o(t_b-t)$ should read $p_{1o}n_o(t_b-t)/\ell$.

Page 32, line 12, $p_{1o}n_o(t_b-t_a)\ell$ should read $p_{1o}n_o(t_b-t_a)/\ell$.

Page 101, equation 3.18 should read

$$T \approx T(t_o) + \left(\frac{Q_m-Q_o}{MC}\right)(t-t_o) \qquad (3.18)$$

LA-3257-MS
UC-80, REACTOR TECHNOLOGY
TID-4500 (37th Ed.)

LOS ALAMOS SCIENTIFIC LABORATORY
OF THE UNIVERSITY OF CALIFORNIA LOS ALAMOS NEW MEXICO

REPORT WRITTEN: March 1965

REPORT DISTRIBUTED: April 8, 1965

OPTIMAL CONTROL OF NUCLEAR REACTOR PROCESSES

by

Ronald R. Mohler

This report consists essentially of a dissertation submitted in partial fulfillment of the requirements for the degree of Doctor of Philosophy in the University of Michigan, 1965.

Contract W-7405-ENG. 36 with the U. S. Atomic Energy Commission

ABSTRACT

Two problems which are analyzed in this study are (1) the minimum-time control of a nuclear-reactor fission process and (2) the optimal control of a direct-cycle heat-exchange process to minimize the consumption of coolant. Interest in these problems has been increased by an attempt to develop nuclear-powered rockets for the space program. The latter problem is particularly significant for the nuclear rocket engine since a decrease in the amount of coolant required can result in a direct increase in payload.

This study analyzes both problems in detail, then synthesizes them in a physically plausible manner. The reactor state is defined by the classic neutron kinetic equations in the first problem. In the latter problem, the system is coupled to a single-stage, heat-exchange model by coolant density reactivity and core temperature reactivity. State-variable techniques and computer computations are utilized in the analysis of these optimal control problems.

The neutronics control must bring the neutron density (reactor power) from an initial steady-state condition to a desired terminal steady-state condition in the minimum time. However, the allowable reactivity change must be limited (i.e., confined to a closed set) for safety reasons. Pontryagin's maximum principle is used along with

physical evidence to show that optimal control is a bang-bang process; i.e., a two-level piecewise-constant variation in reactivity. For this problem, there is no switching or discontinuity in control between end points.

The above problem is treated by the general optimization theory in which the desired terminal phase is defined by a set of points. Once the terminal set (desired neutron density) is reached, it is theoretically possible to maintain steady-state neutron density by means of a continuous terminal variation in reactivity as given by

$$u \equiv \frac{\ell \sum_{i=1}^{6} \dot{C}_i}{n_1} ,$$

where ℓ = neutron mean generation time, $\dot{C}_i$ = time rate of change in density of the ith group of precursors and n_1 = the desired terminal neutron density. Mathematically, this variation in reactivity is in the allowable control set. In practice however, such open-loop control is unstable. By comparison, a dither type of control performs very well. In fact, a simple continuous type of closed-loop control (with reactivity physically constrained to the allowable set) approaches the performance of the optimal system. A describing function analysis is used to estimate the stability of this system.

The bang-bang process is found to be a candidate for the optimal neutronics control with respect to other performance indices. However, the consideration of singular types of solutions shows that the optimal-control trajectory can be a connection of bang-bang trajectories and singular types of trajectories.

The time-optimal neutronic control process is also a required part of reactor control when attempting to minimize propellant consumption of a nuclear rocket engine. Ideally, the optimal variation in coolant mass flow rate is again a bang-bang process. This study considers constraint in reactor power and a stall constraint in the performance of the propellant pumping system. These state-variable constraints are found to further complicate the optimal control process.

PREFACE

This dissertation deals with the problem of controlling nuclear-reactor processes in some optimal manner. After a brief statement of purpose, Chapter I discusses theory and formulates models of a nuclear-reactor fission process, a direct-cycle heat exchanger and a simplified nuclear rocket engine. These systems are found to belong to a general class called bilinear systems.

Chapter II presents an analysis of the optimal control of the classical mono-energetic neutron kinetics. Various constraints on reactivity and state-variables are considered in the analysis of this problem. The theoretic terminal control is found to be unstable due to its open-loop nature. Then a closed-loop dither process is introduced as a terminal control and performs very satisfactorily. For most purposes however, it is shown that a conventional type of continuous closed-loop control may be used.

Optimal control of heat-exchange processes and the nuclear rocket engine are discussed in Chapter III. Coolant density reactivity and conventional temperature reactivity are investigated. In addition to the above neutronic constraints, consideration is given to constraints in reactor power and to constraints in the pumping of coolant.

Chapter IV presents conclusions and an outline of areas which seem fruitful for future research.

Acknowledgements

The author wishes to express heartfelt appreciation to the numerous friends who have made this thesis possible.

Professor Robert M. Howe has constantly been a source of encouragement and enlightening advice. Motivation to do research in this area is largely the result of lectures given by Professor Elmer G. Gilbert, who has provided many valuable suggestions.

The thesis work has been performed in absentia at the Los Alamos Scientific Laboratory (University of California). There the work was done under the guidance of Drs. George N. White and George H. Pimbley, Jr. They have contributed many worthy suggestions and have kept constantly aware of the thesis progress.

In addition to the efforts of the above mentioned advisors, the task of performing thesis work in absentia was made possible by Drs. Joseph E. Perry, Jr. and William H. Crew of Los Alamos. The author is also indebted to the other members of his committee for their interest in this work.

Furthermore, the author wishes to thank: Mark Elder for reading and criticizing the manuscript; Charles P. Milich and Raymond J. Hanson for aid in the analog computer simulations; Otis A. Farmer for help with the digital computer computations; Marjorie Melton, Shirley Cahswell, Donna Barker, Yvonne Johnson and Edward O. Ferdinand for aid in preparing the manuscript; Richard J. Bohl for various bits of information concerning pump performance.

TABLE OF CONTENTS

		Page
ABSTRACT		iii
PREFACE		vii
CHAPTER I, INTRODUCTION		1
1.1	Objectives	1
1.2	Background	1
1.3	Optimal control	3
1.4	Maximum principle	4
1.5	State-variable constraints	9
1.6	Nuclear-reactor processes	12
1.6.1	Neutron kinetics	13
1.6.2	Direct-cycle heat-exchange process	16
1.6.3	The nuclear rocket engine	19
CHAPTER II, OPTIMAL NEUTRONIC CONTROL		23
2.1	Prompt-neutron kinetics	24
2.1.1	Bang-bang control	25
2.1.2	Velocity-limited control	28
2.2	Single-precursor group neutron kinetics	33
2.2.1	Time-optimal control with two state variables n and C	34
2.2.2	Time-optimal control of neutron level	43
2.2.3	Admissibility of the terminal control	45
2.2.4	Consideration of other state variables	46
2.2.5	Time-optimal control with phase-plane constraint	51
2.2.6	Singular solutions	57
2.2.7	Reachable zones of the time-optimal controlled neutronics	62
2.3	Six-presursor group neutron kinetics	64
2.4	Terminal control synthesis	71
2.5	Optimal control and conventional control	82
2.5.1	Time-optimal, suboptimal logarithmic and conventional logarithmic control of a Kiwi-B system	89

TABLE OF CONTENTS (Continued)

	Page
CHAPTER III, OPTIMAL CONTROL OF NUCLEAR-REACTOR DIRECT-CYCLE HEAT-EXCHANGE PROCESSES	97
3.1 Optimal heat-exchange process	98
3.2 Optimal neutronics heat-exchange process	103
3.3 Flow system constraints	113
CHAPTER IV, CONCLUSIONS	119
4.1 Suggestions for further work	120
APPENDIX A, OPTIMAL PROCESSES WITH CONSTRAINED STATE VARIABLES	122
APPENDIX B, SOLUTION TO THE SINGLE-PRECURSOR NEUTRON KINETICS AND NEUTRONIC ADJOINT SYSTEM FOR CONSTANT REACTIVITY	127
APPENDIX C, PHASE-PLANE EIGENVECTORS	130
APPENDIX D, COMPUTATION OF PHASE-PLANE TRAJECTORIES	132
APPENDIX E, NEUTRONICS HEAT-EXCHANGE SWITCHING PROBLEM FOR OPTIMAL STARTUP WITH $Q \leq Q_a$	134
BIBLIOGRAPHY	140

LIST OF TABLES

TABLE		Page
1.1	Precursor-neutron properties for U^{235}	15
1.2	Hypothetical nuclear rocket rated design conditions	22
2.1	Approximate one-delay group neutronic eigenvalues and eigenvector tangents	38
2.2	Describing function for reactivity limiting	85
2.3	Controller gains for data presented in Figures 2.24 and 2.25	91
E.1	Optimal reactor startup trajectory with $Q(t) \leq Q_1$	139

LIST OF ILLUSTRATIONS

FIGURE		Page
2.1	Time-Optimal Increase of Prompt-Neutron Density	27
2.2	Time-Optimal Decrease of Prompt-Neutron Density	27
2.3	Time-Optimal Startup of Prompt-Neutron Kinetics with Velocity-Limited Control	27
2.4	Neutron Density vs Neutron-Precursor Density Minimal-Time Trajectories	36
2.5	One-Precursor-Group Adjoint Trajectories for a Bang-Bang Reactivity Process	40
2.6	Neutron-Precursor Density vs Time Rate of Change of Neutron-Precursor Density for a Bang-Bang Reactivity Process	40
2.7	n vs $\dot{n}$ Bang-Bang Controlled Phase-Plane Trajectories	48
2.8	Bang-Bang Controlled Trajectories Showing the Effect of Neutron Source	50
2.9	Power Constrained Minimal-Time System Transients for a Single-Precursor Model	56
2.10	Analog Computer Diagram of a Bang-Bang Controlled One-Delay-Group Reactor System	58
2.11	Computer Simulated C vs $\dot{C}$ Minimal-Time Trajectories With Constraints in Power and Reactivity	59
2.12	Six-Delay-Group Neutronic Adjoint Transients, with Time Reversed ($t_1 \rightarrow t_o$) and $p_j(t_1) = 0$, ($j = 2,\ldots,7$)	67
2.13	Analog Computer Diagram of the Neutronic Adjoint System	68
2.14	Comparison of Time-Optimal Controlled Neutronics	72
2.15	Failure of the Theoretical Terminal Control Power Response Due to Small Control System Errors	75
2.16	Relay-Hysteresis Characteristic	77
2.17	Synthesis of the Neutronic Time-Optimal Startup Control Process	79

LIST OF ILLUSTRATIONS (Continued)

FIGURE		Page
2.18	Typical Reactivity Pulses During Terminal Dither Control	80
2.19	Typical Reactor Power Pulses During Terminal Dither Control	81
2.20	Bang-Bang Controlled Neutron Kinetics with a Continuous Terminal Control	83
2.21	Frequency Response of an Open-Loop Neutronic Control System Showing Effect of Reactivity Limiting	86
2.22	Bang-Bang Controlled Neutronics with a Proportional Terminal Control	87
2.23	Time-Optimal Controlled Neutronics with $\gamma = 1.3$ and Dither Terminal Control	90
2.24	Classical Logarithmic Power Controlled Startup of a Kiwi-B Neutron Kinetics	92
2.25	Subminimal-Time Startups of a Kiwi-B Neutron Kinetics with Various Closed-Loop Logarithmic Power Controllers	93
2.26	Minimum-Time Startup of a Kiwi-B Neutron Kinetics with $u \leq \gamma\beta$	94
3.1	Ideal Optimal Startup of a Heat-Exchange Process	102
3.2	Minimal Propellant Consumption Startup with Dither Terminal Control	110
3.3	Bang-Bang Control of Neutronics Heat-Exchange Process with $\gamma = 1.5$	112
3.4	Bang-Bang Control of Neutronics Heat-Exchange Process with $\gamma = 1.6$	112
3.5	Hypothetical Pump Performance Map	113

LIST OF ILLUSTRATIONS (Continued)

FIGURE		Page
3.6	Closed-Loop Nuclear Rocket Engine Control System	117
3.7	A Simple Type of Closed-Loop Nuclear Rocket Engine Control System	117

Chapter 1
INTRODUCTION

The present need for optimal control of nuclear-reactor systems has been brought about by the application of such systems to the space program and the military program.

1.1 Objectives

The primary objective of this study is to examine the problem of controlling nuclear reactors in some optimal manner. In particular, the minimal-time control of the neutron kinetics with reactivity constraints is to be analyzed in detail and synthesized in a practical and physically realizable manner. It is shown that a two-level piecewise-constant control may be the optimal reactor control for a portion of the time with respect to a class of performance criteria. Also consideration is to be given to the startup and shutdown of a simplified nuclear rocket engine so as to minimize the consumption of propellant.

Phase-space constraints and control velocity limits are to be considered in the study. Modern control theory, along with analog and digital computer simulations, are to be utilized to analyze and synthesize the optimal control.

1.2 Background

Optimal control of the neutron kinetics has been considered in other studies. T. P. Mulcahey[1] (in a 1963 Purdue University Ph.D. dissertation) designed a suboptimal reactor control system without mathematical foundation. In another paper, Shen and Haag[2] made a non-linear transformation to arrive at a simple linear system. By use of dynamic programming, they found that an extremely complicated controller

minimizes a mean-square error of the transformed system. The error, however, is a complicated function of reactivity and neutron level. Optimal control of neutron level does not necessarily follow.

In addition to this dissertation (which has been summarized in Reference 3) very recent work on optimal control of neutron kinetics has been reported by Rosztoczky and Weaver[4] and by I. Kliger[5]. By means of the maximum principle (to be discussed later), Rosztoczy and Weaver have analyzed the optimal shutdown of a nuclear reactor so as to minimize xenon poison buildup. Meanwhile, Kliger has analyzed the minimal-time control of neutron density by application of Holder's inequality. In his work Kliger assumed that the system constraint appeared as a functional relationship involving reactivity and neutron level. This dissertation considers different constraints and generally different problems than previously analyzed.

The optimization problems treated in this study differ from problems handled by the classical calculus of variations in that the allowable control set is a closed set. But if the allowable set is open, then a number of important necessary conditions for a control to be optimal are found in the classical calculus of variations[6,7].

In recent years the optimal control problem has been analyzed by the maximum principle[8], dynamic programming[9] and extensions of the calculus of variations[6]. Kalman[10] shows that a version of the maximum principle arises from the Hamiltonian-Caratheodory formulation of the calculus of variations while dynamic programming is based on the principle of optimality[9]. This principle states that if the performance index is Markovian, then an optimal control is optimal with respect to any state which results along the optimal trajectory of the system. The performance index is Markovian if it is a function of the initial

state and a functional of the control from the initial time to the terminal time where the initial time is considered to be any initial time. C. A. Desoer[11] derives the maximum principle from the principle of optimality.

L. I. Rozonoer[12], as well as L. S. Pontryagin and his collaborators[8], show that for certain problems the maximum principle is a necessary condition for a control to be optimal and is further a sufficient condition for the optimal control of certain systems jointly linear in the state vector and control vector.

1.3 Optimal control

Modern control theory is usually concerned with the general class of processes which can be described by a system of ordinary differential equations,

$$\frac{dx_i}{dt} = f_i(x_1,\ldots,x_n;u_1,\ldots,u_m) \qquad (i = 1,\ldots,n), \tag{1.1}$$

with prescribed initial conditions. Here $x_i(t)$ are the state variables of the process, $u_1(t),\ldots,u_m(t)$ are the control variables and t is time. In this study it is assumed that $\partial f_i/\partial x_j$ are continuous in x_q and u_k for all i, q, j and k. (1.1) is frequently written in vector notation,

$$\dot{\vec{x}} = \vec{f}(\vec{x};\vec{u}) \quad , \tag{1.2}$$

where the dot represents differentiation with respect to time. Here $\vec{x}$ is the state vector with components $x_1(t),\ldots, x_n(t)$. $\vec{u}$ is the control vector with components $u_1(t),\ldots,u_m(t)$. The control vector

must belong to an admissible class. $\vec{u}(t)$ is an admissible control if it is piecewise continuous and lies in a closed region U, i.e., $\vec{u} \in U$. (It will be assumed that U is time invariant in this dissertation.)

An optimal control problem may be stated as follows: Given a process described by (1.2), determine an admissible control $\vec{u}(t)$ that will transfer the process from some prescribed initial state

$$\vec{x}(t_0) = \vec{x}_0 \tag{1.3}$$

(where t_0 = initial time) to some terminal state

$$\vec{x}(t_1) = \vec{x}_1 \tag{1.4}$$

(where t_1 = terminal time) in a manner designed to minimize an index of performance J,

$$J = \int_{t_0}^{t_1} C(\vec{x}; \vec{u})\, dt\,, \tag{1.5}$$

where C is frequently called the cost function.

1.4 Maximum principle

The following formulation of the maximum principle is only a formal presentation. The reader is referred to Chapter 1 of Reference 8 for precise theorems and explanations.

Suppose one is interested in showing the optimality of some given trajectory $\vec{x}(t)$ [where $\vec{x}(t)$ is a solution to (1.2) for some $\vec{u}(t)$] which connects a given initial condition, $\vec{x}(t_0) = \vec{x}_0$, with a given terminal condition, $\vec{x}(t_1) = \vec{x}_1$. Although the initial time is specified, the terminal time is assumed to be free in this study. For such a trajectory to be optimal it is necessary that a costate vector $\vec{p}(t)$ is related to $\vec{x}(t)$ through Hamilton's equations. Hamilton's equations are discussed

below and relate the state vector of the system to a costate vector by means of a scalar function. The form of the optimal control is that which maximizes this scalar function. A simple application of this theory is presented in Section 2.1.1; this analysis should afford the reader a better understanding of the method.

For convenience the system may be considered to be of order n + 1 by letting the cost function be f_{n+1} and adding the equation $\dot{x}_{n+1} = f_{n+1}$ to (1.2) with $x_{n+1}(t_o) = 0$. Then Hamilton's equations, which form the basis of the maximum principle, take the following form:

$$\frac{d\bar{x}}{dt} = \bar{f}(\vec{x};\vec{u}) = \frac{\partial \mathcal{R}}{\partial \bar{p}} \qquad (1.6)^*$$

[with specified end conditions, $\bar{x}(t_o) = \bar{x}_o$ and $\bar{x}(t_1) = \bar{x}_1$]

and

$$\frac{d\bar{p}}{dt} = -\frac{\partial \mathcal{R}}{\partial \bar{x}} ,$$

where $\bar{p}$ is a costate vector, not identically zero, $\bar{x}$ is a state vector and both are of order n + 1. It is assumed in this study that $\bar{f}$ is not an explicit function of t.** The scalar $\mathcal{R}$ in (1.6) is

$$\mathcal{R}(\vec{x};\bar{p};\vec{u}) = (\bar{p},\bar{f}) = \sum_{i=1}^{n+1} p_i f_i \quad . \qquad (1.7)$$

- - - - - - - - - - - - - - - -

* For convenience, the partial derivative of a scalar with respect to a vector is considered to be a vector rather than a row vector in this dissertation.

** A time-variant system may be transformed to one which is time invariant by defining $x_o = t$ where $x_o(t_o) = t_o$ and $x_o(t_1) = t_1$, with $\dot{x}_o = 1.0$.

Then the Hamiltonian $\mathcal{H}$ is defined by

$$\mathcal{H}(\vec{x};\bar{p}) = \max_{\vec{u}\in U} \mathcal{R}(\vec{x};\bar{p};\vec{u}) \quad . \tag{1.8}$$

That is, the Hamiltonian is an absolute maximum with respect to all controls in the allowable set. In order that $\vec{u}(t)$ force $\vec{x}(t)$ from some initial point $\vec{x}(t_0) = \vec{x}_0$ to some terminal point $\vec{x}(t_1) = \vec{x}_1$ so as to minimize $J = x_{n+1}(t_1)$, it is necessary the $\vec{u}(t)$ and $\vec{x}(t)$ are related to a continuous costate vector $\bar{p}(t)$ by equations (1.6) to (1.8). These equations, along with the necessary continuity conditions given in conjunction with (1.1), form the maximum principle. Furthermore it is shown in Chapter 1 of Reference 8 that the Hamiltonian is a constant and identically equal to zero for the free end-time problem. Also p_{n+1} is a non-positive constant if equations (1.6) to (1.8) are satisfied. That is,

$$\mathcal{H}(\vec{x};\bar{p}) \equiv 0 \tag{1.9}$$

and

$$p_{n+1} \leq 0 \tag{1.10}$$

for $t_0 \leq t \leq t_1$.

From (1.7) it is seen that the costate system is adjoint to the original system (1.2). Thus

$$\frac{d\bar{p}}{dt} = -\frac{\partial \mathcal{R}}{\partial \bar{x}} = -\left[\frac{\partial \bar{f}}{\partial \bar{x}}\right]^T \bar{p} \ , \tag{1.11}$$

where the superscript T refers to a matrix transpose.

If the cost function is unity, the process is time optimal. Then the maximum principle may be formulated as follows:

$$\mathcal{R} = p_{n+1} + R \ , \tag{1.12}$$

where $R = (\vec{p},\vec{f})$ and the system is again of the order n. Then Hamilton's equations are

$$\frac{d\vec{x}}{dt} = \vec{f}(\vec{x};\vec{u}) = \frac{\partial R}{\partial \vec{p}} \qquad (1.13)$$

$$[\text{with } \vec{x}(t_0) = \vec{x}_0 \text{ and } \vec{x}(t_1) = \vec{x}_1]$$

and

$$\frac{d\vec{p}}{dt} = -\frac{\partial R}{\partial \vec{x}} \quad .$$

The Hamiltonian H is an absolute maximum of R with respect to all admissible controls:

$$H(\vec{x};\vec{p}) = \max_{\vec{u}\in U} R(\vec{x};\vec{p};\vec{u}) \quad . \qquad (1.14)$$

Again it is necessary that equations (1.12) to (1.14) are satisfied along with the necessary end conditions if the control and trajectory are to be time-optimal for $t_0 \le t \le t_1$. Also, the necessary continuity conditions must be valid. The Hamiltonian for this minimal-time problem is a non-negative constant,

$$H(\vec{x};\vec{p}) \ge 0 \quad , \qquad (1.15)$$

for $t_0 \le t \le t_1$. Again, the costate system is adjoint to (1.2):

$$\dot{\vec{p}} = -\left(\frac{\partial \vec{f}}{\partial \vec{x}}\right)^T \vec{p} \qquad (1.16)$$

$[\vec{p}(t) \not\equiv 0]$.

If the foregoing equations which formulate the maximum principle are satisfied by only one trajectory which satisfies the required end conditions and if (from physical arguments about the problem) it is known that an optimal trajectory must exist, then the discovered trajectory

is the unique optimal trajectory[8, 10]. Note, however, that the mathematical question of existence of an optimal trajectory is quite involved and will not be discussed here.

In case the system is jointly linear in the state $\vec{x}$ and the control $\vec{u}$, i.e. as defined by

$$\dot{\vec{x}} = A\vec{x} + B\vec{u} \tag{1.17}$$

($\vec{x}$ is of dimension n), then for certain problems the maximum principle is sufficient for a control to be optimal. Furthermore, for such problems the time-optimal control (with each component of the control magnitude constrained) is a piecewise-constant process. If the eigenvalues of the A matrix in (1.17) are real, it is shown on pages 120-123 of Reference 8 that there is a maximum of (n-1) switchings between constraints in each control variable.

The previous formulations have assumed that the terminal phase is fixed, while the terminal time is assumed free. In this study it is necessary to consider the case for which the terminal phase may be confined to a specified smooth hypersurface S_1 [i.e., $\vec{x}(t_1) \in S_1$]. If T_1 is the plane tangent to S_1 at the resulting terminal phase $\vec{x}(t_1) = \vec{x}_1$, it is necessary that the system costate vector $\vec{p}(t_1)$ be orthogonal to T_1 at $\vec{x}_1$. Let $\emptyset(\vec{x}) = 0$ define the terminal hypersurface of interest. Then the necessary costate condition may be written as follows:

$$\vec{p}(t_1) = \upsilon \frac{\partial \emptyset}{\partial \vec{x}} ,$$

where υ is a nonzero constant.

When $\vec{x}_1$ is known beforehand the problem becomes the classical one with a fixed terminal point. The mathematical details of this problem,

along with the more general case (i.e., both end points confined to specified smooth manifolds, with $\vec{p}(t)$ orthogonal to the corresponding manifold's tangent plane) is discussed in detail in Reference 8, pages 45-50.

1.5 State-variable constraints

In addition to control constraints, the process is frequently constrained in its state variables. Optimal control of processes with restricted phase co-ordinates was pioneered by Pontryagin, Boltyanskii, Gamkrelidze and Mishchenko (see Chapter 6 of Reference 8). Later this work was related to the classical calculus of variations by L. D. Berkovitz[13]. Recent contributions in this area include publications by S. S. L. Chang[14] and Bryson, Denham and Dreyfus[15].

This dissertation follows the work of Reference 8. A summary of such work is presented in Appendix A. The object of this section is to review the theory presented in Appendix A for the case of scalar control. Only the necessary conditions (i.e., necessary for the scalar control case) presented here are used to discuss the neutronic constraint problem in Chapter II. One interested in the more complicated optimal-control problem with phase constraint and vector control should read Appendix A. The necessary conditions for the case of vector control are considerably more complicated than those given below and only tend to confuse the reader interested in neutron-kinetic applications. After obtaining an optimal control by physical arguments in Chapter III, the more general theory is used to substantiate the optimal startup for a nuclear rocket engine in Appendix E.

The optimization problem considered here consists of selection of an allowable scalar control whose phase trajectory $\bar{x}$ lies in a given fixed

region G of the (n+1) dimensional phase space, satisfies the state equations [given by (1.1) along with necessary end conditions] and minimizes a performance index $J = x_{n+1}(t_1)$ [given by (1.5)].

Following Appendix A, let the region G be defined by

$$S(\bar{x}) \leq 0. \tag{1.18}$$

Assume that: (1) $S(\bar{x})$ is negative (i.e., optimal motions are not on the phase-constraint boundary) for the time interval (t_0, t_a), (2) $S(\bar{x})$ is zero (i.e., motions are on the phase-constraint boundary) for the interval (t_a, t_b) and (3) $S(\bar{x})$ is negative (i.e., motions are not on the phase-constraint boundary) for the interval (t_b, t_1).

During the time that trajectories are not on a phase-constraint boundary [i.e., during the intervals of time (t_0, t_a) and (t_b, t_1)], the previous conditions stated by the maximum principle are valid.

For the interval (t_a, t_b) the solution is on a phase-constraint boundary and

$$S[\bar{x}(t)] \equiv S(\bar{x}) \equiv 0. \tag{1.19}$$

Equation (1.19) requires that all time derivatives $S^{(k)}$ must vanish. Assume that the required u(t) may be computed from $\dot{S} = 0$, where

$$\dot{S}(\bar{x};u) = \frac{dS(\bar{x})}{dt} = \left[\frac{\partial S(\bar{x})}{\partial \bar{x}}\right]^T \bar{f}(x;\vec{u}) \quad . \tag{1.20}$$

Furthermore, assume that such required u(t) is an interior point of U (the set of allowable controls). If an optimal trajectory is on a

constraint boundary, it is shown in Appendix A that the costate vector must be a solution of

$$\dot{\bar{p}} = -\left\{\frac{\partial \bar{f}(\vec{x};u)}{\partial \bar{x}} - \frac{\partial \bar{f}(\vec{x};u)}{\partial u}\left[\frac{\partial \dot{S}(\bar{x};u)}{\partial u}\right]^{-1}\left[\frac{\partial \dot{S}(\bar{x};u)}{\partial \bar{x}}\right]^{T}\right\}^{T} \bar{p} \; ; \qquad (1.21)$$

where

(1) $\frac{\partial \dot{S}(\bar{x};u)}{\partial \vec{u}} \neq 0$,

(2) p_{n+1} = a nonpositive constant,

(3) $\bar{p}(t_a+)$ is a nonzero vector and $\bar{p}(t_a+)$ is not collinear with $\partial S(\bar{x})/\partial \bar{x}$. [The relation between $\bar{p}(t_a+)$ and $\bar{p}(t_a-)$ is discussed below.]

Further, for the interval (t_a, t_b) it is necessary that $\dot{\rho}$ is non-positive, where

$$\rho = \frac{\partial \mathcal{H}(\vec{x};\vec{p};u)}{\partial u}\left[\frac{\partial \dot{S}(\bar{x};u)}{\partial u}\right]^{-1}. \qquad (1.22)$$

Equation (1.21) represents n equations of the vector form:

$$\dot{\vec{p}} = -\left\{\frac{\partial \vec{f}(\vec{x};u)}{\partial \vec{x}} - \frac{\partial \vec{f}(\vec{x};u)}{\partial u}\left[\frac{\partial \dot{S}(\vec{x};u)}{\partial u}\right]^{-1}\left[\frac{\partial \dot{S}(\vec{x};u)}{\partial \vec{x}}\right]^{T}\right\}^{T} \vec{p} \qquad (1.23)$$

and one equation:

$$\dot{p}_{n+1} = 0, \text{ with } p_{n+1} \leq 0.$$

For the whole interval of time (t_0, t_1) the Hamiltonian is

$$\mathcal{H}(\vec{x};\bar{p}) \equiv 0.$$

During the interval of time (t_a, t_b) the maximum principle states

$$\mathcal{R}(\vec{x};\bar{p};u) = [\bar{p},\bar{f}(\vec{x};u)] = 0,$$

where u(t) is the control required to keep $\vec{x}(t)$ on the phase-constraint boundary.

Again, for the minimal-time problem let

$$\mathcal{R}(\vec{x};\bar{p};u) = R(\vec{x};\vec{p};u) + p_{n+1} ,$$

where $R(\vec{x};\vec{p};u) = [\vec{p},\vec{f}(\vec{x};u)]$. Then for the interval (t_o, t_a) the maximum principle states as above that

$$H(\vec{x};\vec{p}) = \max_{u\in U} R(\vec{x};\vec{p};u) = \text{a non-negative constant}$$

Since $\mathcal{H} = 0$ and p_{n+1} = a non-positive constant for the entire interval (t_o, t_1), $R(\vec{x};\vec{p};u)$ = a non-negative constant for the interval (t_a, t_b), where u(t) is the control required to keep $\vec{x}(t)$ on the phase-constraint boundary. Again $H(\vec{x};\vec{p})$ is a non-negative constant for all time (t_o, t_1).

From equations (A.7) and (A.9) with $S(\bar{x}) = S(\vec{x})$, the costate variables may be discontinuous at the entrance corner to the phase-constraint boundary, i.e.,

$$\vec{p}(t_a-) = \vec{p}(t_a+) + \mu \frac{\partial S(\vec{x})}{\partial \vec{x}} . \qquad (1.24)$$

An alternate equation (A.8) is not needed in this thesis. Across exit corners, the costate variables are continuous, i.e.,

$$\vec{p}(t_b-) = \vec{p}(t_b+) . \qquad (1.25)$$

1.6 Nuclear-reactor processes

This dissertation is primarily concerned with the minimal-time control of a nuclear-fission process. The problem is then extended

to include a heat-exchange process. A study is made of the optimal control of a nuclear rocket engine. In order to understand the optimal control of such systems, it is necessary to first consider their dynamical behavior and the necessary assumptions to arrive at a workable model.

1.6.1 Neutron kinetics

The classical one-energy group spatially independent neutron kinetics are heuristically developed below. A similar development, as well as a rigorous treatment of this system, is presented in reference 16, pages 10-20, and reference 17, pages 223-232. Define the effective multiplication factor k_e to be the ratio of the average number of neutrons in any one generation to the average number of neutrons in the immediately preceding generation for a given reactor of finite size. The mean generation time ℓ is the average time which elapses between successive neutron generations in a finite reactor. Then, if all neutrons are produced promptly, the average change in neutron density n per generation is

$$\ell \frac{dn}{dt} = (k_e - 1)\, n \ . \tag{1.26}$$

Let reactivity $\delta k = k_e - 1$.

Then

$$\frac{dn}{dt} = \frac{\delta k}{\ell} n \ . \tag{1.27}$$

The idea of a reactor period T (with $T = n/\dot{n}$) stems from (1.27). A portion β of the neutrons generated in each fission is delayed. These delayed neutrons are emitted from certain precursors (radioactive fission products) which are formed in the fission process of the fuel

nuclei. The rate of formation of delayed neutrons in any group is equal to the rate of decay of the corresponding precursor and hence the rate of formation of all delayed neutrons is $\sum_i \lambda_i C_i$, where λ_i is the decay constant of the ith delay group with density C_i. Six of these precursors have been observed. Hence, from (1.26) the rate of change of neutron density dn/dt is given as

$$\frac{dn}{dt} = \frac{\left[k_e(1-\beta)-1\right]}{\ell} n + \sum_{i=1}^{6} \lambda_i C_i \quad . \tag{1.28}$$

The rate of change of the precursor density is the birth rate minus the death rate, or

$$\frac{dC_i}{dt} = \frac{k_e \beta_i n}{\ell} - \lambda_i C_i \tag{1.29}$$

($i = 1,\ldots,6$), where β_i is the portion of neutrons which is delayed due to the ith precursor group and $\sum_{i=1}^{6} \beta_i = \beta$. For most cases the reactor is operated very near $k_e = 1$ (this condition is referred to as criticality). Then equations (1.28) and (1.29) may be approximated very accurately by

$$\frac{dn}{dt} = \frac{\delta k-\beta}{\ell} n + \sum_{i=1}^{6} \lambda_i C_i = \frac{\delta k}{\ell} n - \sum_{i=1}^{6} \dot{C}_i \tag{1.30}$$

and

$$\frac{dC_i}{dt} = \frac{\beta_i}{\ell} n - \lambda_i C_i \quad . \tag{1.31}$$

($i = 1,\ldots,6$).

Although usually negligible, an external neutron source S (used to start the chain reaction) would effect (1.30) as shown below:

$$\frac{dn}{dt} = \frac{\delta k-\beta}{\ell} n + \sum_{i=1}^{6} \lambda_i C_i + S \quad . \tag{1.32}$$

The following assumptions are made in the derivation of equations (1.30) and (1.31): 1) all neutrons are generated at the same average energy; 2) space dependent effects are separable from time dependent relations; 3) the system is near criticality; and 4) delayed neutrons have exactly the same effect as the total population in regards to fissioning fuel nuclei. From assumption (2) it is possible to relate the neutron density in a small region to the total neutron population in the reactor by a proportionality constant. This total population is then proportional to the number of fissions which in turn is proportional to the prompt portion of reactor power. A very small percentage of the power comes from the decay of various fission products and not from the fission process itself. This post-fission power is usually negligible except in the case of large decreases from high power. The properties of delayed neutrons given off in the fission process of U^{235} by thermal neutrons are given in Table 1.1[18]. This spatially independent model is very adequate for control analysis (including optimal control) of conventional reactor designs.

Table 1.1 Precursor-neutron properties for U^{235} fission process by thermal neutrons[18].

Part of Total Neutrons	Decay Constant
$10^3 \beta_i$	λ_i, sec^{-1}
0.22	0.0124
1.43	0.0305
1.28	0.111
2.58	0.301
0.75	1.13
0.27	3.00

The neutron kinetics as defined by (1.30) and (1.31) are linear in the dependent variable n for a time specified reactivity function. The system, however, is generally nonautonomous. Reactivity δk is the forcing function used to control the fission process. This control may take the form of mobile poison control rods or poisoned coolant in the core which absorb neutrons, reflector cylinders on the core periphery which control the reflection of neutrons, or mobile fuel rods.

1.6.2 Direct-cycle heat-exchange process

The heat-exchange process between the reactor core and coolant is complicated, nonlinear and distributed in nature but a finite difference model is frequently utilized to describe the heat-exchange dynamics at prescribed points. The model may be further simplified since reactor cores are generally designed so that there are no major variations in temperature in the radial direction. Then the heat-exchange process may be represented by an average model of one coolant passage. A qualitative description of the heat-exchange dynamics may be obtained with a one-stage model of the reactor (no axial or radial subdivisions). Such a one-stage model is represented below by equations (1.33) to (1.35). These equations may be formulated heuristically by writing an energy balance as follows. The heat rate generated from the fission process is equal to the rate at which heat is stored in the core (which results in a core wall temperature change) plus the rate at which heat is transferred from the core wall to the coolant. That is,

$$Q = MC \frac{dT}{dt} + hA\ (T - T_g) \quad , \qquad (1.33)$$

where

Q = heat rate generated from fission process, proportional to n,

MC = reactor core effective mass heat capacity,

T = average core temperature,

T_g = average coolant temperature,

A = heat-transfer area,

h = heat-transfer coefficient

and

t = time .

The rate of heat transfer to the coolant is equal to the rate of heat storage in the coolant plus the rate of increase in enthalpy of the coolant. That is,

$$hA\,(T - T_g) = w\,c_p\,\frac{dT_g}{dt} + \dot{w}\,c_p\,(T_o - T_i), \tag{1.34}$$

where

w = weight of coolant in the core,

c_p = specific heat of coolant,

$\dot{w}$ = coolant weight flow rate,

T_o = coolant temperature at the core exit

and

T_i = coolant temperature at core entrance.

The average coolant temperature is a weighted average of the inlet and exit temperatures,

$$T_g = \frac{T_i + \theta T_o}{1 + \theta}\ , \tag{1.35}$$

where θ is a positive weighting factor dependent on the axial power distribution.

Equations (1.33) and (1.34) are generally nonlinear since the coefficients are functions of the corresponding temperature. For gaseous coolants the mass heat capacity term $wc_p\dot{T}_g$ is negligible and at high temperature the coefficients are nearly constant with the exception of the heat-transfer coefficient. In nuclear reactors the resistance to heat transfer due to conduction through the core is usually negligible compared to the resistance due to convection through the fluid film. If the coolant is a gas and the flow is turbulent, the convective heat-transfer coefficient is approximately proportional to $\dot{w}^{0.8}$ [19]. With these assumptions and with the coolant weight flow rate specified as a function of time, the heat exchanger is a linear non-autonomous system.

From (1.34) and (1.35), with the coolant mass heat capacity and inlet temperature negligible, it is seen that

$$T \approx \left(\frac{c_p \dot{w}}{hA} + \frac{\theta}{1+\theta}\right) T_o \quad . \tag{1.36}$$

Substitution of (1.36) into (1.33) with T_g related to T_o by (1.35) shows that

$$\frac{dT}{dt} \approx \frac{Q}{MC} - \frac{T}{\tau_h} \quad , \tag{1.37}$$

where (since $h \propto \dot{w}^{0.8} \approx \dot{w}$)

$$\tau_h = MC\left[\frac{\theta}{c_p\dot{w}(\theta+1)} + \frac{1}{hA}\right] \approx \frac{1}{a\dot{w}} \tag{1.38}$$

and

a = a heat-transfer constant.

Notice that (1.37) is approximately bilinear in $\dot{w}$ and T. This simple model is found to be a good approximation of the actual process if the effective mass heat capacity is selected according to the axial position of the temperature of interest.

Heat-exchange processes (including the foundation of the above model) are discussed in detail in Reference 19.

The heat-exchange process is usually coupled to the neutron kinetics by temperature reactivity. As the core temperature increases the core expands and more neutrons escape. Also the various neutron cross-sections change with core temperature. The net effect is usually a negative reactivity feedback which may be approximated by

$$\delta k_t \approx c_t T, \tag{1.39}$$

where c_t is a temperature coefficient of reactivity (usually negative). This coupling has a stabilizing effect on the power reactor. It is important to realize that the coupled neutronics heat-exchange process is a nonlinear system even if the heat-exchange process is linear.

1.6.3 The nuclear rocket engine

Conventional control and dynamic analysis of nuclear rocket engines are treated in Reference 20. Such a system can be approximated by the equations given below along with the above neutronics heat-exchange dynamics equations.

Thrust and specific impulse are variables of prime interest to any rocket engine. Thrust F is approximately derived from the stagnation pressure at the nozzle entrance P_c and the nozzle throat area

A_t [21]. That is,

$$F \approx c_f A_t P_c \ , \tag{1.40}$$

where c_f is a nozzle constant. Coolant or propellant temperature at the nozzle entrance (reactor exit) determines specific impulse I_{sp} as shown by

$$I_{sp} = \frac{F}{\dot{w}} = c_s \ (T_o/MW)^{\frac{1}{2}} \ , \tag{1.41}$$

where c_s = a constant for the nozzle and MW = propellant molecular weight[21]. Equation (1.41) shows the importance of specific impulse to rocket propulsion. The promise of nuclear rockets and hydrogen propellant for space travel is shown by (1.41). Hydrogen is a good moderator and hence a density reactivity further couples the heat exchanger to the neutron kinetics. Assume that the propellant is gaseous in the core. Then the density may be computed from the gas equation:

$$\rho = P/RT_g \ , \tag{1.42}$$

where

ρ = average propellant density in the core ,

R = gas constant

and

P = average propellant core pressure.

The density reactivity contribution is computed by the following:

$$\delta k_\rho = k_\rho \ V\rho \ , \tag{1.43}$$

where

k_ρ = propellant density coefficient of reactivity (positive)

and V = reactor core void volume .

The flow is assumed choked through an exit nozzle and static conditions are approximately equal to stagnation conditions due to the low core exit mach number. Then pressure at the core exit is

$$P_c \approx c_n \dot{w} T_o^{\frac{1}{2}} , \tag{1.44}$$

where c_n = a nozzle constant[21]. With the approximations: $P \propto P_c$ and $T \propto T_g$, the propellant density reactivity is

$$\delta k_\rho \approx \frac{c_\rho \dot{w}}{T^{\frac{1}{2}}} , \tag{1.45}$$

where c_ρ = a constant. The magnitude of propellant reactivity may very well be greater than that of the classical temperature reactivity. Although the reactivity of the propellant is positive, its derivative with respect to temperature is negative. This fact further enhances reactor stability.

A hypothetical nuclear rocket engine configuration (at rated design conditions) is presented in Table 1.2. The dynamics of the propellant flow system will be neglected in this study but constraints due to pump cavitation and stall are discussed in Chapter III.

The computer studies which are to follow in Chapters II and III utilize the data given by Tables 1.1 and 1.2 unless otherwise specified.

Table 1.2 Hypothetical nuclear rocket rated design conditions[20].

Thrust, F	100,000 lb
Specific impulse (with losses), I_{sp}	760 sec
Reactor power , Q	2260 megawatts
Propellant flow rate, $\dot{w}$	130 lb/sec
Reactor exit propellant temperature, T_o	4500° R
Nozzle throat area, A_t	61 $in.^2$
Nozzle expansion ratio,	20
Heat exchanger thermal time constant, τ_h	1.5 sec
Inlet propellant temperature , T_i	120° R
Neutron mean-effective lifetime , ℓ	$3\ (10)^{-5}$ sec
Propellant reactivity , δk_ρ	0.0065
Temperature reactivity , δk_t	-0.0065
Effective core mass heat capacity , MC	1140 $\frac{Btu}{°R}$

Chapter II

OPTIMAL NEUTRONICS CONTROL

The optimal-control problem emphasized in this chapter may be stated as follows: (1) given an initial state of the neutron kinetics, find the allowable control reactivity which transfers the system to a desired state in minimal time; (2) it is required that the system have steady-state initial conditions and a steady-state terminal neutron level; (3) the allowable control reactivity is defined by $|\delta k| \leq \gamma\beta$, where γ is a constant and β is the amount of reactivity required to make the reactor prompt critical. (Prompt criticality exists when the system is critical without the presence of any precursor neutrons.) The value of γ depends on the system design and its application. It will be assumed that the control reactivity is a linear function of control position for the reactivity required. Reactivity δk is replaced by u, the control variable, in the following analysis.

Although the negative reactivity constraint may safely be less than the positive constraint, symmetrical limits are assumed for convenience. This assumption allows the forthcoming equations to be written more compactly without appreciably affecting the results. Furthermore as u becomes greatly negative, control effectiveness is lost due to precursor dominance. Hence, it doesn't make the system much faster if a large negative reactivity constraint is allowed. This lack of controllability for large negative reactivity is shown by Figure 3.2 on page 31 of Reference 16.

Minimal-time startup and shutdown are especially desirable for nuclear rocket engines and nuclear-reactor power generation in space. Physically, the reactivity may be changed very rapidly and control rate of change constraints, particularly for space applications, are frequently negligible. In some instances however (primarily in regard to commercial reactors), safety dictates a low constraint on control velocity. Furthermore, physical constraints require that the neutron density must be positive and less than some maximum.

Time-optimal control will be considered for the prompt neutron kinetics prior to the study of the one-precursor-group model. After a detailed analysis of the one-precursor model, comparisons are made with the six-precursor model.

From physical arguments, one might expect the time-optimal control of these neutronic processes to be maximum allowable effort. The following analysis shows that such control is time optimal but the analysis presents details of the control process which are not so obvious.

2.1 Prompt-neutron kinetics

In order to introduce the more complicated neutronic optimal-control processes, it is convenient to first consider the prompt-neutron kinetics:

$$\frac{dn}{dt} = \frac{u}{\ell}\, n \ . \tag{2.1}$$

This approximation to the neutron kinetics is valid for $\dot{C}$ which is small compared to $\dot{n}$ [see (1.30)and (1.31)]. Assume that the system is originally at steady-state with $u = o$ and $n(t_o) = n_o$. The optimal-control process is to take the neutron level to some prescribed steady-

state level in such a manner as to minimize the time elapsed. The following analysis will give consideration to constraints on reactivity and the rate of change in reactivity.

2.1.1 Bang-bang control

The inner product $(\vec{p},\vec{f})$ for this system (2.1) is

$$R(n;p;u) = \frac{u}{\ell}np \tag{2.2}$$

and the adjoint equation of the system defines the costate:

$$\frac{dp}{dt} = -\frac{u}{\ell}p \ . \tag{2.3}$$

Let the allowable control set U be defined by $|u| \leq \gamma\beta$ (this constraint is seen to limit the inverse reactor period in direct proportion). Again, as shown by (1.15), the Hamiltonian is a non-negative constant:

$$H(n;p) = \max_{u\in U} R(n;p;u) \tag{2.4}$$

and the control which maximizes R lies on the boundary of the allowable set. Hence, the optimal control is a bang-bang process such that

$$u^\circ = \gamma\beta \ \text{sgn}\ np \qquad (\text{sgn}\ F = F/|F|) \tag{2.5}$$

for $t_0 < t < t_1$. Since $n(t) > 0$, switching is determined by the sign of the costate variable p. In other words,

$$u^\circ = \gamma\beta \ \text{sgn}\ p \ . \tag{2.6}$$

Therefore, since p [the solution to (2.3)] cannot change sign for this piecewise-constant control, the optimal increase or decrease in neutron level requires constant maximum or minimum reactivity until the desired terminal neutron level is reached. At the terminal phase,

reactivity is returned to the null position to maintain steady-state. The absolute value of the inverse reactor period is at the maximum value of $\gamma\beta/\ell$ between end points.

Although (2.6) indicates the form of the optimal control, the corresponding state and costate trajectories must be solutions to (2.1) and (2.3). The solutions of these equations,

$$n = n_o \exp\left(\int_{t_o}^{t} u \, d\sigma/\ell\right) \tag{2.7}$$

and

$$p = p_o \exp\left(-\int_{t_o}^{t} u \, d\sigma/\ell\right), \tag{2.8}$$

provide a constant non-negative Hamiltonian, $\gamma\beta n_o \mid p_o \mid/\ell$, with $p(t_o) = p_o$ positive for increasing neutron level and negative for decreasing level. Only the bang-bang control process, however, makes the Hamiltonian a maximum. Furthermore, since only one bang-bang controlled trajectory connects the desired end points, the optimal solution is obviously unique if it is assumed that an optimal control exists. Typical optimal trajectories are shown in Figures 2.1 and 2.2.

Although one variable uniquely defines the state of a first-order system, a plot of n vs $\dot{n}$ is introduced since such plots are used later to treat the one-delay group case. For $u^\circ = \pm \gamma\beta$ the optimal time solutions to (2.1) and (2.3) are

$$n = n_o e^{\pm\gamma\beta(t-t_o)/\ell} \tag{2.9}$$

and

$$p = p_o e^{\pm\gamma\beta(t_o-t)/\ell} \tag{2.10}$$

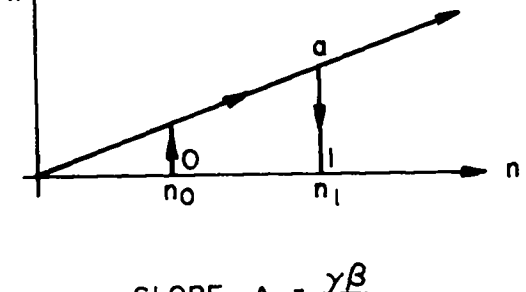

SLOPE A = $\frac{\gamma\beta}{\ell}$
0 - a : u = $\gamma\beta$
a - 1 : u = 0

FIGURE 2.1 TIME-OPTIMAL INCREASE OF PROMPT-NEUTRON DENSITY

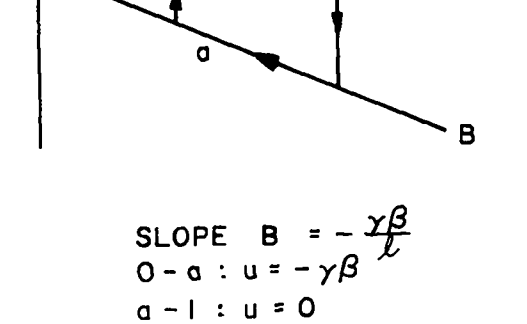

SLOPE B = $-\frac{\gamma\beta}{\ell}$
0 - a : u = $-\gamma\beta$
a - 1 : u = 0

FIGURE 2.2 TIME-OPTIMAL DECREASE OF PROMPT-NEUTRON DENSITY

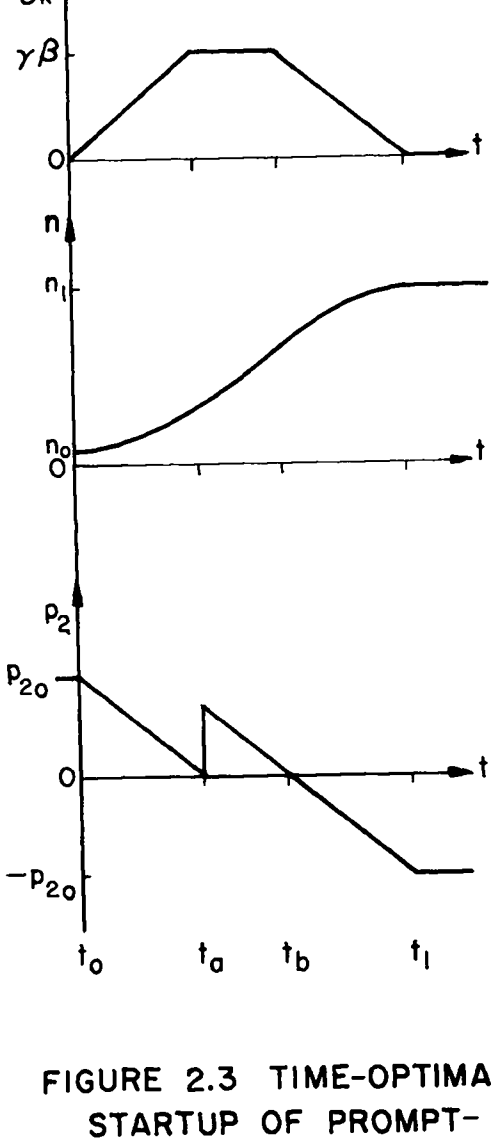

FIGURE 2.3 TIME-OPTIMAL STARTUP OF PROMPT-NEUTRON KINETICS WITH VELOCITY-LIMITED CONTROL

2.1.2 Velocity-limited control

Velocity constraint is sometimes required due to the possibility of failures in the control system (see pages 226-236 of Reference 16).

After the previous analysis it would be expected that the time-optimal control process with velocity-limited control would still be maximum allowable effort. In other words, for a minimal-time increase in neutron level one might hypothesize that reactivity should be increased at its maximum allowable rate until it reaches a maximum allowable value at $t = t_a$. Then at some appropriate time t_b, reactivity should be decreased at its minimum allowable rate until reactivity is zero at $t = t_1$. This zero value should be held to maintain the desired neutron level for $t \geq t_1$. For some problems $n(t_1)-n(t_0)$ or the allowable rate of change of reactivity may be so small that it is necessary to decrease reactivity at the minimum allowable rate before the reactivity magnitude constraint is reached. The following analysis shows for either case that such trajectories do satisfy the necessary conditions set forth by the maximum principle.

Control processes which only use two values, the maximum and minimum allowable velocity, without using the control-magnitude constraint value frequently are called pang-pang control. Similarly, processes which only take on the values of control-velocity constraint and control-magnitude constraint frequently are referred to as pang-bang processes.

With control velocity constraint, it is convenient to define the velocity as a control variable u and the reactivity as a new state variable δk. Then the system is represented by

$$\dot{n} = \frac{\delta k}{\ell} n$$

and

$$\dot{\delta k} = u. \tag{2.11}$$

with $n(t_o) = n_o$ and $\delta k(t_o) = \delta k_o$. Here it is desired to find the time-optimal control which forces the process from some steady-state initial condition, $n(t_o) = n_o$ and $\dot{n}(t_o) = 0$ $[\delta k(t_o) = 0]$, to some higher steady-state terminal condition, $n(t_1) = n_1$ and $\dot{n}(t_1) = 0$ $[\delta k(t_1) = 0]$. Here $|u| \leq \eta\beta$ is a control constraint and $|\delta k| \leq \gamma\beta$ is a phase constraint. Then the phase constraint boundary is defined by $S = |\delta k| - \gamma\beta = 0$.

While $|\delta k| < \gamma\beta$, $t_o < t < t_a$ or $t_b < t < t_1$ and the maximum principle may be applied to this problem. The inner product $(\vec{p},\vec{f})$ and adjoint equations are

$$R = \frac{p_1 n \delta k}{\ell} + p_2 u, \tag{2.12}$$

$$\dot{p}_1 = \frac{-p_1 \delta k}{\ell}$$

and

$$\dot{p}_2 = -\frac{p_1 n}{\ell}. \tag{2.13}$$

Maximization of (2.12) requires a pang-bang process such that

$$u^\circ = \eta\beta \text{ sgn } p_2, \text{ for } |\delta k| < \gamma\beta$$

and

$$u^\circ = 0 \quad , \text{ for } |\delta k| = \gamma\beta \text{ and } \dot{S} = 0. \tag{2.14}$$

With $\delta k = \eta\beta(t-t_o) < \gamma\beta$, the solutions of (2.7), (2.8), (2.12) and (2.14) yield the following for the initial portion of the trajectory:

$$n = n_o \exp [\delta k(t-t_o)/2\ell] , \tag{2.15}$$

$$p_1 = p_{1o} \exp [-\delta k(t-t_o)/2\ell] , \tag{2.16}$$

$$p_2 = p_{2o} - \frac{p_{1o} n_o (t-t_o)}{\ell}$$

and

$$H = |p_{2o}| \ \eta\beta \geq 0 , \tag{2.17}$$

where the o subscripts refer to the initial state and costate, $t_o < t < t_a$, and $t_a = t_o + \gamma/\eta$. Also, p_{1o} and p_{2o} are positive for $n_o < n_1$.

The problem of minimal-time increase in neutron level has the solution which is given below and presented by Figure 2.3. The neutron level for the initial portion of the trajectory is

$$n = n_o \exp [\eta\beta(t-t_o)^2/2\ell] , \tag{2.18}$$

where $t_o \leq t < t_a$. First, suppose that n_o and n_1 are such that $\delta k = \gamma\beta$ for $t_a \leq t \leq t_b$. Then $n(t_a)$ is

$$n_a = n_o \exp (\gamma^2\beta/2\eta\ell) \tag{2.19}$$

and

$$n = n_a \exp [\frac{\gamma\beta}{\ell} (t-t_a)] \tag{2.20}$$

for $t_a \leq t < t_b$. At the constraint exit point, the neutron level $n_b = n(t_b)$ is computed by solving (2.11) from t_1 and n_1 with time reversed. Hence,

$$n_b = n_1 \exp (-\gamma^2\beta/2\eta\ell) , \tag{2.21}$$

where $n_1 = n(t_1)$ and t_1 = terminal time. Then the log of equation (2.20) shows that the time transpired while the trajectory is on the state-variable constraint $\delta k = \gamma\beta$ is computed by

$$t_b = t_a + \frac{\ell}{\gamma\beta} \log \frac{n_b}{n_a} \quad . \tag{2.22}$$

During the final negative control ramp to $\delta k = 0$, the neutron level [as computed from (2.7)] is

$$n = n_b \exp \left\{ \frac{\beta}{\ell} \left[(t-t_b) - \frac{\eta\beta(t^2-t_b^2)}{2} \right] \right\} . \tag{2.23}$$

The maximum principle requires that the adjoint equations have a solution. These solutions are given by (2.16) with $\delta k = \eta\beta(t-t_o)$ and $t_o \leq t < t_a$. At $t = t_a$ and $t = t_b$ the adjoint vector must satisfy certain constraint corner conditions. These conditions are given by (1.24) and (1.25). Although the Hamiltonian is constant and defined by (2.17) for $t_o \leq t \leq t_1$, the costate may be discontinuous across the entrance corner, i.e.,

$$\vec{p}(t_a-) = \vec{p}(t_a+) + \mu \frac{d\vec{S}}{d\vec{x}} \quad , \tag{2.24}$$

where

$$\frac{d\vec{S}}{d\vec{x}} = \begin{bmatrix} 0 \\ \text{sign } \delta k \end{bmatrix} .$$

Across the exit corner the costate is continuous, as shown by

$$\vec{p}(t_b-) = \vec{p}(t_b+) \quad . \tag{2.25}$$

Then, since n(t) and H are continuous for $t_o \leq t \leq t_1$, it is necessary from (2.17) that

$$p_{1a} = p_1(t_a+) = \frac{\ell\eta p_{2o}}{\gamma n_a} = p_1(t_a-) .$$

Therefore, from (2.15) and (2.16)

$$p_{20} = p_{10} n_0 \gamma / \eta \ell$$

and

$$p_2(t_a-) = 0$$

From (2.24) $p_2(t_a+) = \mu = p_{1a} n_a (t_b - t_a)/\ell$. Since $\partial \dot{S}/\partial \vec{x} = \begin{bmatrix} 0 \\ 0 \end{bmatrix}$, it is seen from (1.21), (2.25) and (2.16) that for the interval (t_a, t_b)

$$\begin{aligned} p_1 &= p_{1a} \exp\left[-\gamma\beta(t-t_a)\right] \\ &= p_{10} \exp\left[-\gamma\beta(t-t_0)\right] \end{aligned}$$

and (2.26)

$$\begin{aligned} p_2 &= \mu - p_{1a} n_a (t-t_a)/\ell \\ &= p_{10} n_0 (t_b - t)/\ell . \end{aligned}$$

Hence, since $p_2(t_b) = 0$, $p_2(t_a+) = \mu = p_{1a} n_a (t_b - t_a)/\ell = p_{10} n_0 (t_b - t_a)/\ell$.

Since $\dot{p}_2(t)$ is piecewise-constant of one value, $u(t)$ can only change sign once if the trajectory is to satisfy the necessary conditions at t_0, t_a, t_b and t_1.

During the interval (t_b, t_1), the adjoint variables are again defined by (2.16) with $\delta k = \gamma\beta - \eta\beta(t-t_b)$.

As shown in Figure 2.3, the adjoint variable p_1 is initially selected to be any positive value. Along with p_{10}, the complete solution is determined by n_0 and n_1. Similarly, a solution could be generated for minimal-time decrease in neutron level with $p_1(t_0)$ of arbitrary negative value.

Next, consider a time-optimal startup but suppose n_0 and n_1 are such that $u(t)$ never reaches the constraint boundary $\gamma\beta$; in other words,

n_b from (2.21) is less than n_a from (2.20). Then the maximum principle can be applied as before with $u^\circ = \eta\beta \operatorname{sgn} p_2$. Furthermore, since $\dot{p}_2(t)$ is constant [from (2.13)] there is only one sign reversal of $u^\circ(t)$. For this case:

$$u^\circ = \begin{cases} \eta\beta \ , & t_o \le t < t_a \\ -\eta\beta \ , & t_a < t \le t_1 \end{cases} .$$

t_a is computed below and then may be related to t_1 by $t_1 = t_o + 2t_a$.

The time solutions, (2.15) to (2.17), are again valid with $\delta k = \eta\beta(t-t_o)$ for $t_o \le t < t_a$. . The same solutions describe the time response for $t_a < t \le t_1$ if the o subscripts are replaced by 1 subscripts and time is reversed. Observe that $|p_{21}| = |p_{2o}|$.

Equating the two solutions n(t) (i.e., the solution for $t_o \le t < t_a$ is equated to the solution for $t_a < t \le t_1$) one can compute t_a by

$$(t_a - t_o)^2 = \frac{\ell}{\eta\beta} \log \frac{n_1}{n_o} \ .$$

Time-optimal shutdowns may be computed similarly.

The above results may be applied to the neutron kinetic process in which most of the delayed neutrons are lost to the process. Such systems may be approximated by

$$\frac{dn}{dt} = \frac{u'}{\ell} n \ , \qquad (2.27)$$

where $u' = \delta k - \beta$.

2.2 Single-precursor group neutron kinetics

For many applications and to obtain a qualitative description, the six-group neutron kinetics [as given by (1.30) and (1.31)] may be approximated by a one-delay-group model:

$$\frac{dn}{dt} = \frac{u-\beta}{\ell} n + \lambda C = \frac{u}{\ell} n - \dot{C}$$

and (2.28)

$$\frac{dC}{dt} = \frac{\beta}{\ell} n - \lambda C ,$$

where λ is an average decay constant (computed so that the one-group model approximates the six-group model), $|u| \leq \gamma\beta$, $n(t_0) = n_0$ and $C(t_0) = C_0$. Equation (2.28) may be represented by the vector equation:

$$\dot{\vec{x}} = A(u)\vec{x} = \vec{f}(u,\vec{x}) \tag{2.29}$$

where $|u| \leq \gamma\beta$, $x_1 = n$, $x_2 = C$, and $\vec{x}(t_0) = \vec{x}_0$. This system will be analyzed in some detail since it is of low order and closely approximates the higher-order system for fast control.

2.2.1 Time-optimal control with the two state variables n and C

The logical choice of state variables, following equations (2.28), is neutron density n and neutron-precursor density C. Then the costate is defined by the adjoint system:

$$\dot{\vec{p}} = -A^T(u)\vec{p} , \tag{2.30}$$

where $\vec{p}(t_0) = \vec{p}_0$ and $|u| \leq \gamma\beta$. The optimal trajectory is to connect an initial steady-state n_0, C_0 to a terminal steady-state n_1, C_1 in minimal time. The inner product of $(\vec{p},\vec{f})$ for this system is

$$R(n,C;\vec{p};u) = \frac{u}{\ell} n p_1 + \dot{C}(p_2 - p_1) , \tag{2.31}$$

where $\dot{C}$ is not an explicit function of u. Again R becomes a maximum on the boundary of the allowable control set with a bang-bang process producing the time-optimal control. Since n is positive, the control is determined by

$$u^\circ = \gamma\beta \ \text{sgn}\ p_1 \tag{2.32}$$

and the Hamiltonian is a non-negative constant evaluated on $\vec{x}(t)$ and $\vec{p}(t)$. That is,

$$H(n,C;p) = \frac{\gamma\beta}{\ell}\, n\,|\,p_1\,| + \dot{C}\,(p_2 - p_1) \geq 0. \tag{2.33}$$

The solutions to (2.28) for $u = \pm\,\gamma\beta$ are given in Appendix B and are characterized in the phase plane by a saddle point (for $u = \gamma\beta$) and a stable node (for $u = -\gamma\beta$). Such a phase portrait of n vs C is presented in Figure 2.4. Although trajectories converge sharply to the eigenvectors (to be computed below) in all the phase planes presented in this chapter, it must be realized that each phase trajectory represents a unique solution of the state differential equations (with time eliminated). Hence trajectories really don't coincide and points b, c, d and g (in Figure 2.4 and other forthcoming phase portraits) are on their appropriate trajectory and a very small distance away from the B or D eigenvector. Since the eigenvectors of the A matrix help determine these phase-plane trajectories, their computation will follow.

The eigenvalues of the A matrix for constant u (i.e., the roots of the determinant $|A - I\rho| = 0$) are given by

$$\rho_1,\ \rho_2 = \frac{b \mp (b^2 + 4c)^{\frac{1}{2}}}{2}\ , \tag{2.34}$$

where

$$b = \frac{u - \beta}{\ell} - \lambda \ \text{and}\ c = \frac{u\lambda}{\ell}\ .$$

If $4c \ll b^2$, then the Taylor series for (2.34) indicates that $\rho_1 \approx -c/b$ and $\rho_2 \approx b$. Furthermore, assume that $\lambda\ell \ll \beta - u$ in

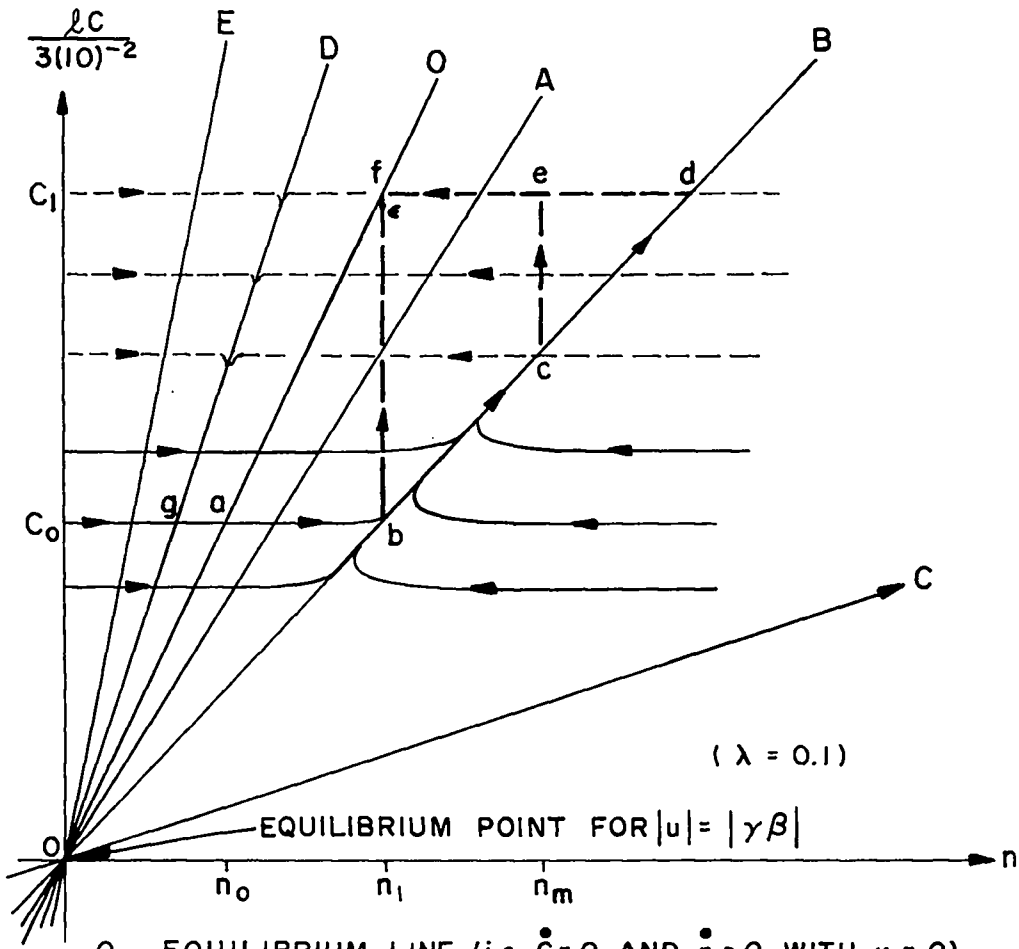

O - EQUILIBRIUM LINE (i.e. $\dot{C}=0$ AND $\dot{n}=0$ WITH $u=0$) WITH $C=\frac{\beta}{\lambda\ell}n$

A - EIGENVECTOR FOR $u = 0.25\beta$

B - EIGENVECTOR FOR $u = 0.5\beta$

C - EIGENVECTOR FOR $u = 0.9\beta$

D - EIGENVECTOR FOR $u = -0.5\beta$

E - EIGENVECTOR FOR $u = -0.9\beta$

SOLID TRAJECTORIES ARE FOR $u = 0.5\beta$

SMALL DASHES ARE FOR $u = -0.5\beta$

FIGURE 2.4 NEUTRON DENSITY VS NEUTRON-PRECURSOR DENSITY MINIMAL-TIME TRAJECTORIES

the above equation for b. (For most reactors $\lambda\ell$ is less than about 10^{-4} seconds.) Then these eigenvalues may be approximated by the following:

$$\rho_1 \approx \frac{\lambda u}{\beta - u} = \frac{\pm \lambda\gamma}{(1 \mp \gamma)}$$

$$\rho_2 \approx \frac{u-\beta}{\ell} = \frac{\beta(\pm \gamma - 1)}{\ell} \quad . \tag{2.35}$$

If $u-\beta \gg \lambda\ell$, the first assumption (i.e., $4c \ll b^2$) requires that $(u-\beta)^2/u \gg 4\lambda\ell$. This assumption is valid for all values of negative reactivity. For positive reactivities, the accuracy of this approximation depends on ℓ and u. For values of u less than $0.6\,\beta$ this approximation is good for most reactors but for larger values of u the approximation is limited to lower values of ℓ (or neutrons of higher energy). If $u = 0.9\beta$ for example, the approximation is only accurate if ℓ should be of the order of $5(10)^{-5}$ sec or less. Hence, the approximation is accurate for many applications such as the nuclear rocket reactor.

The eigenvectors corresponding to these real and distinct roots of the characteristic equation are computed by appendix equation (C.6). With $u = \pm \gamma\beta$, the tangents of these eigenvectors are given as follows:

$$S_1 = \frac{\rho_1 - a_1}{a_2} \approx \frac{-\gamma}{(\gamma \mp 1)} + \frac{\beta\,(1 \mp \gamma)}{\ell\lambda}$$

and

$$S_2 = \frac{\rho_2 - a_1}{a_2} \approx 0 \quad . \tag{2.36}$$

For typical values of ℓ

$$S_1 \approx \frac{\beta}{\ell\lambda} (1 \mp \gamma) ,$$

where $a_1 = (u-\beta)/\ell$ and $a_2 = \lambda$. Table 2.1 presents evaluations of these eigenvector tangents and eigenvalues for $\gamma = 0.5$ and $\gamma = 0.9$. From (2.34), it is readily seen that ρ_2 is slightly smaller than (2.35) indicates for $u = -\gamma\beta$ and slightly larger for $u = \gamma\beta$. Thus, S_2 is slightly negative for $u = -\gamma\beta$ and slightly positive for $u = \gamma\beta$.

Table 2.1

Approximate one-delay group neutronic eigenvalues and eigenvector tangents

u	$0.5\ \beta$	$-0.5\ \beta$	$0.9\ \beta$	$-0.9\ \beta$
ρ_1/λ	1	-0.333	9	-0.47
$\ell\rho_2$	$-0.5\ \beta$	$-1.5\ \beta$	$-0.1\ \beta$	$-1.9\ \beta$
$\ell\lambda S_1$	$0.5\ \beta$	$0.15\ \beta$	$0.1\ \beta+9\ell\lambda$	$1.9\ \beta$
ℓS_2	0+	0-	0+	0-
		For the adjoint system		
S_{1_A}	0.5	1.5	$0.1 + 9\frac{\lambda\ell}{\beta}$	1.9
S_{2_A}	0+	0-	0+	0-

Equation (2.29) indicates that the optimal switching is determined by the adjoint system. Hence, it is of interest to examine the behavior of the costate variables. The time solution to the adjoint system (2.30) is presented in Appendix B.

The eigenvalues of $-A^T(u)$ in equation (2.30) are equal in magnitude but opposite in sign to the eigenvalues of $A(u)$. Despite this

similarity, the eigenvectors are generally very different than those of A(u) as shown by their tangents:

$$S_{1_A} = \frac{\ell}{\beta}(\rho_1 - a_1) \approx (1 \mp \gamma) - \frac{\lambda \ell \gamma}{\beta(\gamma \mp 1)} \quad ,$$

$$S_{2_A} = \frac{\ell}{\beta}(\rho_2 - a_1) \approx 0 \pm \qquad (2.37)$$

and for typical values of ℓ

$$S_{1A} \approx (1 \pm \gamma) \quad .$$

These eigenvector tangents are evaluated for $\gamma = 0.9$ and $\gamma = 0.5$ in Table 2.1.

Figure 2.5 describes the phase behavior of the adjoint system with $u = 0.9\beta$ for positive p_1 and $u = -0.9\beta$ for negative p_1. The phase in the right-half plane is described by a saddle point while that in the left-half plane is typical of an unstable node. Since these adjoint variables are continuous without phase-plane constraints, it is seen from Figure 2.5 that p_1 can only have one zero in finite time. For any value of γ, the eigenvectors for the one-delay-group kinetics are similar to those shown in Figure 2.5, i.e., they are always in the quadrants shown and with the directions indicated. Hence there cannot be more than one switching for the time-optimal bang-bang process.

Since the constant u trajectories are unique solutions of the differential equations of the system, Figure 2.4 indicates there is only one possible trajectory which joins any reachable state from some initial state with a maximum of one switching and therefore such a trajectory

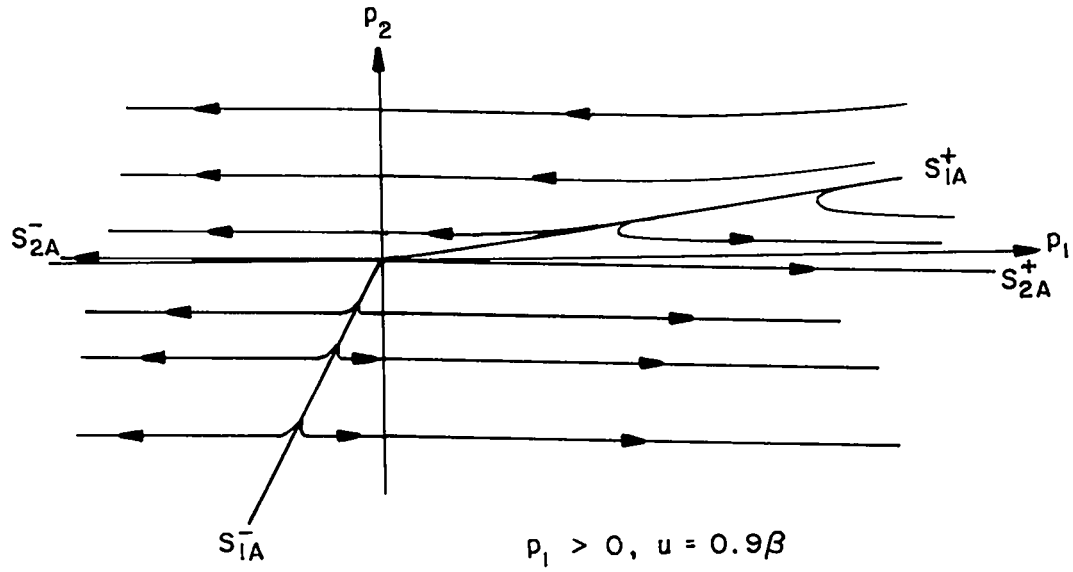

FIGURE 2.5 ONE-PRECURSOR-GROUP ADJOINT TRAJECTORIES FOR A BANG-BANG REACTIVITY PROCESS

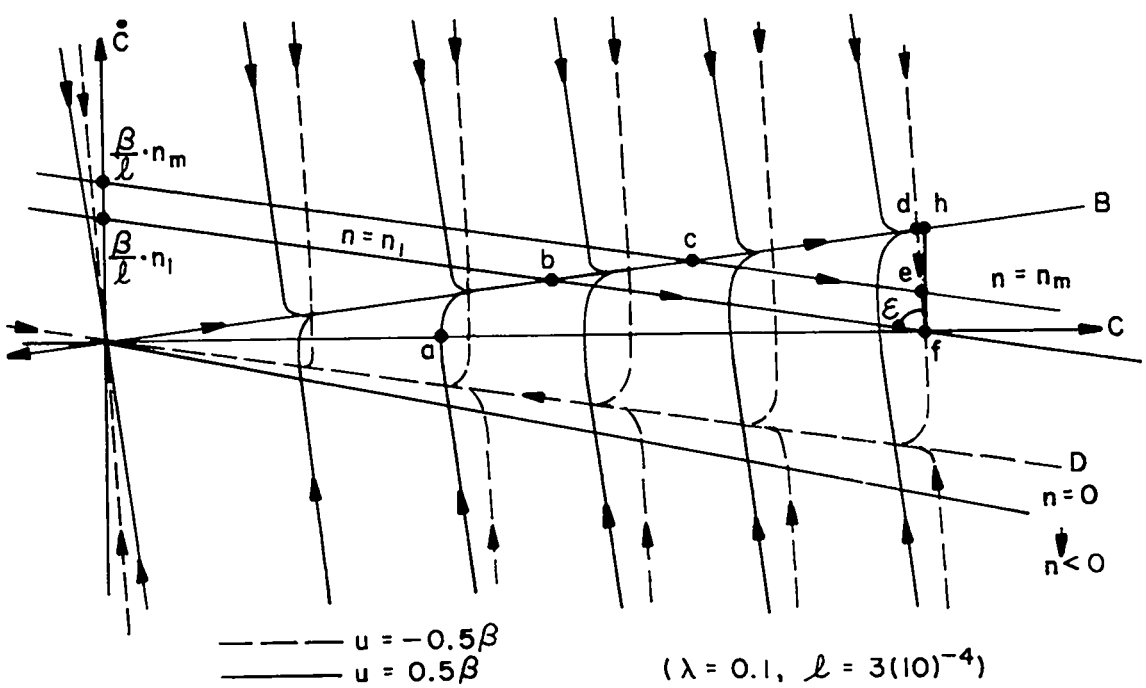

FIGURE 2.6 NEUTRON-PRECURSOR DENSITY VS TIME RATE OF CHANGE OF NEUTRON-PRECURSOR DENSITY FOR A BANG-BANG REACTIVITY PROCESS

(LABELLED POINTS REFER TO SIMILAR POINTS IN FIGURES 2.4 AND 2.7)

must be optimal (e.g., trajectory a-d-f has $u = \gamma\beta$ from a to d and $u = -\gamma\beta$ from d to f). Also the principle of optimality (viz., any portion of an optimal trajectory is optimal) shows that if a desired terminal state can be reached from a given initial state with no switchings and $|u| = \gamma\beta$, then the joining trajectory is optimal.

An example optimal-startup trajectory, linking an initial steady-state phase n_0, C_0 with a desired terminal steady-state phase n_1, C_1 is represented by trajectory a-d-f in Figure 2.4. Initially, the system is in steady-state with zero reactivity. Then reactivity is made equal to the maximum positive constraint $\gamma\beta$ while p_1 is positive. At point d, p_1 goes through zero and becomes negative as reactivity is switched to the minimum negative constraint. When the desired phase point f is reached, reactivity is returned to zero to maintain quiescence. A time-optimal decrease in state is analyzed similarly with p_{10} negative. For steady-state end conditions, the Hamiltonian has the positive value given by the following equation:

$$H(n,C;p) = \frac{\gamma\beta}{\ell} n_0 \ |p_{10}| = \frac{\gamma\beta}{\ell} n_1 \ |p_{11}|, \qquad (2.38)$$

where the 0 subscript represents initial values and the 1 subscript represents terminal values.

The switching point for the time-optimal startup process is conveniently determined by the neutron level n (or the neutron-precursor level C) at point d. Since the trajectory is asymtotic to the eigenvector B in Figure 2.4, for any significant difference, $(n_1 - n_0$, the switching point is nearly independent of the initial state. In many physical systems, it might be desirable to switch to a simple control law which is a continuous function of the system state within some

small predetermined region of the desired terminal phase. The size and shape of this region could be determined by the accuracy of the equations in defining the physical process, the accuracy of the measuring devices and the capability of the new closed-loop control. Hence, the exact switching point might not be too important.

Time may be eliminated from the solutions given by (B.7) if a knowledge of the exact switching point is desired. Then the trajectory passing through any desired phase may be computed as shown in Appendix D. If the desired terminal phase is n_1 , C_1 , the following equation (2.39) must be satisfied at point d in Figure 2.4.

$$\left[\frac{(\rho_{22}+\lambda)C - \frac{\beta}{\ell}n}{(\rho_{22}+\lambda)C_1 - \frac{\beta}{\ell}n_1}\right]^{-\rho_{22}} = \left[\frac{(\rho_{12}+\lambda)C - \frac{\beta}{\ell}n}{(\rho_{12}+\lambda)C_1 - \frac{\beta}{\ell}n_1}\right]^{-\rho_{12}}, \quad (2.39)$$

where the second subscript 2 of ρ refers to $u = -\gamma\beta$. However, as shown in Figure 2.4, $C \approx C_1$ at the switching point.

A time-optimal shutdown is shown in Figure 2.4 by trajectory f-g-a. Again the switching point is almost independent of the initial state and can be determined by n at point g. The exact switching point g, however, could be determined by the equation given below, which is similar to (2.39) with the eigenvalues replaced by ρ_{11} and ρ_{21}; i.e., those for positive reactivity $\gamma\beta$.

$$\left[\frac{(\rho_{21}+\lambda)C - \frac{\beta}{\ell}n}{(\rho_{21}+\lambda)C_1 - \frac{\beta}{\ell}n_1}\right]^{-\rho_{21}} = \left[\frac{(\rho_{11}+\lambda)C - \frac{\beta}{\ell}n}{(\rho_{11}+\lambda)C_1 - \frac{\beta}{\ell}n_1}\right]^{-\rho_{11}}. \quad (2.40)$$

For example, equation (2.39) describes a switching line for a time-optimal startup to a desired terminal phase (n_1 , C_1). Below this line $u = \gamma\beta$ and when this line is reached $u = -\gamma\beta$ until the desired terminal phase is reached. Similarly, equation (2.40) defines a switching line for a time-optimal shutdown with $u = -\gamma\beta$ above the switching line.

If a knowledge of n and C are available, an on-line computation could be made (e.g., digitally or by means of an analog function generator and a comparator) to determine the switching point from (2.39) or (2.40).

2.2.2 Time-optimal control of neutron level

In practice it is generally desirable to traverse from some initial steady-state neutron level to a terminal steady-state neutron level in minimal time without the terminal precursor level necessarily being at steady state. This problem may be specified by merely defining the terminal set to be a line $n = n_1$ in the n vs C phase plane shown in Figure 2.4. Optimization problems with a variable terminal point belonging to a specified hypersurface were discussed in Chapter I, page 8. In general, the costate vector must be orthogonal to the tangent plane of the terminal hypersurface at the free terminal state. In regards to this neutronic control problem, the terminal hypersurface is simply the line $n = n_1$ in the n vs C phase plane. Hence, the adjoint vector must be perpendicular to this terminal line.

With $p_2 (t_1) = 0$ and time reversed, it is seen from Figure 2.5 that $p_1(t)$ can have no zeros for $t < t_1$. Similar plots, with the eigenvectors in the same quadrants, could be obtained for other values of γ. Hence, the time-optimal control with a reactivity constraint

is constant for $t_o < t < t_1$. This fact is substantiated by the solution to the adjoint system with time reversed which is similar to the neutronics solution (B.7).

With $p_2(t_1) = 0$ and time reversed ($t \leq t_1$)

$$p_1 = \frac{p_{11}}{\rho_2 - \rho_1} \left(c_{11}^1 e^{\rho_1 (t_1 - t)} + c_{11}^2 e^{\rho_2 (t_1 - t)} \right), \qquad (2.41)$$

where $p_1(t_1) = p_{11}$, $p_2(t_1) = 0$, $c_{11}^1 = \rho_2 + \frac{\beta}{\ell}(1 \mp \gamma)$, $c_{11}^2 = -\left[\rho_1 + \frac{\beta}{\ell}(1 \mp \gamma)\right]$ and $u = \pm \gamma\beta$. Then, from (3.35) and (B.6) [with ρ_2 slightly larger than (3.35) predicts for $u = \gamma\beta$ and slightly smaller for $u = -\gamma\beta$]

$$c_{11}^1 \approx 0^{\pm} \text{ and } c_{11}^2 \approx -\left[\pm \frac{\gamma\lambda}{(1 \mp \gamma)} + \frac{\beta}{\ell}(1 \mp \gamma) \right] \qquad (2.42)$$

Order of signs is read according to order of $u = \pm \gamma\beta$.

For $u = \gamma\beta$, both coefficients of the exponential terms in (2.41) are of the same sign and $p_1(t)$ cannot have any zeros. Also, for $u = -\gamma\beta$, both coefficients are negative; hence, $p_1(t)$ can have no zeros and there can be no switching in the control process.

The time-optimal solution to the neutron kinetics [equation (2.28)] is again given by (B.7) on the interval (t_o, t_1).

At the terminal time the neutron-precursor level is not yet at steady-state. Therefore, reactivity must be different from zero to maintain constant neutron level $n(t) = n_1$ for $t \geq t_1$. From equation (2.28) it is seen that the following equation is required to hold the neutron level constant:

$$u = \frac{\ell \dot{C}}{n_1} = \beta - \frac{\lambda \ell C}{n_1} . \qquad (2.43)$$

For constant neutron level n_1 and $t_1 \leq t$, the solution to (2.28) is

$$C = \frac{\beta}{\ell\lambda} n_1 + \left[C(t_1) - \frac{\beta n_1}{\ell\lambda} \right] e^{-\lambda(t-t_1)} \quad . \tag{2.44}$$

Then

$$\dot{C} = -\left[C(t_1) - \frac{\beta}{\ell\lambda} n_1 \right] \lambda e^{-\lambda(t-t_1)} \tag{2.45}$$

and

$$u(t) = \left[\beta - \frac{\ell\lambda C(t_1)}{n_1} \right] e^{-\lambda(t-t_1)} \quad . \tag{2.46}$$

With reference to a typical startup trajectory a-b-f, as presented in Figure 2.4, it is seen that $\dot{C}$ diminishes according to (2.45) and Figure 2.6 (phase plane of C vs $\dot{C}$) for $n = n_1$ and would only become zero at $C(t) = \frac{\beta}{\ell\lambda} n_1$, according to equation (2.28). This state is never reached in finite time, as shown by (2.44).

It is interesting to recognize the similarities in the optimal control of the prompt kinetics and the single-precursor-group kinetics; e.g., both require no switching, except at the end points, to vary neutron level from one state to another in minimal time.

2.2.3 Admissibility of the terminal control

The allowable set of controls for the optimization process has been defined by $|u| \leq \gamma\beta$. To assure that the terminal control is contained in the set of allowable controls for the case of unsymmetrical limits, let reactivity be limited by $-\gamma_1\beta \leq u \leq \gamma_2\beta$. From the following analysis it will be seen that the required terminal control belongs to this allowable set for initial equilibrium conditions. From equation (2.46), it is seen that

$$-(1+\gamma_1) \leq -\frac{\ell\lambda C(t_1)}{\beta n_1} \leq \gamma_2 - 1 \qquad (2.47)$$

or

$$(1-\gamma_2)\frac{n_1\beta}{\ell\lambda} \leq C(t_1) \leq (1+\gamma_1)\frac{n_1\beta}{\ell\lambda} . \qquad (2.48)$$

In other words, if $C(t_1)$ satisfies (2.47), the terminal control is in the allowable set. The first of equations (2.36) along with (2.34) shows that, for $u = \gamma_2\beta$, the left side of (2.48) is true for any trajectory which starts from the left side of the B eigenvector in Figure 2.4. That is, since the eigenvector cannot be crossed, the following inequality is valid:

$$C(t) \geq \frac{(1-\gamma_2)\beta n}{\ell\lambda} + \frac{\gamma_2}{1-\gamma_2} n . \qquad (2.49)$$

Then certainly $C(t_1) > \frac{1-\gamma_2}{\ell\lambda}\beta n_1$ and the terminal control $u(t) < \gamma_2\beta$.

From the eigenvector D in Figure 2.4 (for $u = -\gamma_1\beta$) it is seen that for any trajectory which starts to the right of D, the following inequality must be satisfied:

$$C(t) \leq \frac{(1+\gamma_1)\beta n}{\ell\lambda} - \frac{\gamma_1}{1+\gamma_1} . \qquad (2.50)$$

Then certainly $C(t_1) < \frac{\beta}{\ell\lambda}(1+\gamma_1)n_1$ and the terminal control $u > -\gamma_1\beta$. Hence, there is always a step change in reactivity from the boundary and into the allowable set when $n(t) = n_1$ and the required terminal control is in the allowable set thereafter.

2.2.4 Consideration of other state variables

Since the rate of change of neutron level has physical interest

and is usually measured, one would suspect that n and $\dot{n}$ would be a good selection of state variables for control purposes. With state variables n and $\dot{n}$, equation (2.28) may be represented as follows:

$$\frac{d^2n}{dt^2} = \left(\frac{u-\beta}{\ell} - \lambda\right)\frac{dn}{dt} + \left(\frac{\lambda u+\dot{u}}{\ell}\right)n \quad . \tag{2.51}$$

This equation may be written conveniently in vector form (with $x_1 = n$ and $x_2 = \dot{n}$) as

$$\dot{\vec{x}} = A(u, \dot{u})\,\vec{x} \quad , \tag{2.52}$$

where

$$A(u, \dot{u}) = \begin{bmatrix} 0 & 1 \\ \frac{\lambda u+\dot{u}}{\ell} & \frac{u-\beta}{\ell} - \lambda \end{bmatrix} \quad . \tag{2.53}$$

Since the eigenvectors of (2.53) for constant u lie in such a manner that the position vector and velocity vector point in the same direction (see Appendix C), it is apparent that the eigenvectors have slope equal to the eigenvalues of (2.53). These eigenvalues are given by equation (2.35).

Although not drawn to any scale, Figure 2.7 gives a qualitative description of several piecewise continuous n vs $\dot{n}$ phase-plane trajectories, which approximately correspond to continuous trajectories presented in Figure 2.4. In this phase plane, $t_1 - t_0 = \int_{n_0}^{n_1} \frac{1}{\dot{n}}\, dn$ and thus the above time-optimal process is substantiated by the following argument: With maximum or minimum allowable reactivity (i.e., $u = \pm \gamma\beta$), the trajectory is farthest away from the n axis that the control constraint allows. Then the time evolved in changing neutron level between steady-state conditions is minimized by the bang-bang process with no switching between the end states.

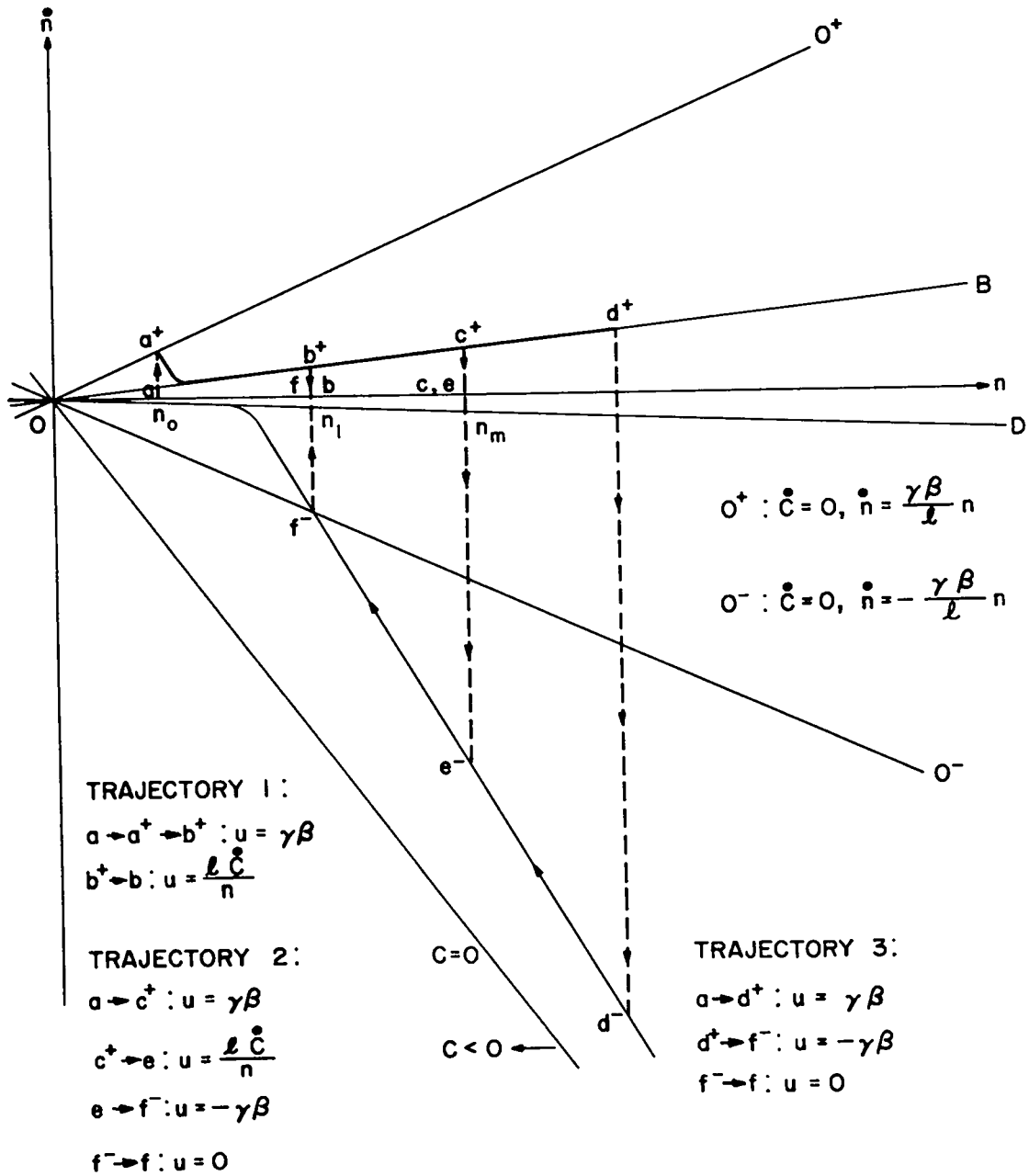

FIGURE 2.7 n VS $\dot{n}$ BANG–BANG CONTROLLED PHASE-PLANE TRAJECTORIES

(LABELLED POINTS REFER TO SIMILAR POINTS IN FIGURES 2.4 AND 2.6)

The discontinuities in $\dot{n}$ at the switching points, however, generally make it an undesirable state variable for the bang-bang controlled process. As shown by equation (2.28) and again below by (2.54), the rate of change of neutron-precursor level $\dot{C}$ is generally continuous for piecewise-continuous reactivity.

$$\frac{d^2C}{dt^2} = \left(\frac{u-\beta}{\ell} - \lambda\right)\frac{dC}{dt} + \frac{\lambda u}{\ell} C \qquad (2.54)$$

The continuity of $\dot{C}$ makes it interesting to study the C vs $\dot{C}$ phase plane. For constant reactivity, the C vs $\dot{C}$ trajectories are identical to the n vs $\dot{n}$ trajectories but the former trajectories have the convenience of continuity between the saddle-point portrait and the stable-node portrait at the switching points. An example of such a superposition is presented in Figure 2.6. Figure 2.8 shows the effect of the neutronic source term (which is generally negligible) as it appears in equation (1.32).

Consider the problem of traversing from some initial steady-state precursor level C_0 to a desired steady-state precursor level C_1 (see Figure 2.4). Again, when the trajectory for maximum or minimum reactivity intersects this set, the adjoint vector is perpendicular to the line $C = C_1$. Therefore, $p_1(t_1) = 0$ and hence from Figure 2.5 with time again reversed, it is seen that there can be no switching in reactivity for $t < t_1$. The control required to hold the neutron-precursor level constant is $u = (\ell\dot{n})/n$. Again, the time-optimality of this process is substantiated by the convenient time relationship in the C vs $\dot{C}$ phase plane. However, the time traversed in going from

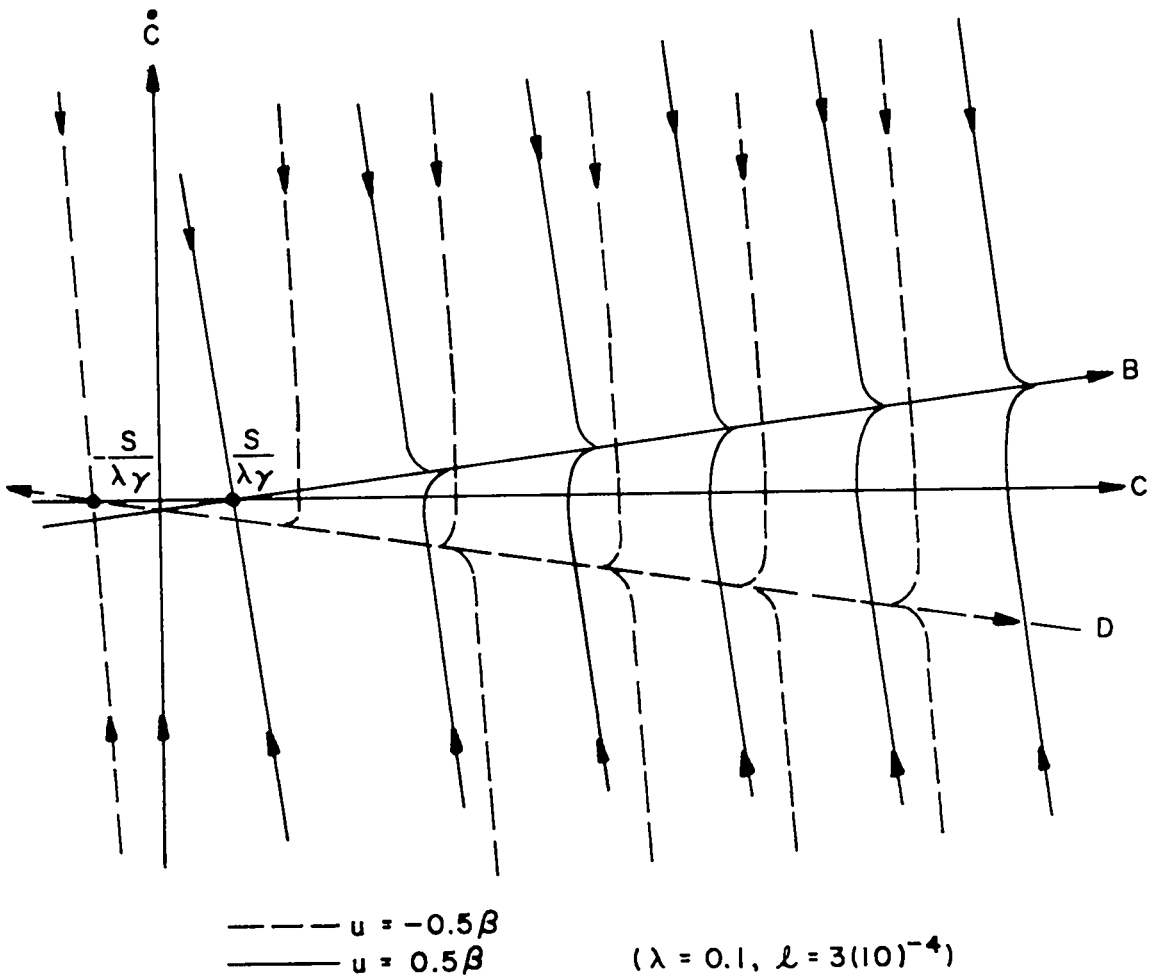

FIGURE 2.8 BANG-BANG CONTROLLED TRAJECTORIES SHOWING THE EFFECT OF NEUTRON SOURCE

point d to point f with $u = \gamma\beta$ in Figure 2.4 and Figure 2.6 is very small and thus the bang-bang control discussed previously (i.e., n_0, C_0 to n_1, C_1 via trajectory a-d-f) is nearly optimal for this new problem also.

2.2.5 Time-optimal control with phase-plane constraint

Another neutronic optimization problem pertains to the analysis of the time-optimal trajectory which links steady-state n_0, C_0 with a desired terminal steady-state n_1, C_1 (see 2.2.1), while including an additional constraint on the amount of overshoot in neutron level.

Suppose there is a requirement of no overshoot in n. It is seen from Figure 2.6 (e.g., see trajectory a-b-f) that neutron-precursor level cannot be increased in such a manner in finite time, because (with $\Delta t = \int_{C_0}^{C_1} \frac{1}{\dot{C}}\, dC$) any steady-state phase ($\dot{C} = 0$) can only be reached or left in finite time by trajectories perpendicular to the axis at $\dot{C} = 0$. A phase very close to the desired phase (see ϵ in Figure 2.6), however, may be reached in finite time. This point ϵ could be reached by a constant reactivity $\gamma\beta$ followed by the variation similar to that defined by (2.43) for the proper n. At point ϵ the trajectory would continue to approach the steady-state terminal phase or a conventional closed-loop control could be introduced so that the phase would approach point f. The optimal trajectory, a-b-ϵ, is shown below to satisfy the necessary conditions of the maximum principle and the optimization techniques with phase-space constraints.

The initial portion of the trajectory (i.e., for $n \leq n_1$) was analyzed by the maximum principle in Section 2.2.1.

Then, in order that the trajectory does not cross the constraining line $n = n_1$ but coincides with this line, it is necessary that the

control be generated according to equation (2.43). Following the designation used in Chapter I, the constraint boundary is represented by $S = n-n_1 = 0$ and $\dot{S} = \dot{n} = (u-\beta)\, n/\ell + \lambda C$. As discussed in Chapter I, the Hamiltonian is constant across the entering corner to the constraint line (point b in Figures 2.4 and 2.6). Hence,

$$H(n,C;\vec{p})\,\Big|_{t_a-} = H(n,C;\vec{p})\,\Big|_{t_a+} \geq 0 \ . \tag{2.55}$$

With the constraint explicitly independent of C, equation (1.24) indicates that the following equations must also be satisfied at the entrance corner.

$$\begin{aligned} p_1(t_a-) &= p_1(t_a+) + \mu \\ \text{and} \qquad & \qquad (2.56) \\ p_2(t_a-) &= p_2(t_a+) \ . \end{aligned}$$

From equations (2.55) and (2.38), with $\dot{n}(t_a+) = 0$, it is seen that

$$\dot{n}p_1 + \dot{C}p_2\,\Big|_{t_a-} = \dot{C}p_2\,\Big|_{t_a+} = H \ , \tag{2.57}$$

where

$$H = \frac{\lambda\beta}{\ell}\, n_o\, |p_{1c}| \ ^{*} \ . \tag{2.58}$$

Furthermore, since $\dot{C}(t_a-) = \dot{C}(t_a+)$ and $p_2(t_a-) = p_2(t_a+)$, it is seen from (2.57) that

$$p_1(t_a-) = 0. \tag{2.59}$$

- - - - - - - - - - - -

* For the sake of brevity, the arguments of a function, e.g., $H(n,C;\vec{p})$, are often dropped in this dissertation where they are obvious or previously defined.

Therefore, it is indicated by Figure 2.5 that the optimal control has no switchings for $t < t_a$. For the optimal trajectory to correspond to the constraining line, one sees from equation (1.23) that the costate dynamics must behave according to

$$\dot{\vec{p}} = -\left[\frac{\partial \vec{f}}{\partial \vec{x}} - \frac{\partial \vec{f}}{\partial u}\left(\frac{\partial \dot{s}}{\partial u}\right)^{-1}\left(\frac{\partial \dot{s}}{\partial \vec{x}}\right)^{T}\right]^{T} \vec{p} \quad . \tag{2.60}$$

For the problem at hand [see (2.28) and (2.29)]:

$$\frac{\partial \vec{f}}{\partial \vec{x}} = \begin{bmatrix} \frac{u-\beta}{\ell} & \lambda \\ \beta/\ell & -\lambda \end{bmatrix} = A(u) \quad , \tag{2.61}$$

$$\frac{\partial \vec{f}}{\partial u} = \begin{bmatrix} n/\ell \\ 0 \end{bmatrix}, \left[\frac{\partial \dot{s}}{\partial u}\right]^{-1} = \ell/n \tag{2.62}$$

and

$$\left[\frac{\partial \dot{s}}{\partial \vec{x}}\right]^{T} = \begin{bmatrix} \frac{u-\beta}{\ell} & \lambda \end{bmatrix} \quad . \tag{2.63}$$

Therefore, the costate is defined by terms appearing in the adjoint equation (2.30) plus other terms given above, which yield

$$\dot{p}_1 = -\frac{\beta}{\ell} p_2$$

and

$$\dot{p}_2 = \lambda p_2 \tag{2.64}$$

for $t > t_a$. The solution to (2.64) for $t \geq t_a$ is

$$p_2 = p_{2a}\, e^{\lambda(t-t_a)}$$

and

$$p_1 = -\frac{\beta p_{2a}}{\ell\lambda}\, e^{\lambda(t-t_a)} + \left(p_{1a} + \frac{\beta}{\ell\lambda} p_{2a}\right) , \tag{2.65}$$

where

$$p_{2a} = p_2(t_a+) \text{ and } p_{1a} = p_1(t_a+) \quad .$$

In order to satisfy (2.56) to (2.58), it is seen from equation (2.45) that $p_1(t_a+) = -\mu$ and

$$p_{2a} = \frac{H}{\left(\frac{\beta}{\ell} n_1 - \lambda C_a\right)} \geq 0, \tag{2.66}$$

where

$$C_a = C(t_a) \quad \text{and} \quad H = \frac{\gamma\beta}{\ell} n_0 |p_{10}| \ ;$$

or

$$p_{2a} = A\,|p_{10}| \quad , \tag{2.67}$$

where

$$A = \frac{\gamma n_0}{\left[1 - \frac{\ell\lambda C_a}{\beta n_1}\right] n_1} \quad .$$

Recognize that $\partial\dot{S}/\partial u$ is nonzero for (t_a, t_b) and $\vec{p}(t_a+)$ is nonzero and noncollinear with $\partial S/\partial\vec{x}$ as required in Section 1.4. Furthermore, since p_{2a} is non-negative, substitution of (2.65) into (2.64) shows that $\dot{p}(t) = \dot{p}_1(t)$ is non-positive for (t_a, t_b) as required in Section 1.4.

The optimal-time responses are defined by equations (2.44), (2.65) and (2.67) for $n(t) = n_1$ and $t_a < t$. Then substitution of $p_{1a} = 0$ into the solution of the adjoint equations (see Appendix B) for $t < t_a$ (with time reversed), yields the following:

$$p_1(t) = \frac{\beta A |p_{1o}|}{\ell(\rho_1 - \rho_2)} \left[e^{\rho_1 (t_a - t)} - e^{\rho_2 (t_a - t)} \right] \qquad (2.68)$$

and

$$p_2(t) = \frac{A |p_{1o}|}{\rho_2 - \rho_1} \left[(\rho_2 + \lambda) e^{\rho_1 (t_a - t)} - (\rho_1 + \lambda) e^{\rho_2 (t_a - t)} \right] . \qquad (2.69)$$

Therefore, [from (2.69)] the necessary relation between the initial costate components is

$$p_{2o} = \frac{A |p_{1o}|}{\rho_2 - \rho_1} \left[(\rho_2 + \lambda) e^{\rho_1 (t_a - t_o)} - (\rho_1 + \lambda) e^{\rho_2 (t_a - t_o)} \right] . \qquad (2.70)$$

The time solutions of the state variables for $t \leq t_a$ are given by equation (B.7) and corresponding optimal phase-plane trajectories are designated as a-b-e in Figures 2.4, 2.6 and 2.7.

Suppose neutron level is allowed to overshoot n_o but not n_m. Then from the previous analysis, along with the Δt relation for Figure 2.6, it is readily deduced that trajectory a-c-e-f is a minimal-time trajectory between points a and f with the added constraint of $n(t) \leq n_m$. Also, part of this trajectory is the time-optimal trajectory between n_o and n_m.

An actual example as obtained from the analog computer is shown in Figure 2.9, where the reactor is started with steady-state initial power level and precursor level. The data may be interpreted as the time-optimal process between the given initial condition and a desired terminal steady-state power level and steady-state precursor level with a power constraint, $Q \leq Q_m = 4.28(10)^6$ Btu/sec; or the process may be considered as time optimal between the given initial condition and a desired terminal steady-state power level Q_m. With $\gamma = 0.9$ and $\ell = 3(10)^{-4}$ sec, it is seen in Figure 2.9 that the time elapsed

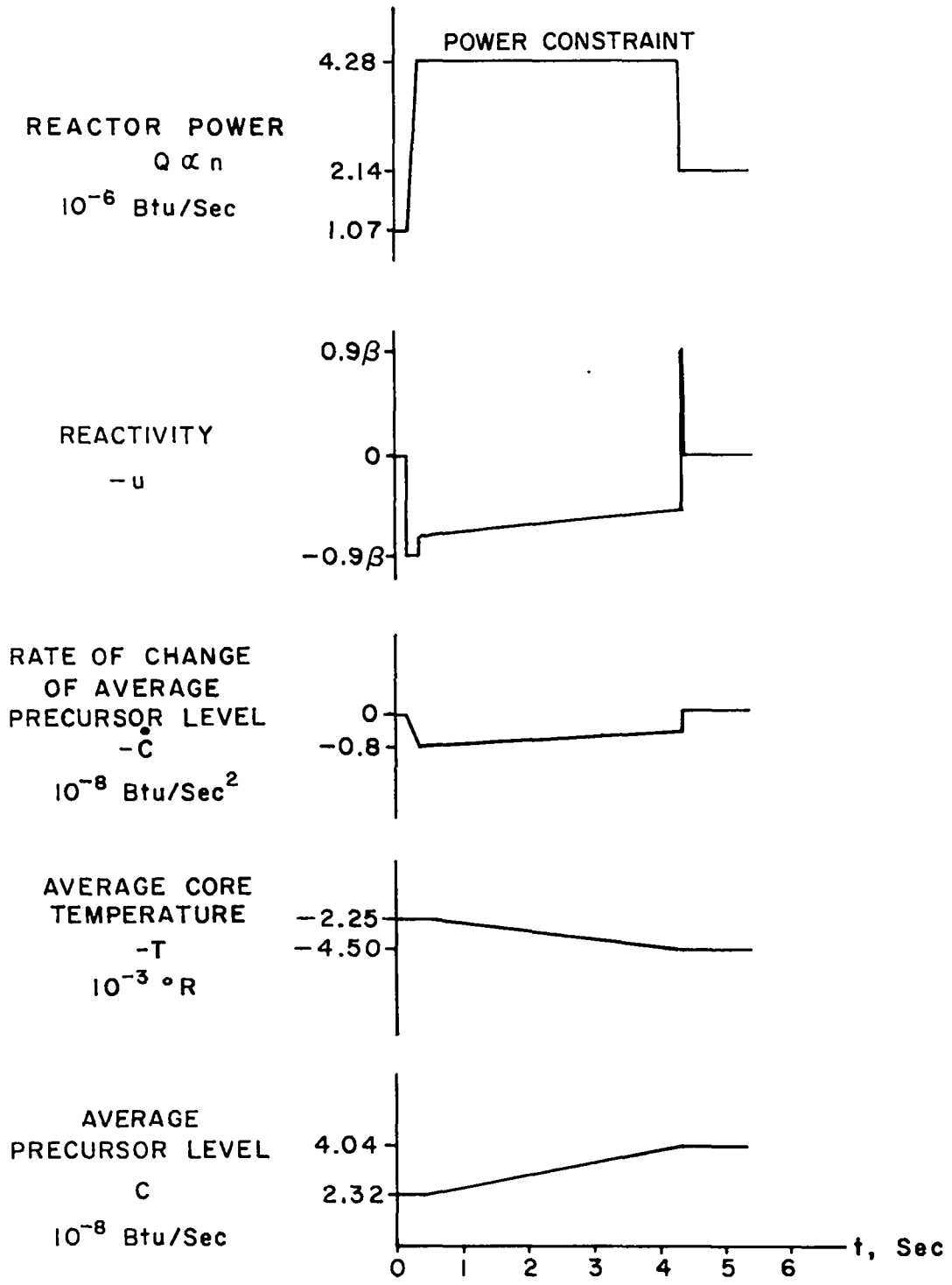

NOTE: RUN STARTS AT $t = 0.2$ Sec

$\ell = 3(10)^{-4}$ Sec, $\lambda = 0.1$ Sec^{-1}

FIGURE 2.9 POWER CONSTRAINED MINIMAL-TIME SYSTEM TRANSIENTS FOR A SINGLE-PRECURSOR MODEL

($\dot{Q} = \dot{C} = 0$ AT END POINTS, SIMILAR RUN IS SHOWN BY TRAJECTORY a-c-e-f IN FIGURE 2.4)

to quadruple the power level is about 0.2 sec. The time elapsed to double the neutron level and force the precursor level to steady-state along with the neutron level at the terminal point is about 4.4 seconds. Such minimal-time startup transients were simulated by the analog computer schematic diagram shown in Figure 2.10. Although an exit gas temperature is recorded, temperature and propellant reactivity coupling were neglected. Notice also that the precursor level is still represented by C but the units of C must be units of power to be consistent with (2.28).

Various optimal trajectories are plotted in Figure 2.11 with the circuit diagram shown in Figure 2.10. Elapsed times, between end points, are listed in the accompanying table. Trajectories 1, 2, 3 and 5 merely compare time-optimal trajectories between various initial quiescent states to a desired terminal quiescent state with the same constraint on neutron level (or power level). Trajectories 4 and 5 show the decrease in transition time for an increase in the maximum neutron level constraint. Trajectories 4, 6 and 7 compare transition times for various constraints in reactivity. Again, these trajectories may be considered as optimal between n_o, C_o and n_m or between n_o, C_o and n_1, C_1. These data indicate a considerable reduction in transition time, $t_1 - t_o$, may be obtained by increasing γ to 0.9.

2.2.6 Singular solutions

In the event that the switching function of the control equation [e.g., p_1 in (2.31)] should vanish for any finite period of time, the control is undefined and is classified as a singular control. If such a singular solution satisfies the necessary conditions of the maximum principle along with the boundary values of the problem,

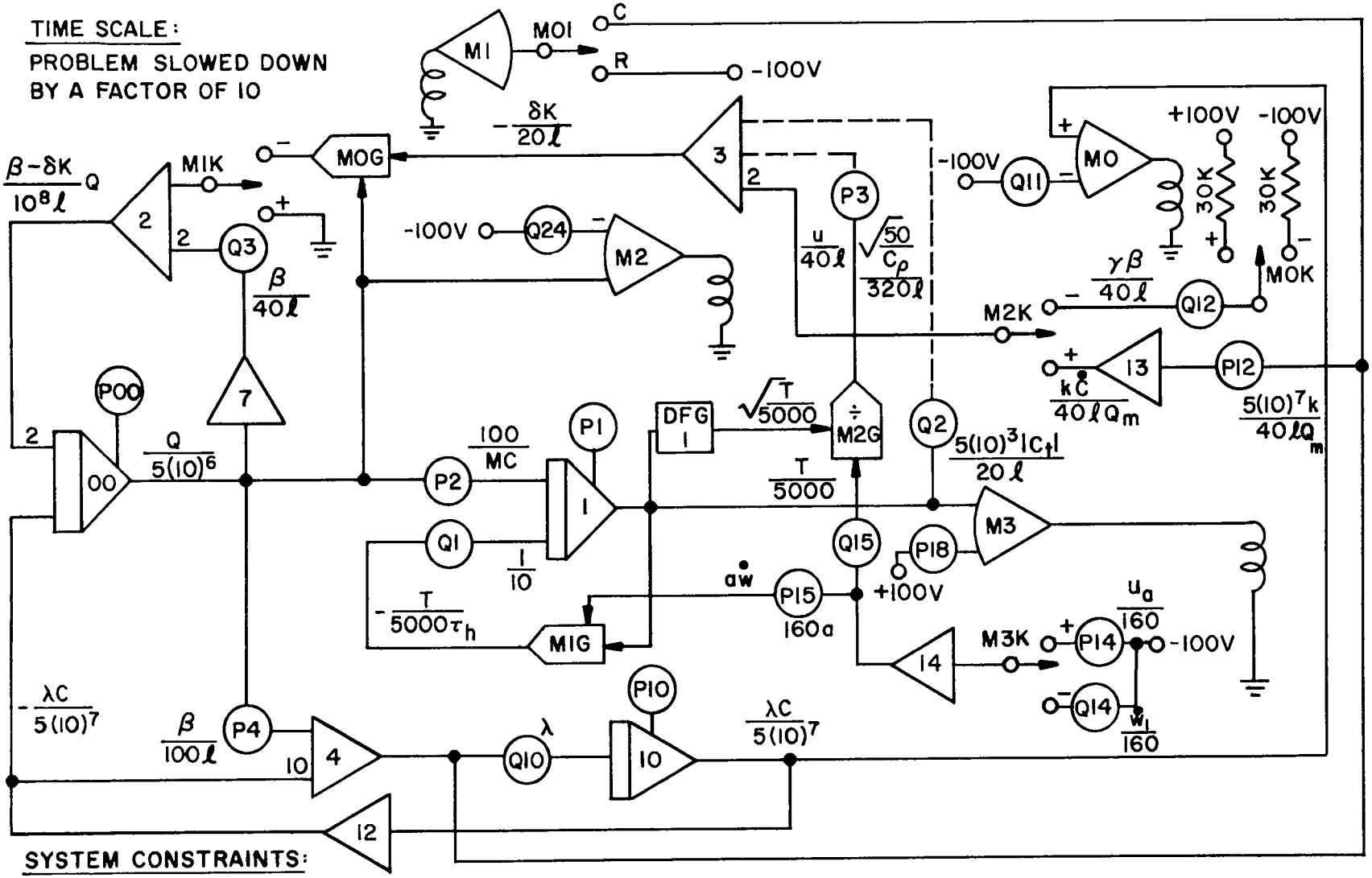

FIGURE 2.10 ANALOG COMPUTER DIAGRAM OF A BANG-BANG CONTROLLED ONE-DELAY-GROUP REACTOR SYSTEM

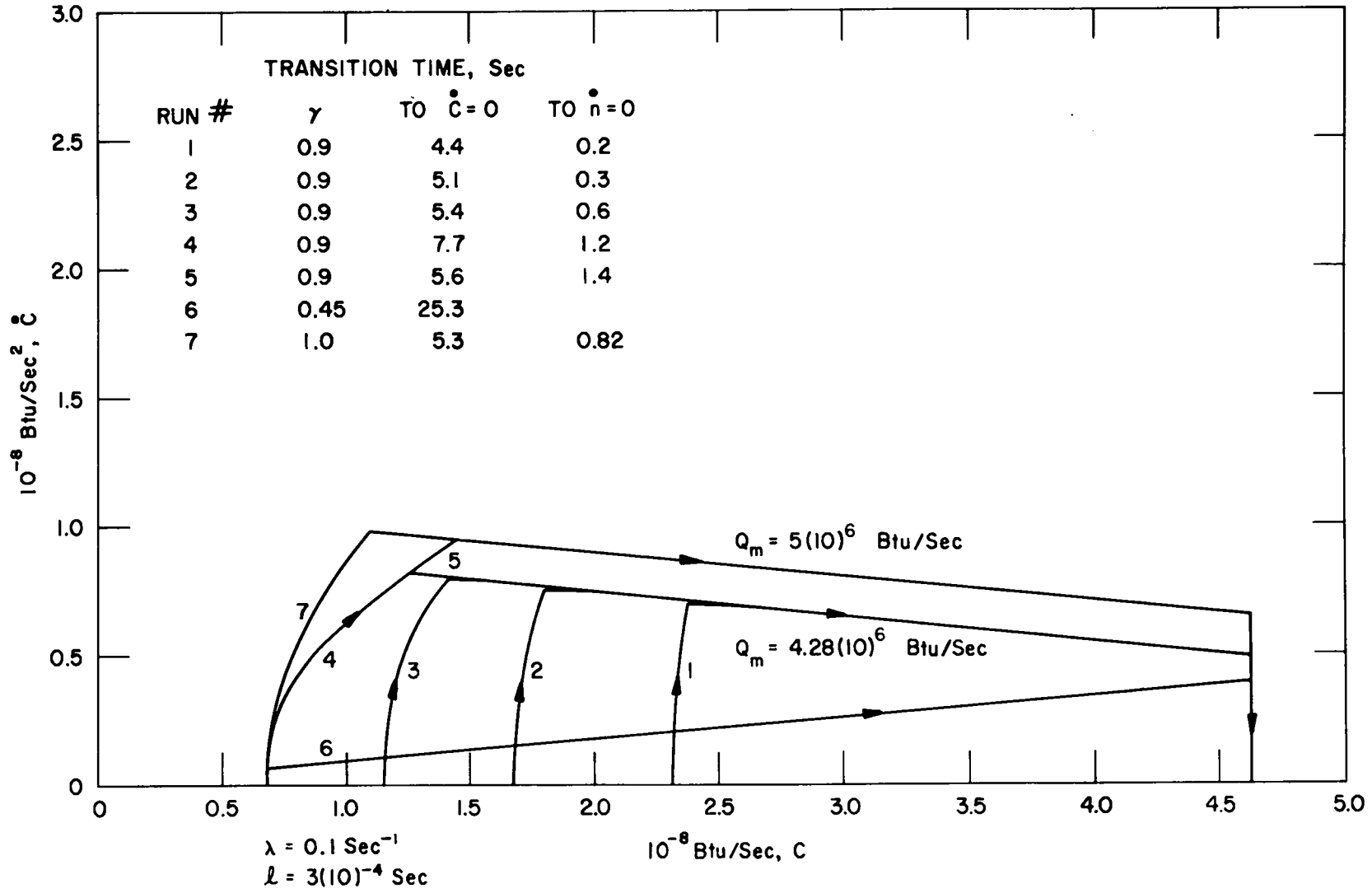

FIGURE 2.11 COMPUTER SIMULATED C VS $\dot{C}$ MINIMAL-TIME TRAJECTORIES WITH CONSTRAINTS IN POWER AND REACTIVITY

the singular control (as indicated in Reference 22) is a candidate for the optimal process. Such control, however, has not appeared in the above optimal-control problems.

Indeed the only possibility of a singular solution to exist in the above neutronic processes is for p_1, the switching function in (2.32), to vanish for some finite interval of time. If $\dot{n} \neq 0$, it is seen from the adjoint equation [see (2.30)],

$$\dot{p}_1 = \frac{u}{\ell} n p_1 + \left(\frac{\beta}{\ell} n - \lambda C\right) (p_2 - p_1), \tag{2.71}$$

that p_1 cannot vanish for any finite time. Hence a singular solution cannot exist since the neutron level and precursor level is positive.

Once the numerical value of the Hamiltonian has been established, then as is shown in **Reference** 22 (see statement 1, page 6), any control which renders such a value for R is a candidate for the optimal control.

Suppose $p_1(t) \equiv 0$, $\dot{n} \equiv 0$, $u = \frac{\ell \dot{C}}{n}$ and $n(t) \equiv n_a$, for $t_a < t < t_b$; then, from (2.31),

$$R = p_2 \dot{C} \ . \tag{2.72}$$

Hence [from (2.28)],

$$\dot{C} = \frac{\beta}{\ell} n_a - \lambda C \ , \tag{2.73}$$

[from (2.71)]

$$\dot{p}_1 = 0$$

and

$$\dot{p}_2 = \lambda p_2 \ . \tag{2.74}$$

The solutions to (2.73) and (2.74) are:

$$C = \frac{\beta}{\ell\lambda} n_a + \left[C_a - \frac{\beta n_a}{\ell\lambda}\right] e^{-\lambda(t-t_a)} \tag{2.75}$$

[where $C_a = C(t_a)$],

$$p_1 = p_{1a}$$

and (2.76)

$$p_2 = p_{2a}\, e^{\lambda(t-t_a)} \quad ,$$

where $p_{1a} = p(t_a)$ and $p_{2a} = p_2(t_a)$. Substitution of (2.73), (2.75) and (2.76) into (2.72) yields

$$R = \left[\frac{\beta}{\ell} n_a - \lambda C_a\right] p_{2a} \quad . \tag{2.77}$$

Then $R = H$ if

$$p_{2a} = \frac{H}{\frac{\beta}{\ell} n_a - \lambda C_a} \quad . \tag{2.78}$$

For example, with the Hamiltonian given by (2.38):

$$p_{2a} = \frac{\gamma n_o |p_{1o}|}{n_a - \frac{\lambda \ell}{\beta} C_a} \quad . \tag{2.79}$$

For steady-state initial conditions, the denominator of (2.79) is positive for time-optimal increases in n and is negative for time-optimal decreases in n. The adjoint trajectories given in Figure 2.5 indicate the possibility of $p_{1a} = 0$, (with p_{2a} positive for $u = \gamma\beta$ and negative for $u = -\gamma\beta$) and hence, along with (2.79), a singular type of solution does exist for $\dot{n} \equiv 0$. With respect to the previous analyses, such a solution is only optimal for the problem with neutron-level constraint and the problem with a free terminal state. However, the optimal control of these processes was obtained properly in a different manner, as analyzed in sections 2.2.5 and 2.2.3 respectively. Notice that the optimal control problem with phase-plane constraint also allows a jump discontinuity in p_1 at

$t = t_a$. Other singular solutions do not meet the required end conditions.

Even though singular control is of little significance for the minimal-time neutronic control problems, it can be important for other neutronic optimization problems. Since the neutron kinetic equations (2.28) are linear in the control, it is readily seen from the maximum principle that a bang-bang reactivity variation is a candidate for the optimal control if the cost function is linear in the control. For these problems singular control could be important and it is generally possible to construct singular control surfaces by means of the equations developed in Reference 22.

Although the conditions required by the maximum principle have only been necessary for the control to be optimal, consideration of singular solutions and the dynamics of the system substantiates the uniqueness of the optimal process. The simple relations for the time changes in the n vs $\dot{n}$ and C vs $\dot{C}$ phase planes have been very useful in this respect.

2.2.7 Reachable zones of the time optimal controlled neutronics

From Figure 2.4 it is seen that for bang-bang control processes, any steady-state condition is reachable from any state with physical constraints of $C \geq 0$, $n \geq 0$ and $|u| \leq \gamma\beta$. Typical trajectories are shown in Figure 2.4 for $\gamma = 0.5$, along with several first quadrant eigenvectors for various values of γ. Note, however, that states to the right of the eigenvector for positive reactivity are not reachable from states to the left of the same eigenvector (e.g., eigenvector B in Figure 2.4). Similarly, states to the left of the eigenvector for negative reactivity (e.g., eigenvector D in Figure 2.4) are not reachable from states

to the right. The eigenvectors of interest are approximated by equation (2.36). Thus the zones which are unreachable are set off by lines whose slopes are approximately proportional to $\frac{1 - \gamma}{\ell}$ for $u = \gamma\beta$, and to $\frac{1 + \gamma}{\ell}$ for $u = -\gamma\beta$. However, any physical limit of $n \leq n_m$ constrains the reachable zones to the left of n_m. In practice, one would not be interested in attaining these unreachable states anyway. In fact, constraints have been applied to guarantee that we can't attain these undesirable states.

These limitations on the reachable zones are also obvious from Figures 2.6, 2.7 and 2.11. For example, in the phase plane of n vs $\dot{n}$, it is not possible to reach states above the line $\dot{n} = (\gamma\beta/\ell)n$ or below the line $\dot{n} = -(\gamma\beta/\ell)n$ from the steady-state and only can these lines be reached with an abrupt change in $u = \pm \gamma\beta$. A small constraint in control velocity further limits the reachable zone to periods somewhere between the eigenvectors of slope given by (2.34) and shown by lines B and D in Figure 2.4. The line of $\dot{C} = 0$ has the equation $\dot{n} = (u/\ell)n$ while $\dot{n} = 0$ requires that $\dot{C} = (u/\ell)n$, but $\dot{n}$ and $\dot{C}$ can only be zero if $u = 0$. From Figures 2.7 and 2.11, it is seen that from states between the eigenvectors only similar states can be reached. Again, the reachable zones are further constrained by the line of constant n_m or $\dot{C} = \beta/\ell\ n_m - \lambda C$. Obviously, zones for negative n or C are physically unreachable. The lines of $n = 0$ and $C = 0$ have slopes of $-\lambda$ and $\frac{-(1 + \gamma)\beta}{\ell}$ in Figures 2.11 and 2.7 respectively. The source term in the neutronics equations (1.32) does increase the reachable zones slightly as shown by Figure 2.8 (e.g., $n = 0$, $C = 0$ can be left in finite time).

In general then, in addition to the mean neutron generation time, the reachable zones are limited by constraints in reactivity and neutron level. These constraints are caused by physical and safety considerations. The eigenvectors in Figures 2.6 and 2.7, however, have their slopes approximated by (2.35). Hence, if the lower limit can be reduced, the unreachable zones below line D in Figures 2.6 and 2.7 and to the left in Figure 2.4 may be further reduced. The mean neutron generation time ℓ, in addition to affecting reachable zones, also affects the switching point of the bang-bang control process. This result is obvious from the effect of ℓ on the indicated eigenvectors in Figure 2.4; i.e., since the slope is approximately inversely proportional to ℓ [see (2.36)] the neutron level at the switching point is also approximately inversely proportional to ℓ. Also from (2.34) and Figures 2.6 and 2.7, the total elapsed time varies directly with ℓ.

The neutronic system is controllable in the sense that any steady-state can be transferred to any other steady-state in finite time (i.e., for $0 \leq n \leq n_m$ and $0 \leq C$). From (2.34), it can be seen that the control variable has little effect on one mode of response for $u \ll \beta$. With the terminal control $u = \ell\dot{C}/n_1$, it is seen from Figure 2.6 that the state $\dot{C} = 0$ is not reachable in finite time.

2.3 Six-precursor group neutron kinetics

The one-energy-group neutron kinetic equations were introduced in Chapter I along with the assumptions made for this classic six-delay group model. For the minimal-time control problems, these equations are repeated below for convenience.

$$\frac{dn}{dt} = \frac{u-\beta}{\ell}\, n + \sum_{i=1}^{6} \lambda_i C_i = \frac{u}{\ell} n - \sum_{i=1}^{6} \dot{C}_i$$

and (2.80)

$$\frac{dC_i}{dt} = \frac{\beta_i}{\ell} n - \lambda_i C_i \quad (i=1,\ldots,6)$$

with

$$|\, u \,| \leq \gamma\beta \text{ and } \beta = \sum_{i=1}^{6} \beta_i \ .$$

The inner product $(\vec{p},\vec{f})$ is

$$R = \frac{u}{\ell} n p_1 + \sum_{i=2}^{7} \dot{C}_{i-1} (p_i - p_1) \ . \tag{2.81}$$

R is again a maximum for the control on the constraint boundary of the allowable control set and hence, for motion evaluated on the interval (t_0, t_1)

$$H(n,C_i;\vec{p}) = \max_{u\in U} R(n,C_i;\vec{p};u) \geq 0 \ . \tag{2.82}$$

The optimal control is again bang-bang with the form of solution given by

$$u^{\circ} = \gamma\beta \ \text{sgn}\ p_1 \tag{2.83}$$

since $n(t) > 0$.

It is necessary that the costate be defined by the adjoint equations:

$$\frac{dp_1}{dt} = \frac{\beta-u}{\ell}\, p_1 - \sum_{i=2}^{7} \frac{\beta_{i-1}}{\ell}\, p_i$$

and (2.84)

$$\frac{dp_i}{dt} = \lambda_{i-1}\ (p_i - p_1), \ i = 2,\ldots,7 \ .$$

Again, the problem of most physical interest is one for which the terminal set is a hypersurface $n = n_1$ in a seven dimensional phase space

while the initial state is usually a fixed point. The costate vector is then orthogonal to the tangent plane of the terminal hypersurface which implies that

$$p_i(t_1) = 0, \quad \text{for } i \neq 1 . \tag{2.85}$$

A computer search for various values of γ with time reversed shows that $p_1(t)$ the solution to (2.84) with u given by (2.83), cannot change sign for $t < t_1$ if (2.85) is satisfied. Hence, there can be no switching in reactivity. Various such transients obtained from an analog computer simulation are shown in Figure 2.12. From (2.85) we see that it is unnecessary to check other terminal magnitudes of p_1 since the value of γ alone determines the form of solution and therefore the number of zeros. This is seen from the solution to (2.84) for a fixed u, $p_1(t_1)\,[a_1 \exp \rho_1(t-t_1) + \ldots + a_7 \exp \rho_7(t-t_1)]$, where t decreases from t_1 and the constant coefficients a_i and ρ_i (i=1,..., 7) depend on u, but are independent of $p_1(t_1)$. Here $p_1(t_1)$ is positive for $u(t_1)$ positive and negative for $u(t_1)$ negative. But there is no change in sign of $p_1(t)$ or switching of u(t).

An analog computer circuit diagram of the neutronics adjoint system which was used to obtain Figure 2.12 is presented in Figure 2.13.

The terminal control required to maintain steady-state conditions at the terminal set $n(t) = n_1$ is obtained from (2.80) with $\dot{n} = 0$. This theoretical terminal control is given by

$$u = \frac{\ell}{n_1} \sum_{i=1}^{6} \dot{C}_i . \tag{2.86}$$

The following analysis shows that with initial steady-state conditions the above terminal control satisfies the inequality constraints, $-\gamma_1 \beta \leq u \leq \gamma_2 \beta$. Inequality constraints are considered to show that the

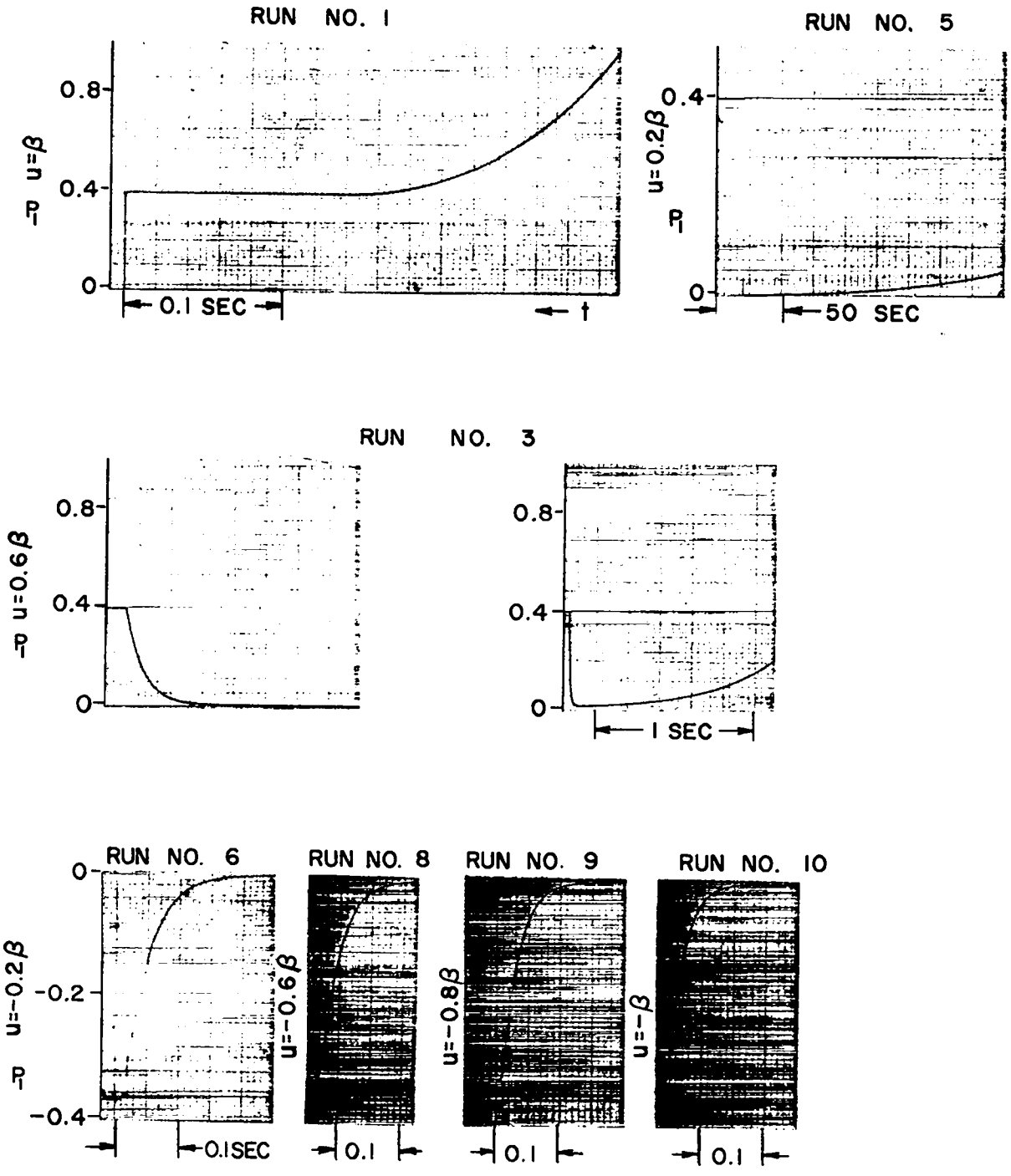

FIGURE 2.12 SIX-DELAY-GROUP NEUTRONIC ADJOINT TRANSIENTS, WITH TIME REVERSED ($t_1 \rightarrow t_0$) AND $p_j(t_1)=0$ $(j=2,\cdots,7)$

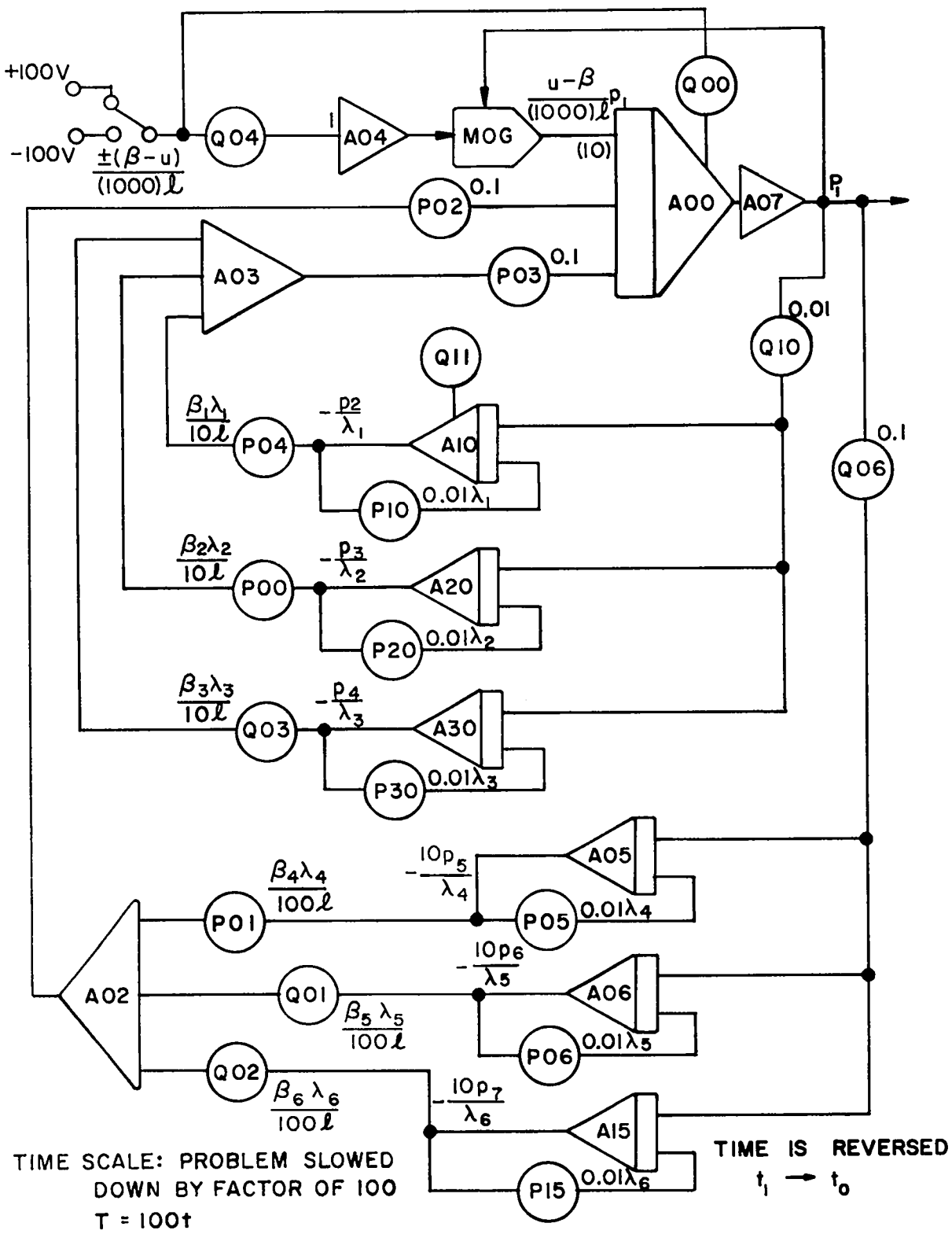

FIGURE 2.13 ANALOG COMPUTER SIMULATION OF THE NEUTRONICS ADJOINT SYSTEM

arguments are general in this respect. The solution to (2.80) for $t_1 < t$ with $n(t) = n_1$ is

$$C_i = \frac{\beta_i}{\ell\lambda_i} n_1 + \left[C_i(t_1) - \frac{\beta_i n_1}{\ell\lambda_i}\right] e^{-\lambda_i(t-t_1)} \quad ; \tag{2.87}$$

then

$$u(t) = \sum_{i=1}^{6} \left[\beta_i - \frac{\ell\lambda_i C_i(t_1)}{n_1}\right] e^{-\lambda_i(t-t_1)} \quad . \tag{2.88}$$

If equation (2.88) is substituted into the control constraint inequality, it is seen that the following relation is necessary for u(t) to belong to the allowable set:

$$-\gamma_1 \le 1 - \frac{\ell}{\beta n_1} \sum_{i=1}^{6} \lambda_i C_i(t_1) \le \gamma_2$$

or

$$(1-\gamma_2) \frac{\beta n_1}{\ell} \le \sum_{i=1}^{6} \lambda_i C_i(t_1) \le (1 + \gamma_1) \frac{\beta n_1}{\ell} \quad . \tag{2.89}$$

Although this condition only shows that u(t) satisfies the constraints at $t = t_1$, it is shown next that the terms enclosed by brackets in (2.88) are all negative or all positive hence proving the inequality at $t = t_1$ proves it for $t > t_1$.

Suppose n and C_i are at steady-state initially and $u = \gamma_2\beta > 0$ for the interval (t_o, t_1). Then, since neutrons are born at a faster rate than they are lost for positive reactivity, $\dot{n}(t)$ is positive. (This is substantiated by the responses given on pages 29-31, Reference 16.) Furthermore, if $\dot{n}(t)$ is positive, and $\dot{C}_i(t_o)$ is zero, each precursor level increases since precursors are born at a faster rate than they decay for positive reactivity. That is $\lambda_i C_i(t) < \beta_i n(t)/\ell$

[or $\dot{C}_i(t)$ is positive] and $C_i(t_1) < [\beta_i n(t_1)]/(\ell\lambda_i)$. Then if $n(t_1) = n_1$,

$$\sum_{i=1}^{6} \lambda_i C_i(t_1) < \frac{\beta n_1}{\ell} ,$$

and certainly

$$\sum_{i=1}^{6} \lambda_i C_i(t_1) < (1+\gamma_1) \frac{\beta n_1}{\ell} .$$

Furthermore, since $\dot{n}(t_1-)$ is positive (for $u = \gamma_2\beta$ from t_0 to t_1), and $n(t)$ and $C_i(t)$ are continuous at $t = t_1$, (2.80) shows that

$$(1-\gamma_2) \frac{\beta n_1}{\ell} < \sum_{i=1}^{6} \lambda_i C_i(t_1).$$

A similar argument can be made for $u = -\gamma_1\beta$ and $n_0 > n_1$. Hence, $\dot{C}_i(t)$ is negative and from (2.87)

$$C_i(t_1) > \frac{\beta_i n_1}{\ell\lambda_i} \quad (i=1,\ldots,6).$$

Then certainly

$$\sum_{i=1}^{6} \lambda_i C_i(t_1) > (1-\gamma_2) \frac{\beta}{\ell} n_1 .$$

Also, since $\dot{n}(t_1-)$ is negative, (2.80) shows that

$$\sum_{i=1}^{6} \lambda_i C_i(t_1) \leq (1+\lambda_1) \frac{\beta n_1}{\ell} .$$

Summarizing these results, the equation

$$(1+\gamma_1)\frac{\beta}{\ell} n_1 > \sum_{i=1}^{6} \lambda_i C_i(t_1) > (1-\lambda_2) \frac{\beta}{\ell} n_1 , \qquad (2.90)$$

is a valid relation for time-optimal increases or decreases in state with steady-state initial conditions. Hence, the terminal control satisfies the required inequality constraints.

The above analyses of this section produce the same results that

were obtained for the single precursor model. Furthermore, in many cases time response of the single-precursor model can closely approximate that of the six-precursor model. A comparison of such optimal responses for six-precursor groups and one-average-precursor group is presented in Figure 2.14. Notice that n(t) is held essentially constant by a multiple bang-bang or dither control process. Such a process is discussed below. Utilization of the arithmetric average decay constant shows that there is hardly any noticeable difference for such fast transients. If slower transients are of interest, it is necessary to reduce the average λ in order to closely approximate the reactor neutron kinetics. Then one would generally expect the optimal-control analysis of the one-average-precursor-group model to apply to the actual six-precursor-group system.

2.4 Terminal control synthesis

It has been shown that the theoretical control required to maintain a constant terminal neutron level $n(t) = n_1$ is $u = \lambda \sum_{i=1}^{6} \dot{C}_i / n_1$. Such a variation in reactivity, however, is open loop and cannot be implemented in practice due to errors in measurement and synthesis.

If there exists a small error in the measurement of n, then the following analysis shows a divergence in neutron level. Suppose the error in the measurement is represented by Δn, and the theoretic terminal control can be engaged in zero time at $t = t_a$. The one-delay-group neutronics approximation with $u = \lambda \dot{C}/n_1$ is

$$\frac{dn}{dt} = \dot{C} \left(\frac{n}{n_1} - 1\right) \tag{2.91}$$

for $t_a \leq t$. Let $n = n_1 + \Delta n$ and $C = C_1(t) + \Delta C$. Then neglecting

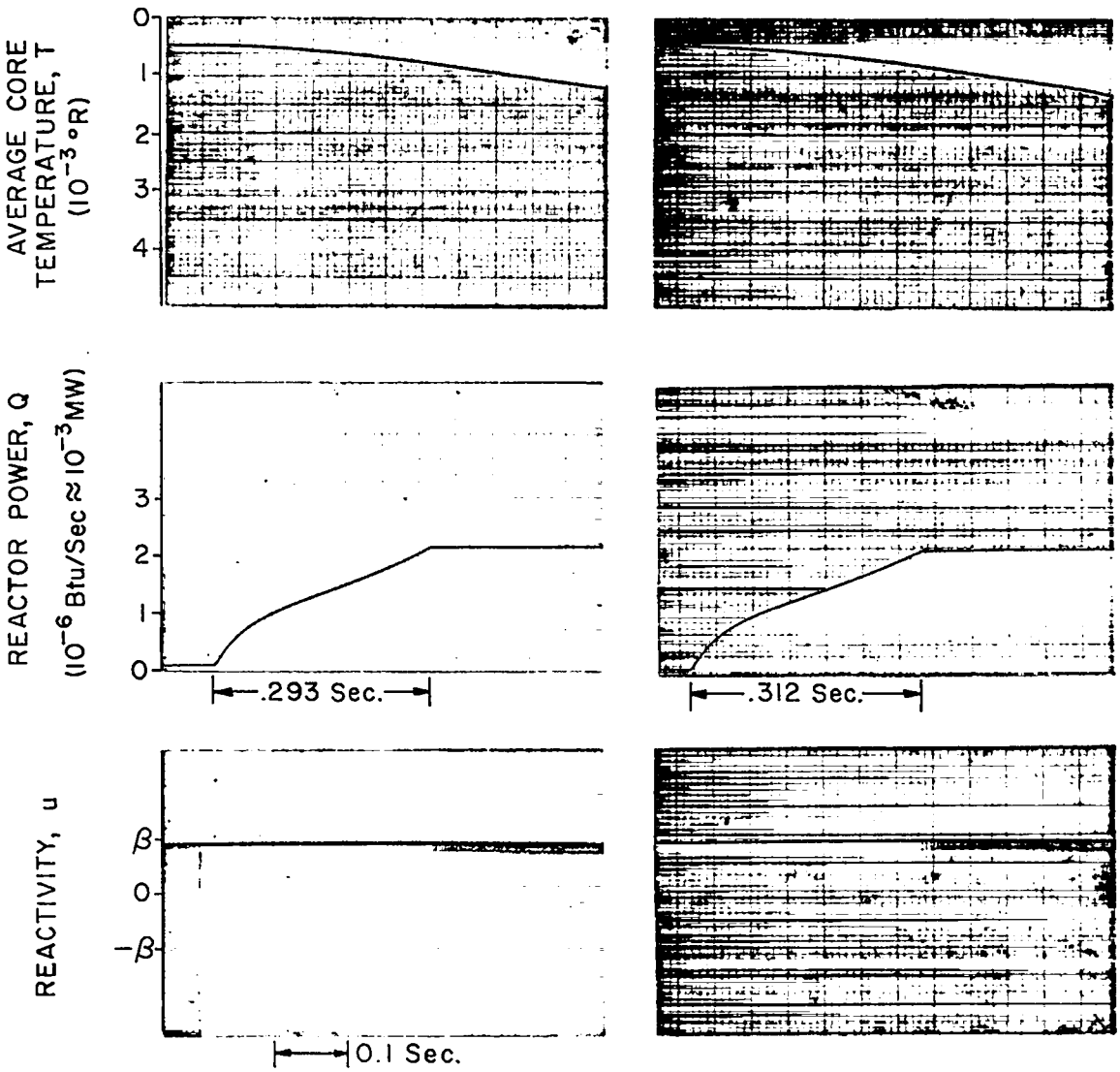

$\lambda = 0.4\ \text{Sec}^{-1}$

$u = 0.9\beta$ for $Q < Q_1 = 2.2(10)^6$ Btu/Sec.

$Q \propto n$

FIGURE 2.14 COMPARISON OF TIME-OPTIMAL CONTROLLED NEUTRONICS

second-order terms (2.91) becomes

$$\Delta\dot{n} \approx \frac{\dot{C}_1}{n_1}\,\Delta n \quad , \tag{2.92}$$

which has the following solution:

$$\Delta n \approx \Delta n_a \exp\left\{\frac{1}{n_1}\left[C_1(t) - C_{1a}\right]\right\} , \tag{2.93}$$

where $\Delta n_a = n(t_a) - n_1$ and $C_{1a} = C_1(t_a)$. From (2.28) the response in precursor level $C_1(t)$ due to the theoretical terminal control is

$$C_1(t) = \frac{\beta}{\ell\lambda} n_1 + \left(C_{1a} - \frac{\beta}{\ell\lambda}\, n_1\right) e^{-\lambda(t-t_a)} . \tag{2.94}$$

If (2.93) is approximated by the linear terms of a Taylor series for small $[C_1(t)-C_{1a}]/n_1$,

$$\Delta n \approx \Delta n_a \left[1 + \frac{C_1(t)-C_{1a}}{n_1}\right] . \tag{2.95}$$

Hence, one might expect the divergence in neutron level to vary in a manner similar to the variation in precursor level for small changes in $\Delta n(t)$ and $C_1(t) - C_{1a}$. The following argument, however, shows that for certain conditions the divergence of $\Delta n(t)$ may be described by a time constant that is smaller than $1/\lambda$.

Consider (2.94) for $(t-t_a) \ll 1/\lambda$:

$$C_1(t) = \frac{\beta}{\ell\lambda} n_1 + \left(C_{1a} - \frac{\beta}{\ell\lambda} n_1\right)[1-\lambda(t-t_a)+\ldots]$$

or

$$C_1(t) \approx C_{1a} + \left(\frac{\beta}{\ell\lambda}\, n_1 - C_{1a}\right)\lambda(t-t_a).$$

Then, from (2.93)

$$\Delta n \approx \Delta n_a \exp\left[(\beta/\ell\lambda - C_{1a}/n_1)\lambda(t-t_a)\right] \quad . \qquad (2.96)$$

At equilibrium $C = (\beta/\ell\lambda)n$, but thereafter n(t) increases faster than C(t) for positive reactivity (e.g., see trajectory a-b, Figure 2.4) and decreases faster for negative reactivity. Equation (2.36) and Figure (2.4) show that if n_1 is much larger than n_o then $\beta/\ell\lambda$ is much more than C_{1a}/n_1. For example, consider trajectory a-b-f in Figure 2.4 with C at point b equal to C_{1a}. Using the approximations for (2.36) $C_{1a}/n_1 \approx (1-\gamma)\beta/\ell\lambda$. Hence the rate of divergence of $\Delta n(t)$ depends on C_{1a}/n_1, but for $n_1 >> n_o$ the divergence can be considerably faster than that predicted by (2.95). Such an instability is not surprising since the basic problem is the failure of an open-loop control. The same problem exists in attempting to maintain constant n(t) with steady-state initial conditions.

The failure of this control is shown more accurately by Figure 2.15. These various power transients were obtained from an analog computer simulation for very small changes in the constant term of the theoretical terminal control. The initial dropoff or rise in power ∩ (when terminal control is engaged) is due to negative or positive Δn_a, as explained by (2.96). The subsequent long-period rise, however, is due to the reactivity not decaying to zero as it should, but decaying to a small positive value due to inaccuracies in computer equipment. (It could just as well be negative, in which case Q would would finally decrease exponentially.) In a similar manner, analog computer solutions show that use of n(t) instead of n_1 in the denominator of the terminal control yields an unstable solution.

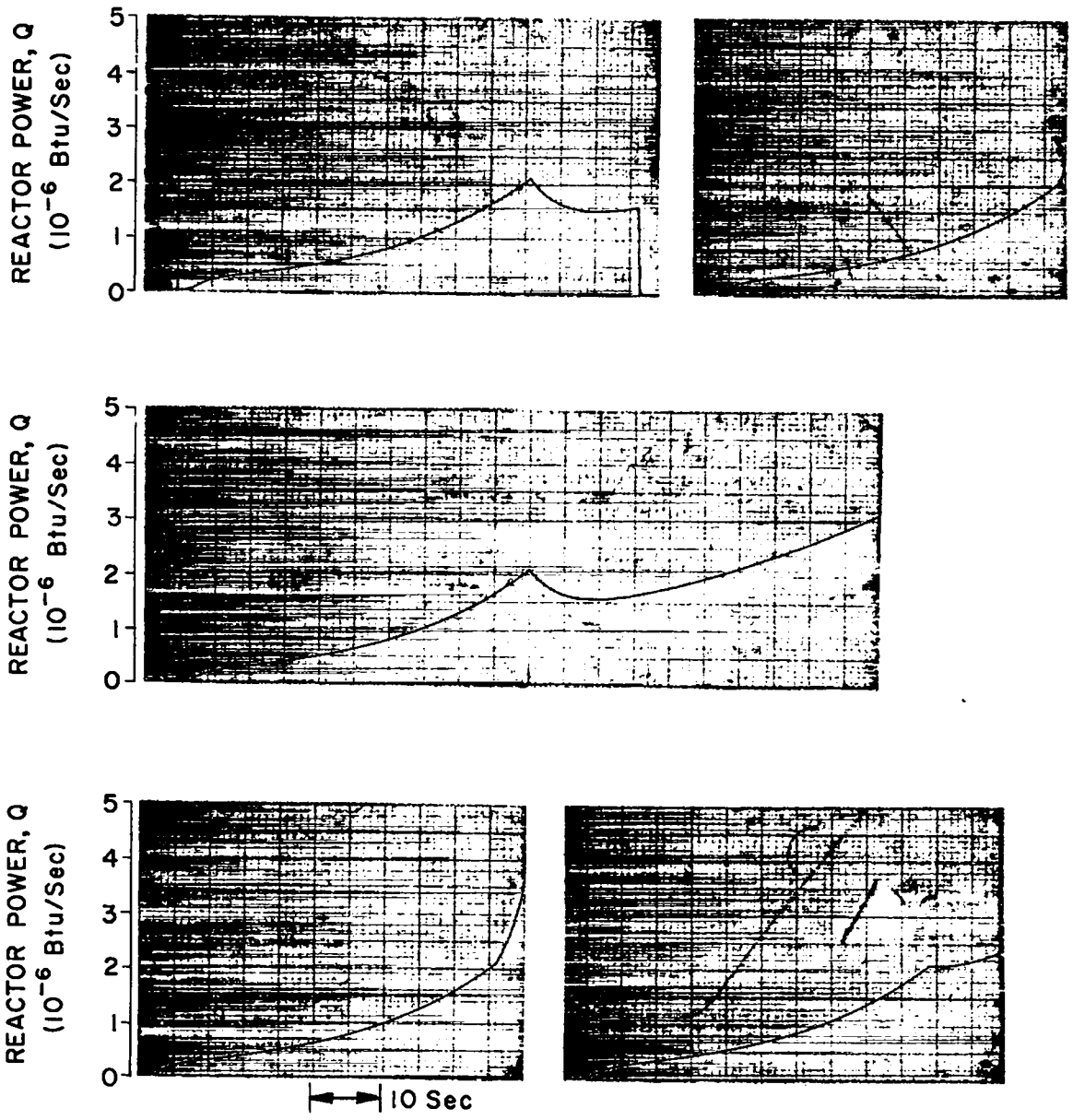

FIGURE 2.15 FAILURE OF THE THEORETICAL TERMINAL CONTROL POWER RESPONSE DUE TO SMALL CONTROL SYSTEM ERRORS ($\ell = 3(10)^{-4}$, $\gamma = 0.4$ AND SIX PRECURSOR MODEL)

The terminal control for the simulation shown in Figure 2.15 was switched into the simulation (which has time slowed down by a factor of ten) by a fast acting differential relay system. This relay system has a frequency variant hysteresis characteristic, which is shown in Figure 2.16. The input to the differential relay was a sawtoothed wave of various frequencies, for the results shown in Figure 2.16. Just as this characteristic enters into the simulation, it could enter into the actual control synthesis of a physical reactor.

Since failure of the theoretic terminal control may be attributed to its open-loop nature, closed-loop control should certainly be investigated. Such control is studied below in Section 2.5 but for the moment consider a control which is more closely related to the above theoretic terminal control.

Although the theoretic terminal control is unstable, intuitively it might be expected that a multiple bang-bang type of control (which switches to values above and below the theoretical value) is worth investigation. The following discussion presents an example of such control, which was successfully tested on an analog computer and is called a dither control process. For a time-optimal startup followed by such a dither process, reactivity should be $\gamma\beta$ until $n(t) = n_1 + \Delta$, where 2Δ is a predetermined amount of hysteresis (see Figure 2.17) of very small positive magnitude. At this time reactivity switches to a low approximation to the theoretically required process [i.e., $u(t)$ is smaller than but approximately defined by (2.86)] until $n(t) = n_1 - \Delta$. Then reactivity is switched to $\gamma\beta$ again and the process continues

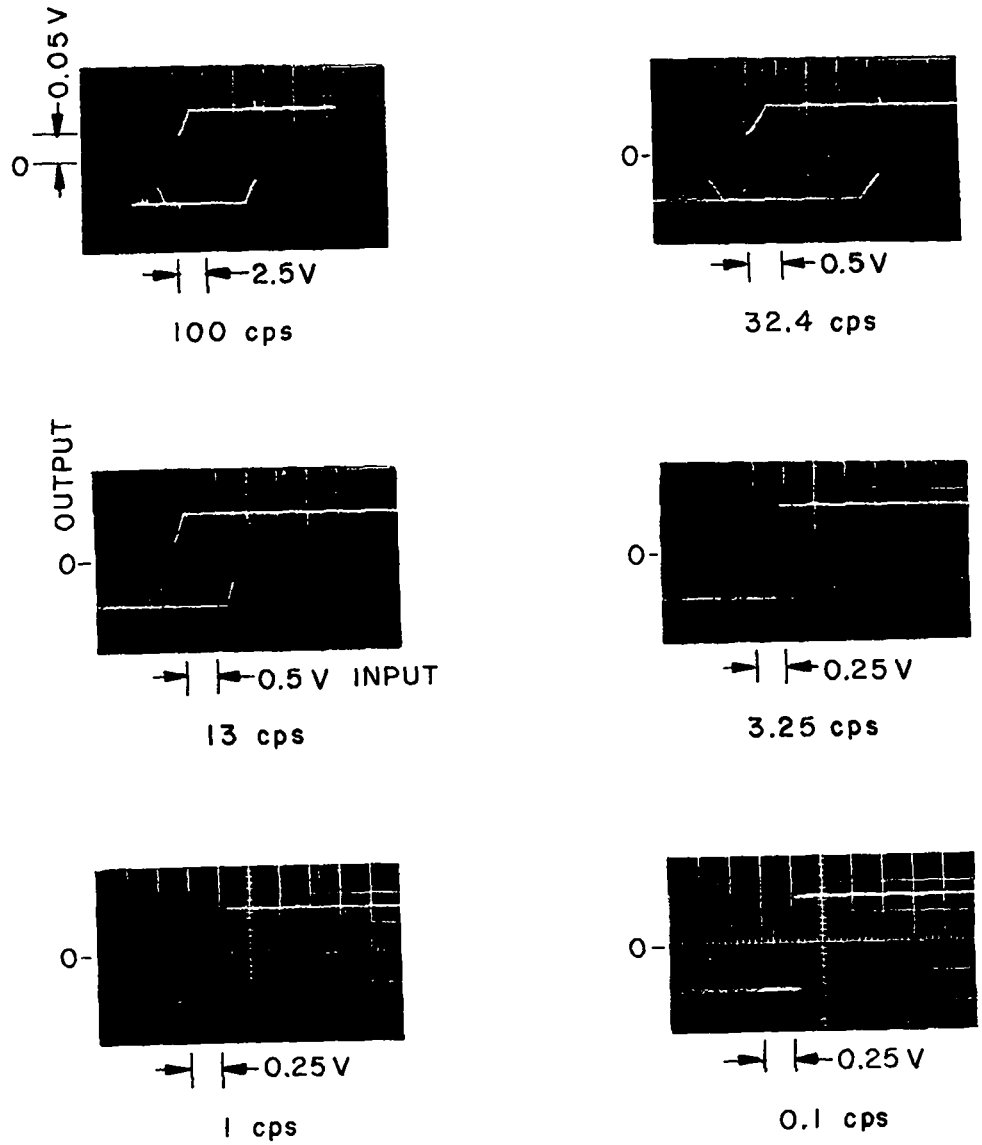

INPUT VOLTAGE IS A SAW-TOOTHED WAVE, 15.6 VOLTS PEAK TO PEAK, WITH THE FREQUENCY INDICATED

FIGURE 2.16 RELAY-HYSTERESIS CHARACTERISTIC UTILIZED IN TERMINAL CONTROL STUDIES

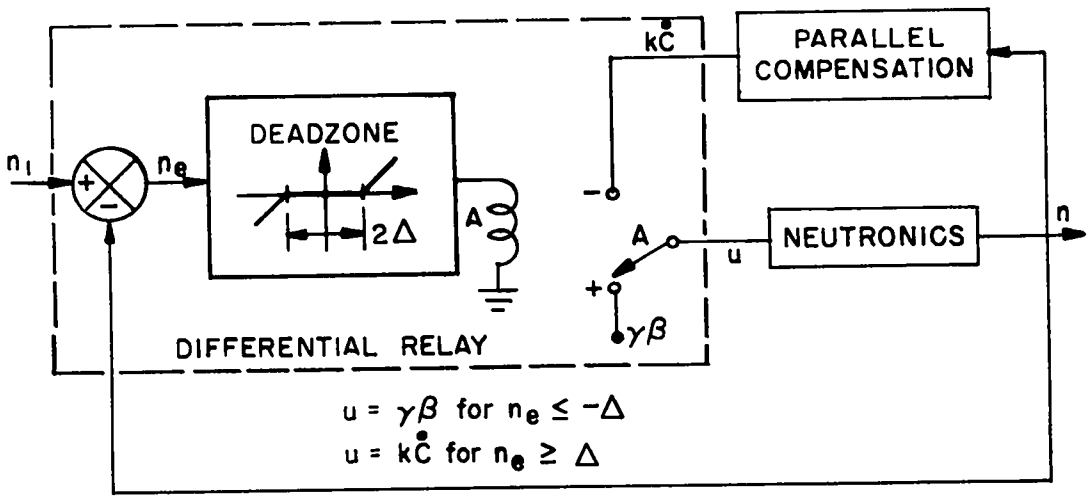

ANALOG COMPUTATION OF $k\dot{C}$ (PARALLEL COMPENSATION)

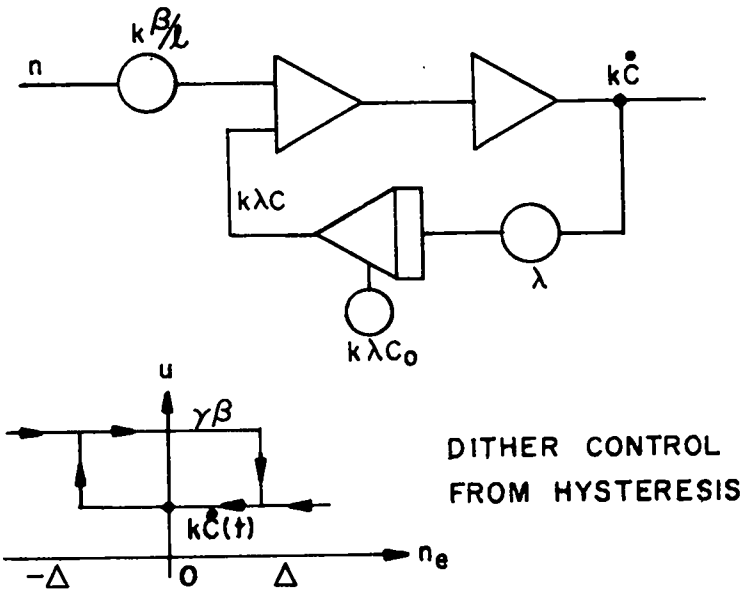

DITHER CONTROL FROM HYSTERESIS

FIGURE 2.17 SYNTHESIS OF THE NEUTRONIC TIME-OPTIMAL STARTUP CONTROL PROCESS (WITH A DITHER TERMINAL CONTROL)

repeatedly. The synthesis of this control process (which utilizes a differential relay with hysteresis is presented in Figure 2.17.

During the dither process, relay A in Figure 2.17 oscillates between the positive and negative positions. That is, relay A is in the positive position with $u = \gamma\beta$ for $n_e \leq -\Delta$ and in the negative position with $u = k\dot{C}$ for $n_e \geq \Delta$. k is set so that the parallel compensation output $k\dot{C}$ is slightly lower than that of the theoretic control. The dither process as it results from hysteresis in the differential relay is shown at the bottom of Figure 2.17.

Typical reactivity pulses and power transients of such an actual dither process, as obtained using the analog computer to mechanize Figure 2.17, are shown by Figures 2.18 and 2.19. Although finite switching time was not discussed above, it is included in this synthesis of the dither process. The simulation was slowed down by a factor of ten (from that of the original simulation) in order to study the frequency variant effect of the relay system. It is seen that power variations are reduced considerably by slowing down the problem and effectively decreasing the hysteresis. The hysteresis characteristic of the differential relay is presented in Figure 2.16. The lack of symmetry of the reactivity pulses in Figure 2.18 is caused by the spring forcing of the relay in one direction and the magnetic forcing in the opposite direction. Application of solid-state devices to the synthesis of such a physical system would be very desirable.

The results of analog computer simulated time-optimal startups have been shown by Figures 2.9 and 2.14. Both of these systems actually utilized the dither terminal control system to maintain a neutron

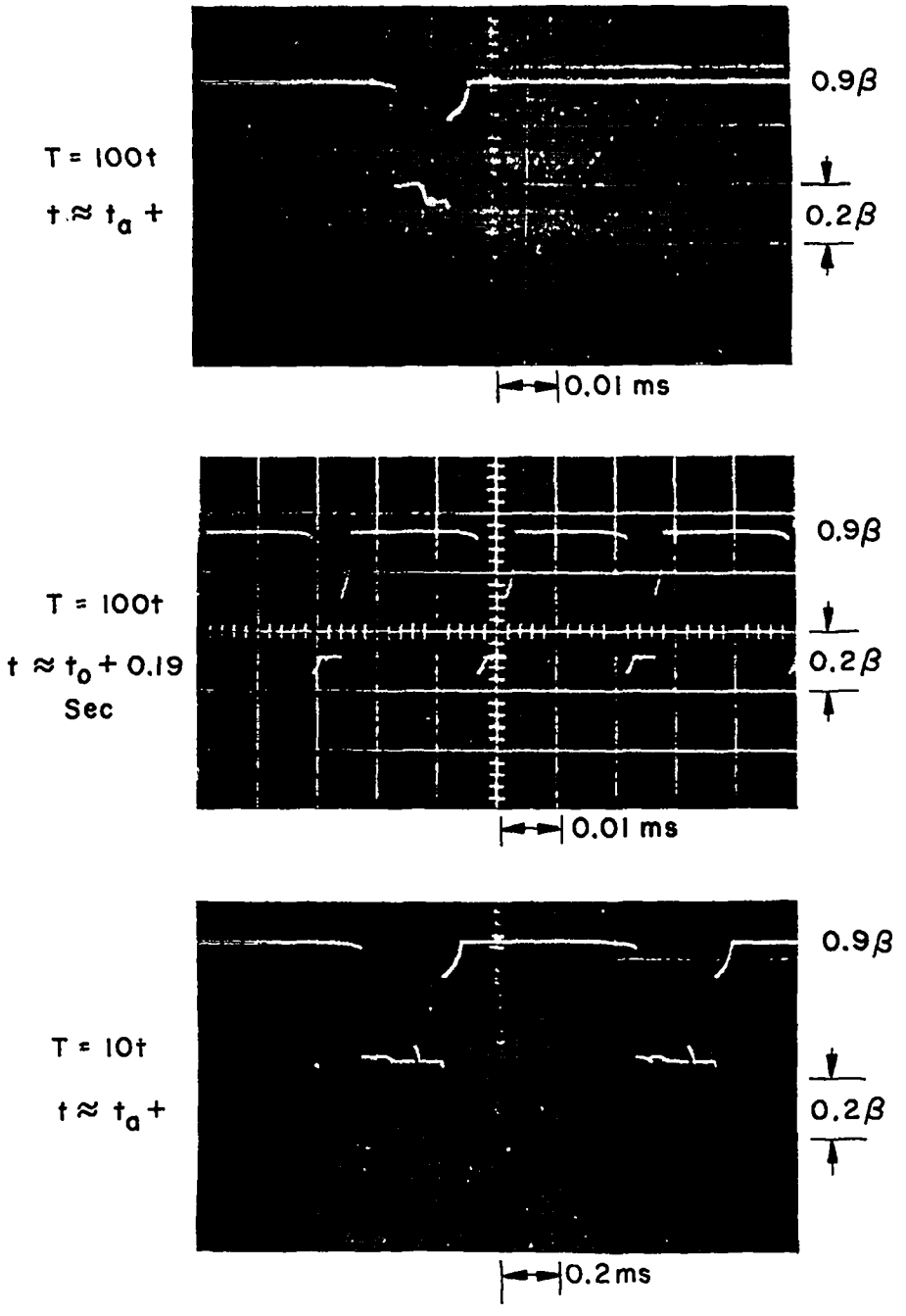

T = COMPUTER TIME
t_a = TIME AT WHICH DITHER CONTROL IS ENGAGED
REAL TIME IS INDICATED ON ALL GRAPHS
TIME INCREASES FROM RIGHT TO LEFT

FIGURE 2.18 TYPICAL REACTIVITY PULSES DURING TERMINAL DITHER CONTROL

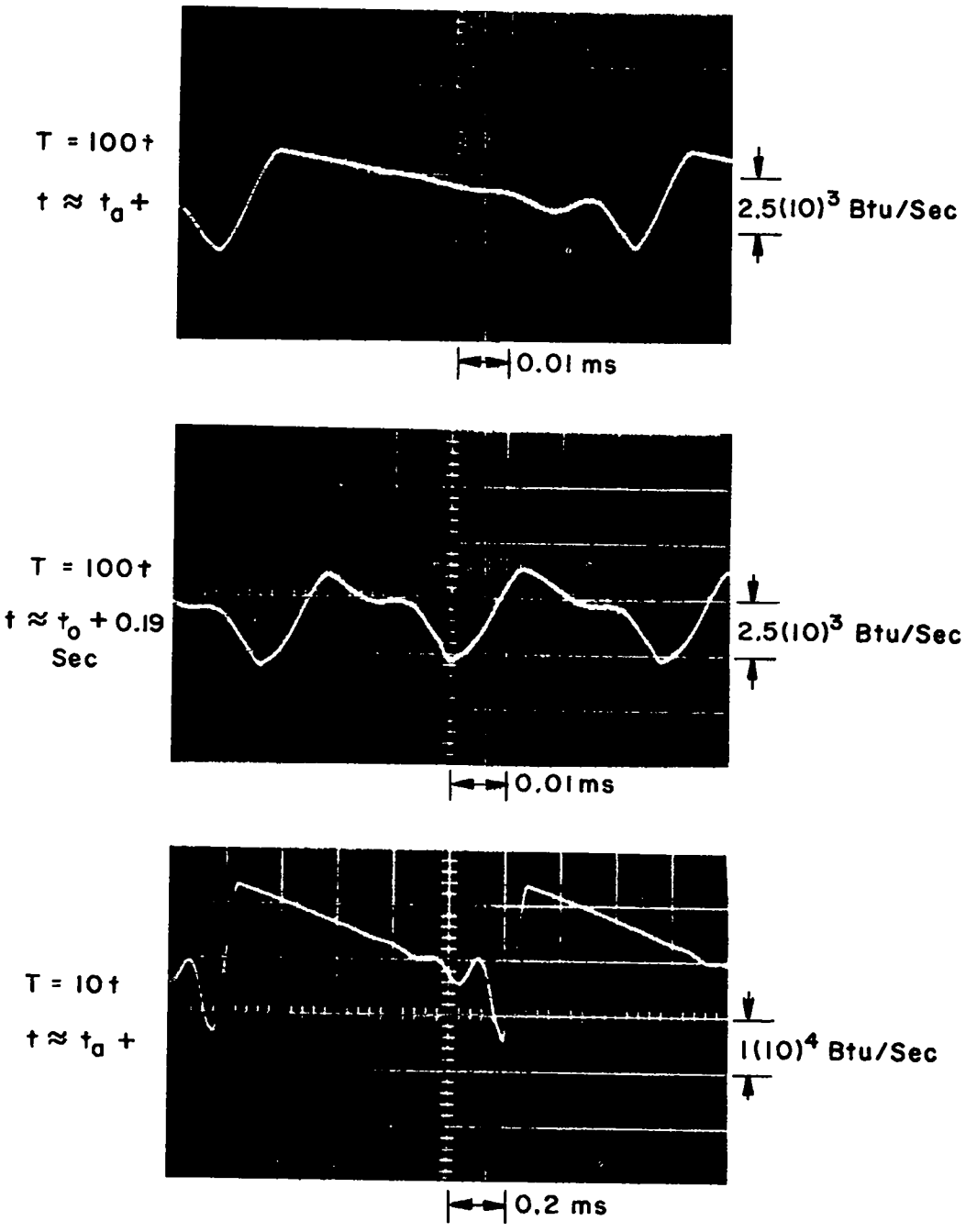

T = COMPUTER TIME
t_a = TIME AT WHICH DITHER CONTROL IS ENGAGED
REAL TIME IS INDICATED ON ALL GRAPHS
TIME INCREASES FROM RIGHT TO LEFT

FIGURE 2.19 TYPICAL REACTOR POWER PULSES DURING TERMINAL DITHER CONTROL

density that is essentially constant; only the theoretical control, however, is recorded in Figure 2.9.

2.5 Optimal control and conventional control

The key to the synthesis of the time-optimal control appears to be the ability to maintain neutron density essentially constant while the precursor level is not near steady-state.

Although the bang-bang neutronic control is synthesized very simply, the required terminal control is slightly more complicated. In many cases a conventional type of closed-loop control is satisfactory and may even approach the performance of the optimal process. Even for these cases, however, the optimization analysis provides a yardstick of performance. One convenient technique of approximating the optimal process is to synthesize a continuous feedback control system which is fast acting but limited in control variations. The startup of such a system is shown in Figure 2.20. Initially, the system is at steady-state with a neutron level of less than one-twentieth of the terminal level. Then 0.9$ of reactivity is added until the neutron level is about one-eighth of the terminal value. At that time, a proportional-plus-integral type of feedback controller replaces the constant control process. The controller was introduced at that time to limit the magnitude of the controller integral signal. (Below, in Section 2.5.1, it is shown that by controlling the log of power the loop may be closed for the entire run. Also, if integral control were limited separately, a limited effort proportional-plus-integral control could probably be introduced immediately.) This controller is defined as follows:

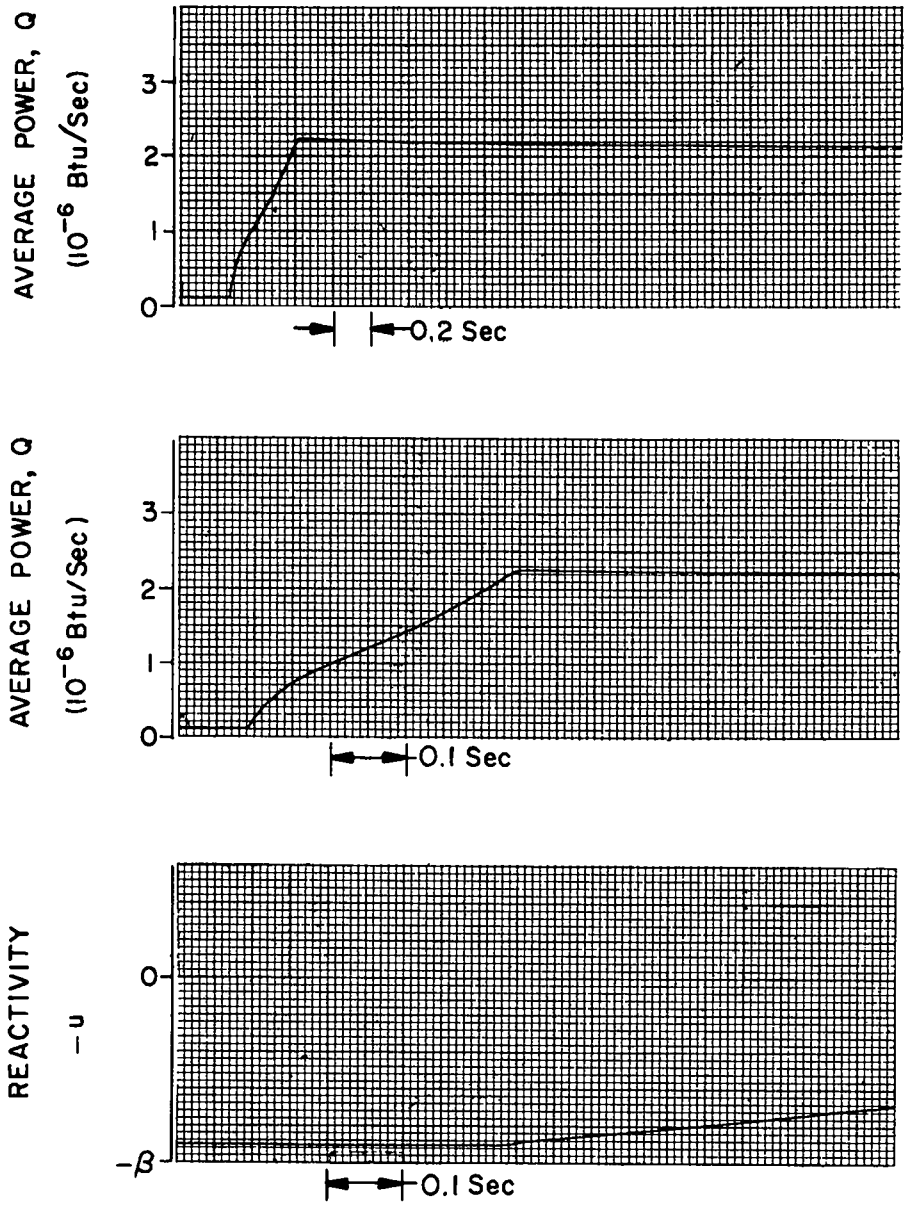

CONSTRAINT: $u \leq 0.9\beta$

FIGURE 2.20 BANG-BANG CONTROLLED NEUTRON KINETICS WITH A CONTINUOUS TERMINAL CONTROL

$$u = 1.87\ (10)^{-9}\ Q_e + 6.24\ (10)^{-9} \int^t Q_e\ d\sigma\ , \qquad (2.97)$$

where $Q_e = Q_1 - Q$ Btu/sec and $Q \propto n$. Due to the high gain of the system, the reactivity stays at its constrained value of 0.9β until the terminal state is approached. After this small rise time, Q(t) has a small overshoot followed by a slow decay toward the desired steady-state value. The slow decay is caused by the slow birth of precursor neutrons. For most applications such small overshoot is insignificant and this simple suboptimal closed-loop control could be utilized. Nevertheless, the dither terminal control (as shown in Figure 2.14) maintains constant power more accurately.

The describing function N for the simple limiting nonlinearity is given in Table 2.2[23]. Then Figure 2.21 presents Nyquist plots of the open-loop transfer function. The limiting nonlinearity is represented by the critical-point locus, -1/N(A). Transfer functions of changes in power with respect to both changes in reactivity [plot (a)] and changes in power error [plot (b)] are plotted there. Sketches (a) and (b), shown at the top of Figure 2.21, approximate $\Delta Q/\Delta u(j\omega)$ and $\Delta Q/\Delta Q_e(j\omega)$ mappings of the s-plane contour shown in sketch (c). Sketch (a) also approximates the shape of $\Delta Q/\Delta Q_e(j\omega)$ for proportional control. Applying the Nyquist stability criterion (with the -1 point replaced by -1/N in Figure 2.21) indicates that the system cannot have a limit cycle.

The transient response of a system with only proportional control is presented in Figure 2.22. In this case, the simple control was carefully engaged at the desired terminal power but due to the precursor neutrons the error again approaches zero very slowly. The lack of

Table 2.2 Describing function for reactivity limiting[23].

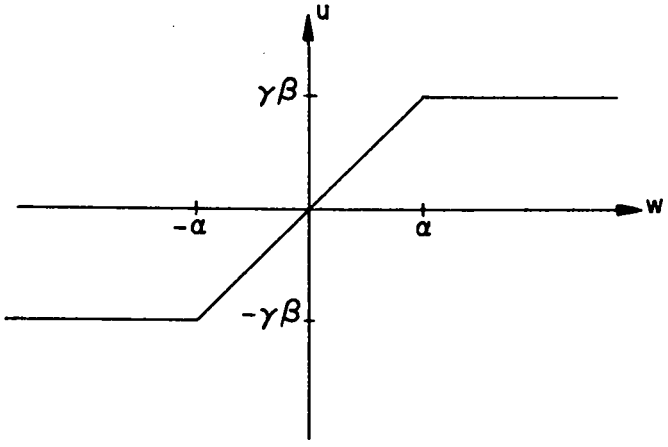

$N(A) = \frac{\gamma\beta}{\alpha}$ for $w < \alpha$

$N(A) = \frac{\gamma\beta}{\pi\alpha}(2\Phi+\sin 2\Phi)$, for $w > \alpha$

where

A = amplitude of input sine wave

w = input

u = limited reactivity

$\Phi = \arcsin(\alpha/A)$

A/α	$N(A) \times \alpha/\gamma\beta$	$\frac{1}{N(A)}$ for $\alpha=\gamma\beta$
0 to 1	1.0	1.0
1.5	0.76	1.32
2.0	0.6	1.67
3.0	0.42	2.38
4.0	0.32	3.1
6.0	0.22	4.54
8.0	0.16	6.25
10.0	0.12	8.33
20.0	0.064	15.6
50.0	0.0255	39.2
100.0	0.0127	78.5

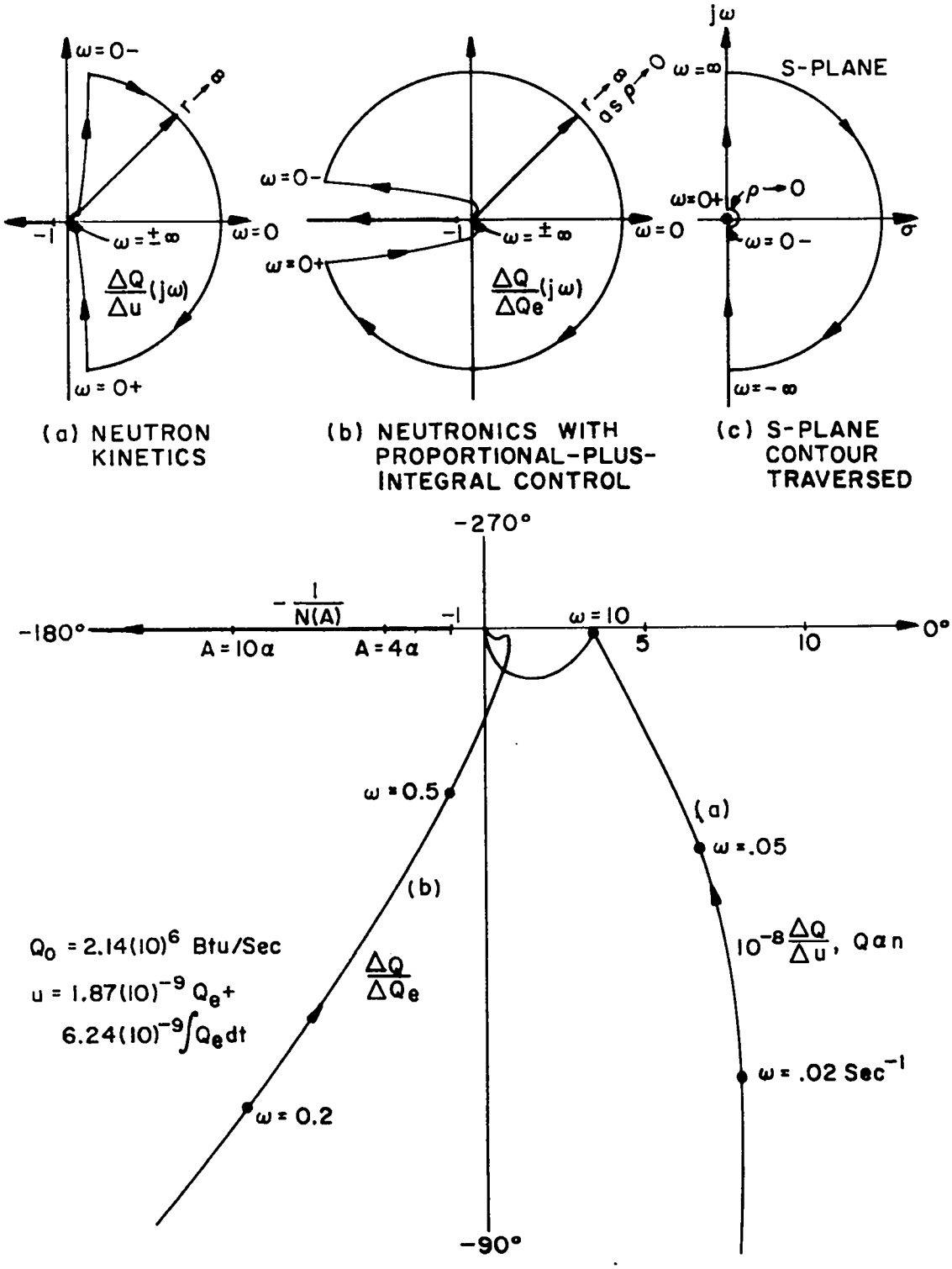

FIGURE 2.21 FREQUENCY RESPONSE OF AN OPEN-LOOP NEUTRONIC CONTROL SYSTEM – SHOWING EFFECT OF REACTIVITY LIMITING (SIX PRECURSOR MODEL)

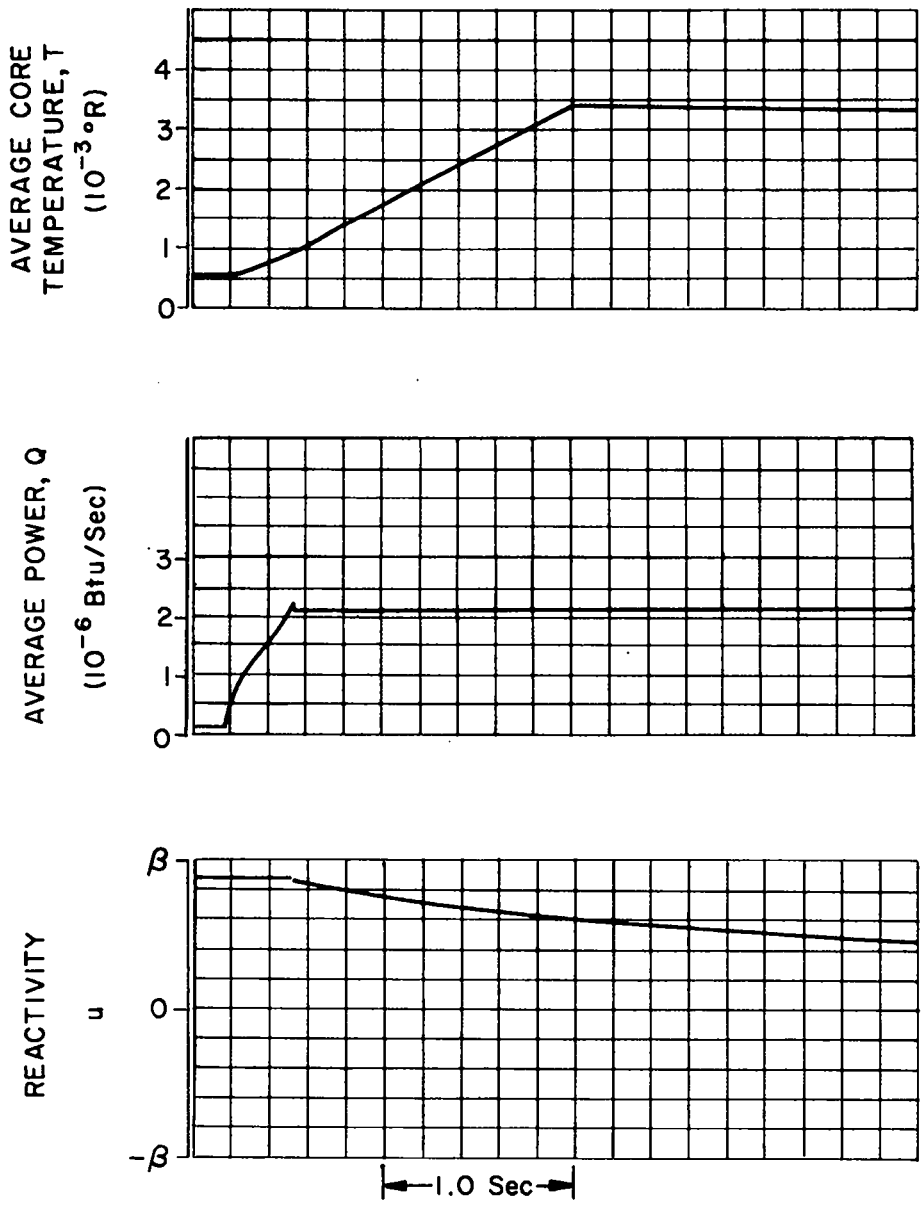

CONSTRAINT: $u \leq 0.9\beta$

FIGURE 2.22 BANG-BANG CONTROLLED NEUTRONICS WITH A PROPORTIONAL TERMINAL CONTROL

integral control causes the residue of this slow mode to be slightly larger and its response slower than that of Figure 2.20. Notice, however, that Figure 2.21 shows that the neutron kinetics with simple proportional closed-loop control is more stable than if the system is controlled according to (2.97).

In addition to the usual precautions, which must be taken in making conclusions based on describing-function analysis, it should be realized that the neutron kinetics as defined by (2.28) represent a structurally unstable system[24] (i.e., any small change in reactivity from zero, changes the qualitative phase behavior). At zero reactivity, the neutronics phase plane shown in Figure 2.4 has a border-line sort of portrait and there exists a line of equilibrium points. Similarly, for the six-delay-group neutronics there exists an equilibrium line in a seven-dimension phase space. For a slight positive reactivity the C vs n portrait is characteristic of a saddle point and for a slight negative reactivity the phase-plane portrait is characteristic of a stable-node type of behavior. For the problems considered here however, the response is of such short duration that the transfer-function analysis is a good approximation. Furthermore, the describing function approach is a valid approximation since (1) the limiting non-linearity is time invariant and (2) harmonics greater than the first are attenuated.

Although an average core temperature is computed in the analog computer simulation and shown in Figures 2.14 and 2.22, no reactivity coupling was considered at this time. Coolant mass flow rate was held at a minimum constant value but was increased to maintain steady-state at the terminal point. Such variations in flow rate will be discussed

as optimal in Chapter III. Notice that the temperature transient indicates a desirable type of response.

Figure 2.23 shows that the dither control is adequate for a start-up time as low as 9 ms, where the terminal power is again more than twenty times the initial power.

2.5.1 Time-optimal, suboptimal logarithmic, and conventional logarithmic control of a Kiwi-B system

The variations in dynamic behavior of the neutron kinetics with neutron level n or power level Q, may be seen crudely from a transfer function of the linearized neutron kinetics[16]. This function is

$$\frac{\Delta Q}{\Delta u} = \frac{Q_o \prod_{i=1}^{6} (s+\lambda_i)}{\ell \, s \prod_{i=1}^{6} (s+r_i)} \quad ;$$

where Δu is a perturbation about zero reactivity which causes a power perturbation, ΔQ, about some steady-state power Q_o; s is the Laplace transform complex variable; and r_i locates the poles of the transfer function. By feeding back the logarithm of power, the dynamics are roughly independent of power as shown by

$$\frac{\Delta \log Q}{\Delta u} = \frac{\Delta Q/Q_o}{\Delta u} \quad .$$

Using this type of control, conventional design procedures provide good performance for extremely low powers as well as for high power levels. In this section logarithmic proportional-plus-integral control is compared to a time-optimal process.

A Nyquist plot [see Figure 2.21, plot (b)], indicates that stability of closed-loop neutronic systems, which employ proportional-plus-integral control, increases with loop gain. Systems with high gain, however, require more reactivity than those of low gain and as

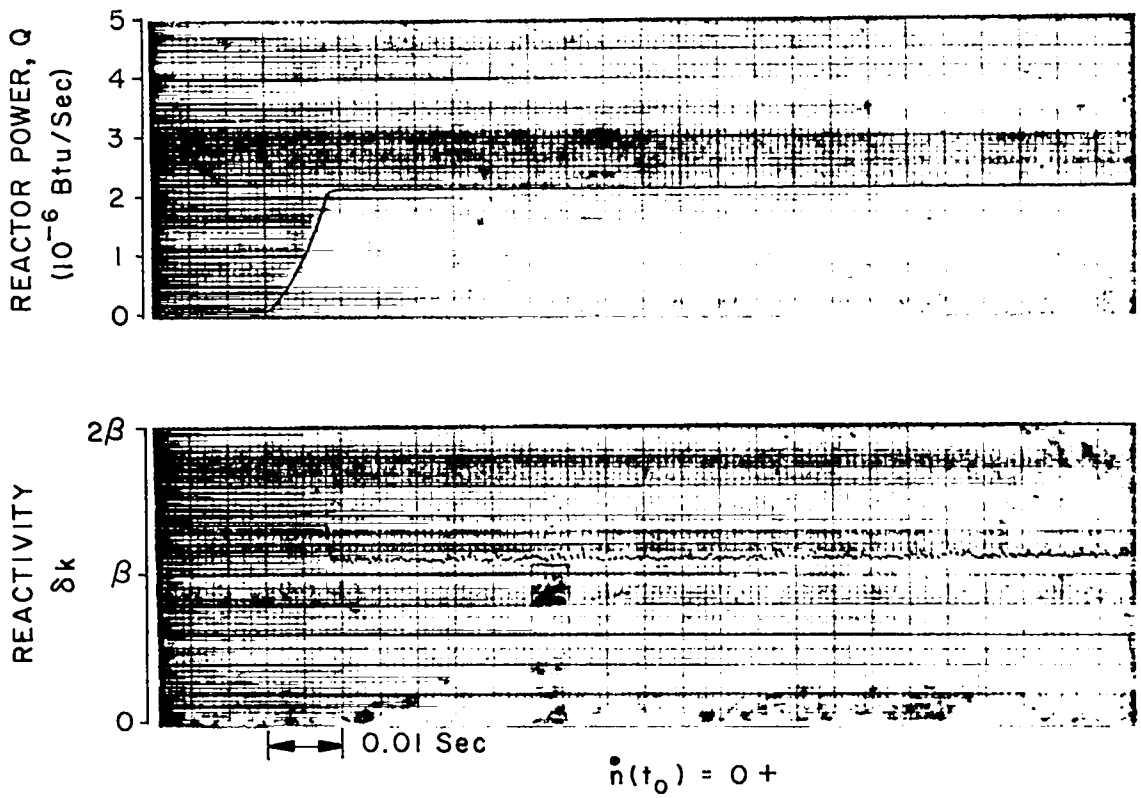

FIGURE 2.23 TIME-OPTIMAL CONTROLLED NEUTRONICS WITH $\gamma = 1.3$ AND DITHER TERMINAL CONTROL

discussed previously, reactivity should be limited for safety reasons. For nuclear rockets, a limit of 0.9β is a safe constraint.

Various logarithmic proportional-plus-integral controller designs are shown by Table 2.3. Then Figures 2.24 and 2.25 present startup data for a Kiwi-B (nuclear rocket test reactor) system which uses these closed-loop control systems. In all cases, logarithmic power demand is stepped from steady-state log Q_o to about log 24 Q_o at the initial time. Figures 2.24 and 2.25 are plotted against such a slow time scale so that the slow mode of response may be examined. These data are compared below to time-optimal startups shown in Figure 2.26.

Table 2.3 - Controller gains for data presented in Figures 2.24 and 2.25

Run No.	Proportional Gain k_p	Integral Gain k_i, sec^{-1}
1	$6.5\ (10)^{-3}$	$1.3\ (10)^{-4}$
2	$3.25\ (10)^{-3}$	$3.9\ (10)^{-4}$
3	$5.71\ (10)^{-4}$	$1.17\ (10)^{-2}$
4	$2.6\ (10)^{-3}$	$2.6\ (10)^{-2}$
5	$3.25\ (10)^{-3}$	$6.5\ (10)^{-3}$
6	$6.5\ (10)^{-3}$	$3.25\ (10)^{-3}$

Control Equation:

$$\delta k = k_p \log_{10} Q_d/Q + k_i \int^t \log_{10} Q_d/Q \, d\sigma$$

The minimal-time startup with $u = 0.9\beta$ is given in Figure 2.26 and requires about 0.12 sec to increase power by a factor of twenty four. Again, in Figure 2.26, the desired terminal power is maintained

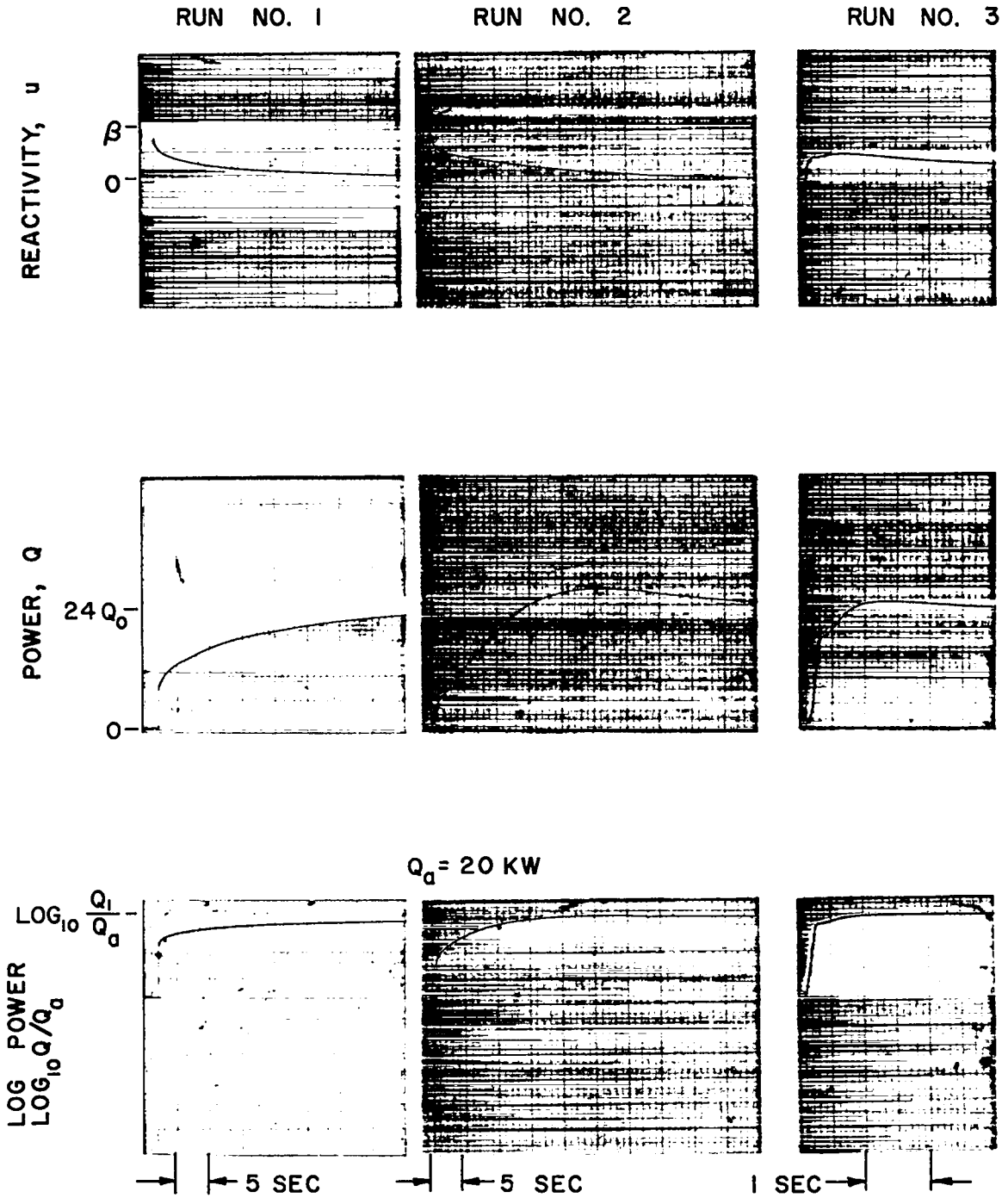

CONTROLLERS ARE GIVEN IN TABLE 2.3

FIGURE 2.24 CLASSICAL LOGARITHMIC POWER CONTROLLED STARTUP OF A KIWI-B NEUTRON KINETICS

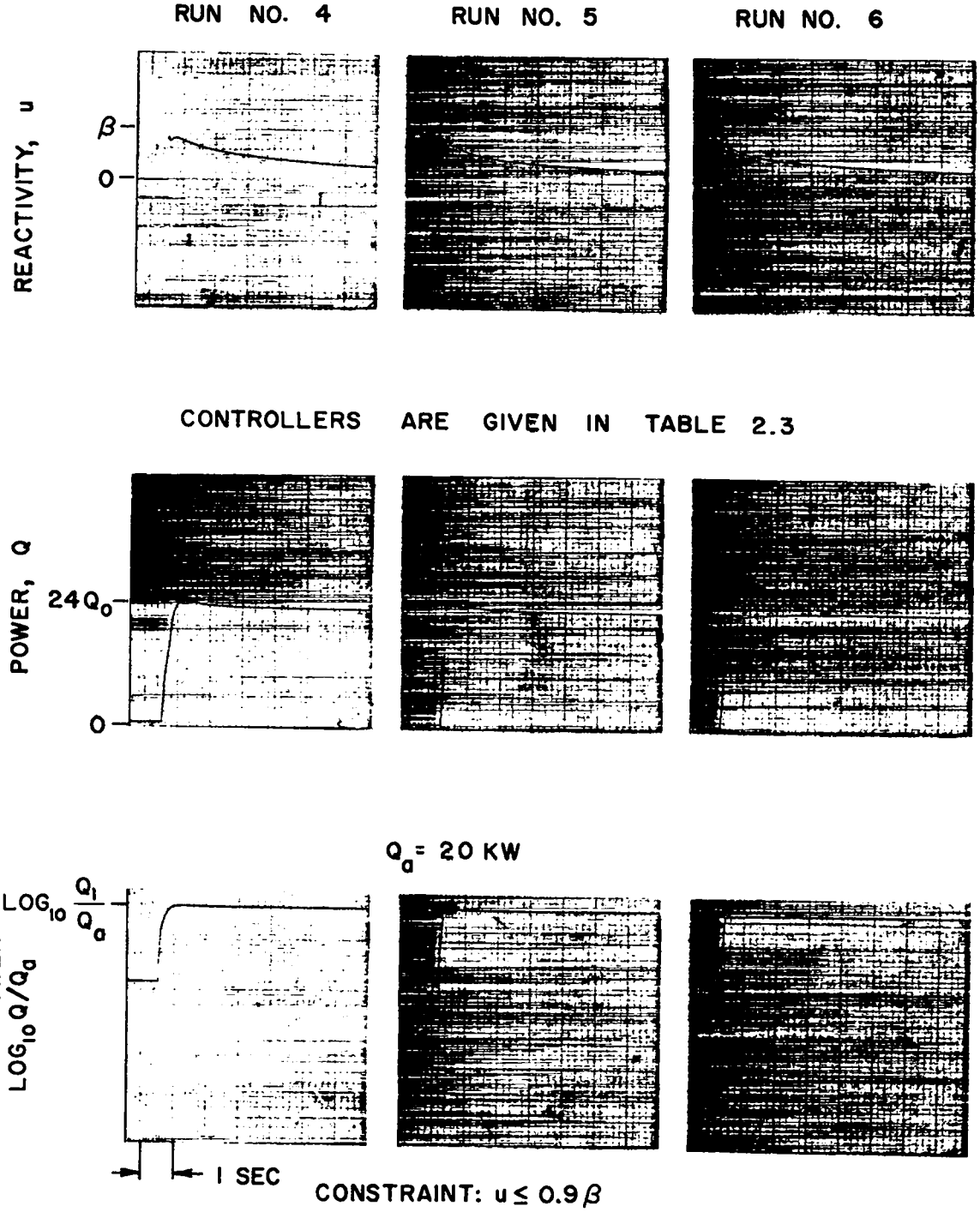

FIGURE 2.25 SUBMINIMAL-TIME STARTUPS OF A KIWI-B NEUTRON KINETICS WITH VARIOUS CLOSED-LOOP LOGARITHMIC POWER CONTROLLERS

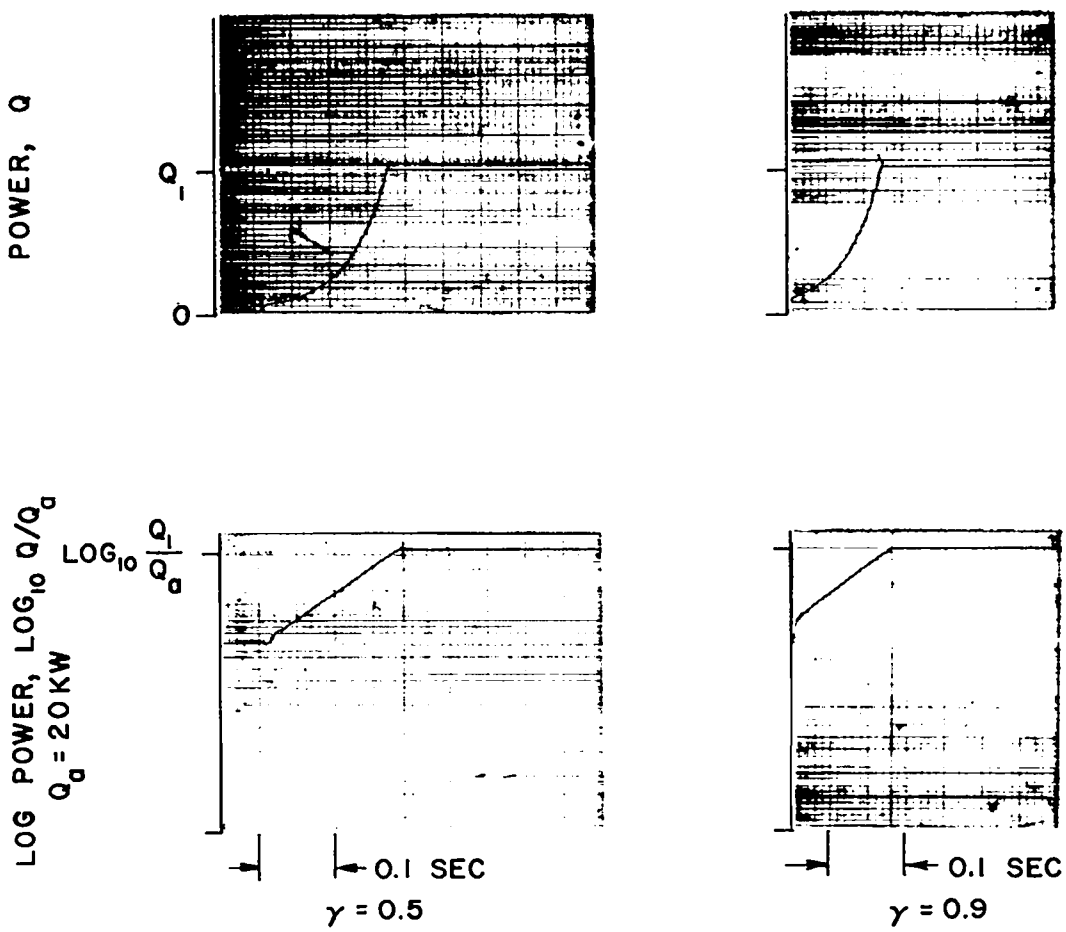

FIGURE 2.26 MINIMUM-TIME STARTUP OF A KIWI-B NEUTRON KINETICS WITH $u \leq \gamma\beta$

by a dither process. Two suboptimal startups, with the same end conditions as those given in Figure 2.26 are shown by Figure 2.25. Though similar to the suboptimal controller discussed above [see equation (2.97) and Figures 2.20 and 2.22], the use of a fast-correcting logarithmic controller (with reactivity limited to values less than 0.9β) allows the loop to be closed during the entire operation. Controller gains for these sub-optimal designs are given under runs 5 and 6 in Table 2.3. Again, the suboptimal control requires the same time difference as the optimal control to reach a value close to the desired terminal value for runs 5 and 6. This initial fast rise is followed by a slow decay toward the desired terminal value. This slow decay is again caused by the slow birth of precursor neutrons. For most applications either run 5 or 6 would be very satisfactory. In other cases (e.g., in fast reactors with low thermal time constants) very little overshoot, if any can be allowed and run 6 would be more desirable.

By cut and try, a controller of the suboptimal category (e.g., as given in Table 2.3 under run 4) can be designed which requires no more than a specified amount of reactivity. The suboptimal startup with reactivity less than 0.9β is presented by run 4 in Figure 2.25. For run 4, however, reactivity never quite reaches 0.9β and rise time is slower than that of runs 5 and 6.

For many applications such suboptimal startups would be sufficient. Though the suboptimal control is synthesized in a simple manner and may be more desirable for these cases, the optimal startup has still provided a measure of performance.

Various nonoptimal startups are presented in Figure 2.24. Notice that runs 1 and 2 require approximately 0.9β of reactivity at the

start and exhibit performance that is far from time optimal. Without knowledge of the time-optimal startup, a designer could unwittingly use such a nonoptimal controller.

A conservative nonoptimal startup (to a step increase in logarithmic power demand) with reactivity always less than 0.5β is exhibited by run 3 in Figure 2.24. The corresponding controller design is given in Table 2.3. After reaching the desired power in about 0.6 sec, the power or neutron level overshoots the desired value by about 8 percent and slowly decays toward the desired terminal power $Q_1 = 24\ Q_0$. Such response is far from optimal for the minimal-time startup, with $\gamma = 0.5$, is presented in Figure 2.26 and requires about 0.17 sec.

Summarizing these comparisons we see that it is possible to design and synthesize a suboptimal neutronic control by conventional means. Knowledge of the optimal performance, however, is required to evaluate the conventional controller. Further, the small terminal transient of slow decay (which always exists for simple suboptimal control with finite gain) hardly appears if the terminal control is a closed-loop dither process.

Chapter III

OPTIMAL CONTROL OF NUCLEAR-REACTOR DIRECT-CYCLE HEAT-EXCHANGE PROCESSES

As discussed previously, the heat exchanger and neutronics as separate processes are bilinear in the state variables and the control variables (reactivity and coolant weight flow rate). As a coupled process the system is generally nonlinear, but in any event, the system is approximately linear in the control variables. Hence, with reference to the maximum principle, the bang-bang control may be optimal for a class of performance indices if the control is constrained. Again, for trajectories on state variable constraint boundaries, for periods of singular solutions or when the desired phase is reached, the optimal control will not generally be bang-bang.

The assumptions and dynamic equations of the heat-exchange model are discussed in the introduction. This model is most important to describe the state of high-power reactors. The optimal-control problem considered below may be stated as follows: Given an initial reactor steady-state, bring the system to a desired terminal steady-state so as to minimize the consumption of coolant. For a nuclear rocket engine, pounds of propellant saved will allow less bulky propellant tanks and more payload. Although nuclear rockets allow a much higher specific impulse than chemical rockets, their engines are heavier and more complex than their chemical counterparts. Minimization of the nuclear system weight becomes necessary.

With a negligible inlet temperature, the time rate of change of average core temperature as presented by (1.37) is

$$\frac{dT}{dt} = \frac{Q}{MC} - \frac{T}{\tau_h} \quad , \tag{3.1}$$

where $T(t_o) = T_o$, $\dot{T}(t_o) = 0$. Here T is the average core temperature and Q is the rate of heat generated in the reactor. Letting the weighting factor $\theta = 2$ in equation (1.38) (this value of θ is found to be a good estimate for many reactors[20]), we obtain the following expression for the thermal time constant τ_h:

$$\tau_h \approx MC \left[\frac{2}{3\, c_p\, \dot{w}} + \frac{1}{hA}\right] \approx \frac{1}{a\dot{w}} \quad . \tag{3.2}$$

3.1 Optimal heat-exchange process

Consider the optimal control of (3.1) between steady-state end points so as to minimize coolant consumption with flow rate constrained as follows:

$$u_a \le \dot{w} \le u_b \, , \tag{3.3}$$

with $\dot{w}(t_o) = u_a$. u_a is a minimum flow rate necessary to insulate substantially the reactor from its outside pressure shell. This outside shell is necessary to hold a high-pressure reactor together but cannot withstand extremely high temperature. For gross decreases in power, it may be necessary to increase u_a in order to remove the post-fission after-heat. u_b is the maximum flow rate the coolant system can develop.

For the time being, assume that the reactor power Q can be changed instantly with the following constraint:

$$0 \le Q \le Q_m$$

and

$$Q(t_1) = Q_1 \, , \tag{3.4}$$

where Q_m is the rated design power of the reactor. The cost function for this problem is coolant flow rate. Then, with reference to Chapter I [equation (1.7)], $(\bar{p},\bar{f})$ is

$$\mathcal{R}(T;\bar{p};Q,\dot{w}) = \dot{T}p_1 + \dot{w}p_2 = \frac{1}{MC}Q - a\dot{w}T\ p_1 + \dot{w}p_2 \qquad (3.5)$$

and the Hamiltonian is

$$\mathcal{H}(T;\bar{p}) = \max_{\vec{u}\in U} \mathcal{R}(T;\bar{p};Q,\dot{w}) \ . \qquad (3.6)$$

Equation (3.5) is made a maximum by

$$Q^\circ = \begin{cases} Q_m & \text{for } p_1 > 0 \\ 0 & \text{for } p_1 < 0 \ . \end{cases} \qquad (3.7)$$

and

$$\dot{w}^\circ = \begin{cases} u_a & \text{for } p_2 - aTp_1 < 0 \\ u_b & \text{for } p_2 - aTp_1 > 0 \ . \end{cases} \qquad (3.8)$$

The costate is defined by the adjoint equation:

$$\dot{p}_1 = a\dot{w}p_1 \qquad (3.9)$$

and p_2 is a non-positive constant. The solution to (3.9) is

$$p_1 = p_{1o} \exp\left(a\int_{t_o}^{t} \dot{w}\, d\sigma\right) , \qquad (3.10)$$

where $p_{1o} = p_1(t_o)$. p_1 cannot change sign since $a\dot{w}$ is always positive and there is no switching for $t_o < t < t_1$. Hence, to increase temperature it is required that

$$Q^\circ = Q_m \qquad (3.11)$$

for $t_o < t < t_1$ and p_{1o} is positive.

Since the system (3.1) is initially at steady-state with the minimum coolant flow rate [i.e., $\dot{w}(t_o) = u_a$], the required initial power is

$$Q_o = MC_a u_a T_o \quad . \tag{3.12}$$

At the terminal time it is desired that $\dot{T}(t_1) = 0$, $T(t_1) = T_1$ and $Q(t_1) = Q_1$; then from (3.1)

$$\dot{w}(t_1) = \frac{Q_1}{MCaT_1} \quad . \tag{3.13}$$

Since temperature is increased most rapidly by low coolant flow rate $\dot{w}$ and high reactor power Q [see (3.1) and (3.2)], it is obvious that the minimal coolant trajectory utilizes $\dot{w} = u_a$ between end points. Thus from (3.10)

$$p_1 = p_{1o} \exp [a\, u_a\, (t - t_o)] \tag{3.14}$$

on the interval (t_o, t_1). After discussing the temperature transient, it is shown below that this constant coolant flow process along with (3.14) satisfies the maximum principle. Thus the optimal process involves constant maximum power and constant minimum propellant flow rate between end points. Switching occurs at the end points to leave or reach the steady-state conditions. An optimal decrease in state with the above initial and terminal conditions reversed is caused by the above variation in power and flow rate with time reversed.

Solutions to (3.1) for constant coolant flow rate are discussed next so that the core temperature transient may be defined for the optimal process analyzed above and below in section 3.2. Equation (3.1) is a linear differential equation of first order if Q(t) and $\dot{w}(t)$ are functions of time. This equation is made exact by multiplication by an integrating factor $\exp[\int a\dot{w}dt]$. Then the solution to (3.1) is

$$T = \frac{\exp(-a\int \dot{w}\, dt)}{MC} \int \exp(a\int \dot{w}\, dt)\, Q\, dt + c\, \exp(-a\int \dot{w}\, dt) \qquad (3.15)$$

(c is a constant of integration)

If $\dot{w}$ is constant and Q(t) is defined for $t \geq t_o$, equation (3.15) may be written as

$$T = T(t_o)e^{-a\dot{w}(t-t_o)} + \frac{e^{-a\dot{w}t}}{MC} \int_{t_o}^{t} e^{a\dot{w}\sigma}\, Q\, d\sigma \quad . \qquad (3.16)$$

Then for a step change to the power level Q_m applied at $t = t_o$,

$$T = \left[T(t_o) - \frac{Q_m}{MC\ a\dot{w}}\right] e^{-a\dot{w}(t-t_o)} + \frac{Q_m}{MC\ a\dot{w}} \quad . \qquad (3.17)$$

For very small coolant flow rate, (3.17) may be represented by the linear terms of a Taylor series. Then the solution to (3.1) is

$$T \approx \left[T(t_o) + \frac{Q_m - Q_o}{MCa\dot{w}}\right] e^{-a\dot{w}(t-t_o)} \quad . \qquad (3.18)$$

See Attached Errata Sheet

Optimal startup trajectories (for the idealized problem analyzed above) are presented in Figure 3.1.

That $\dot{w} = u_a$ (for $t_o \leq t < t_1$) satsifies the adjoint system, is shown by substituting (3.14) and (3.17) into the switching function $p_2 - aTp_1$. With $p_{1o} > 0$, this function has no zeros. Also $\mathcal{H} \equiv 0$ [see (3.6)] requires that

$$p_{2o} = p_{1o}\left\{aT(t_o) - [Q(t_1) - Q(t_o)]/MC\ u_a\right\} \quad . \qquad (3.19)$$

From these trajectories, another physical constraint can be conveniently considered. Thermal stresses in the reactor core are roughly minimized by utilization of a linear increase in average core temperature. These thermal stresses however, frequently

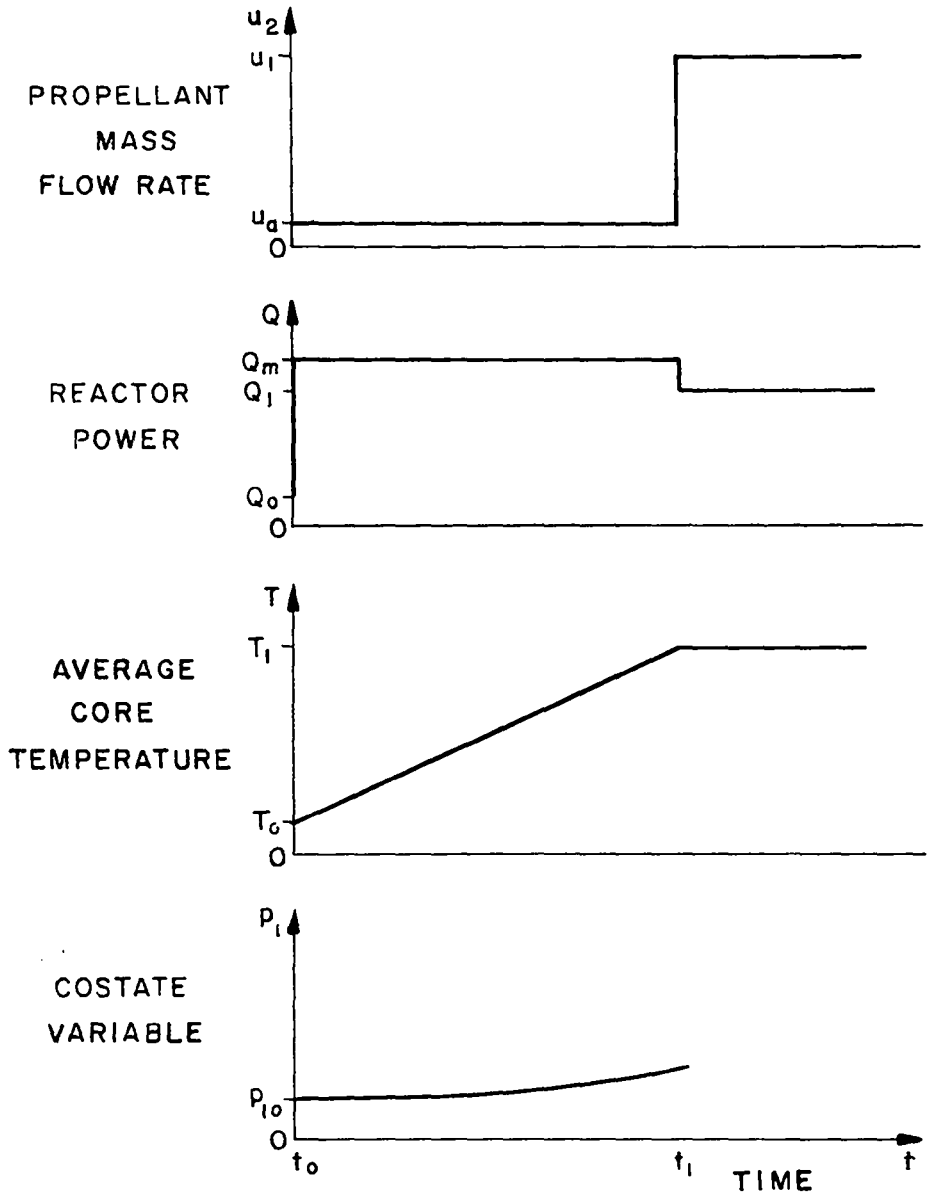

FIGURE 3.1 IDEAL OPTIMAL STARTUP
OF A HEAT-EXCHANGE PROCESS

necessitate a constraint on $\dot{T}$. At low flow rates equation (3.18) shows that this new constraint may be approximated by a constraint on power. (Such a power constraint Q_m may very well be less than the rated design power.)

It is obvious from the system dynamics that the above minimal-propellant process is also one of minimal heat energy and minimal time. Although the power and coolant flow rate cannot be changed instantly, their change can be very rapid compared to the temperature response (see the minimal-time neutronics control as analyzed in 2.2.2). Core temperature reactivity and coolant density reactivity coupling as discussed below complicates the process somewhat.

3.2 Optimal neutronics heat-exchange process

Suppose the rate of change of the precursor-neutron densities and the reactivity coupling are negligible. Then the neutronics heat-exchange process may be represented by the following equations:

$$\dot{Q} = \frac{u_1}{\ell} Q$$

and (3.20)

$$\dot{T} = \frac{Q}{MC} - a u_2 T,$$

where

u_1 = reactivity, δk

and

u_2 = coolant weight flow rate, $\dot{w}$

The allowable control set is defined by:

$$|u_1| \leq \gamma\beta$$

and (3.21)

$$u_a \leq u_2 \leq u_b ,$$

where $u_a > 0$.

Consider the optimal programming problem with given initial and terminal steady-state conditions such that $T(t_o) = T_o$, $u_a(t_o) = u_a$, $T(t_1) = T_1$ and $Q(t_1) = Q_1$. Find the optimal trajectories if the cost function is $f_3 = u_2$ and there is no constraint on power. Then $(\bar{p},\bar{f})$ is

$$\mathcal{R}(Q,T;\bar{p};\vec{u}) = \frac{u_1}{\ell} Q p_1 + \frac{Q}{MC} p_2 - a u_2 p_2 T + u_2 p_3 . \tag{3.22}$$

$\mathcal{R}$ is made a maximum by a bang-bang process such that

$$u_1^o = \gamma\beta \text{ sgn } p_1 , \tag{3.23}$$

$$u_2 = u_b, \text{ for } p_3 - aTp_2 > 0$$

and

$$u_2 = u_a, \text{ for } p_3 - aTp_2 < 0.$$

The costate is defined by the adjoint system:

$$\dot{p}_1 = -\frac{u_1}{\ell} p_1 - \frac{1}{MC} p_2 ,$$

$$\dot{p}_2 = a u_2 p_2$$

and

$$\dot{p}_3 = 0. \tag{3.25}$$

The solution to (3.20) (for constant control with $t_o = 0$) is computed as follows:

$$Q = Q_o \exp(u_1 t/\ell), \tag{3.26}$$

where

$$Q(0) = Q_o = MC a u_2(0) T(0) .$$

The average core temperature is obtained from (3.16). Then

$$T = T_o e^{-a u_2 t} + \frac{e^{-a u_2 t}}{MC} \int_0^t e^{a u_2 \sigma} Q(\sigma)\, d\sigma , \tag{3.27}$$

where

$$T(0) = T_o .$$

Similarly, the solution to (3.25) is

$$p_3 = \text{a constant} \leq 0, \tag{3.28}$$

$$p_2 = p_{20} e^{au_2 t}, \tag{3.29}$$

$$p_1 = e^{-u_1 t/\ell} \left[p_{10} - \frac{1}{MC} \int_0^t e^{-u_1 \sigma/\ell} \, p_2 \, (\sigma) \, d\sigma \right] . \tag{3.30}$$

or

$$p_1 = p_{10} e^{-u_1 t/\ell} + \frac{p_{20}}{MC\left(\frac{u_1}{\ell} + au_2\right)} \left(e^{-u_1 t/\ell} - e^{au_2 t} \right) , \tag{3.31}$$

where

$$p_1(0) = p_{10} \text{ and } p_2(0) = p_{20} .$$

These solutions, (3.26) to (3.31), are substituted into (3.22) to obtain

$$R = \frac{p_{20} Q_0}{MC} \left(1 - \frac{u_1}{\ell \rho} + \frac{au_2}{\rho} \right) e^{\rho t} + \frac{u_1}{\ell} Q_0 \left(p_{10} + \frac{p_{20}}{MC\rho} \right)$$

$$+ u_2 \, p_3 - au_2 \, p_{20} \left[T_0 + \frac{Q_0}{MC\rho} \right] , \tag{3.32}$$

where

$$\rho = \frac{u_1}{\ell} + au_2 .$$

It is necessary however, that the Hamiltonian is zero; i.e.,

$$\mathcal{H}(Q, T; \bar{p}) \equiv 0. \tag{3.33}$$

Equation (3.33) can only be satisfied if

$$p_3 = p_{30} \leq 0 ,$$

$$p_{20} = 0 = p_2 \tag{3.34}$$

and

$$p_1 = p_{1o}\, e^{-\frac{u_1}{\ell} t} \quad , \tag{3.35}$$

where, from (3.32),

$$p_{1o} = -\frac{\ell u_2^\circ p_{3o}}{u_1^\circ} \quad . \tag{3.36}$$

Then for optimal startup $p_{1o} > 0$ and for optimal shutdown $p_{1o} < 0$. Since the switching functions in (3.23) and (3.24) cannot change sign, the optimal control between end points is constant with $u_1^\circ = \gamma\beta$ for startups, $u_1^\circ = -\gamma\beta$ for shutdowns and $u_2^\circ = u_a$ for either. At the terminal end it is necessary that u_2° be instantly increased to $Q_1/MCaT_1$ for startup and u_2° is decreased instantly to u_a at the initial time for shutdown. Q is computed from (3.26). The corresponding terminal reactivity and initial reactivity are zero for steady-state conditions.

The above analysis establishes a background for optimal control of the more involved six-delay-group neutronics heat-exchange processes which are to follow. Rather than analyze the complicated costate of the system, the following analysis will depend on an understanding of the system dynamics, as well as the maximum principle, in order to obtain optimal trajectories. Total reactivity and coolant weight flow rate will be treated as control variables with magnitude constraints on flow rate and total reactivity. The end points of these control variables will be specified by the end states in question. Furthermore, power is constrained to have no overshoot. Again total consumption of coolant is the performance index to be minimized in the following work.

The neutronics heat-exchange process may be approximated by a mono-energetic neutron kinetics and a single-lump heat-exchange model. This model is discussed in the introduction and is very accurate in defining the temperature at any point if the proper mass heat capacity is utilized. Such a model with inlet coolant temperature neglected, is described by the following system of equations:

$$\frac{dQ}{dt} = \frac{u_1 - \beta}{\ell} Q + \sum_{i=1}^{6} \lambda_i C_i = \frac{u_1}{\ell} Q - \sum_{i=1}^{6} \dot{C}_i , \tag{3.37}$$

$$\frac{dC_i}{dt} = \frac{\beta_i}{\ell} Q - \lambda_i C_i \qquad (i=1,\ldots,6) \tag{3.38}$$

and

$$\frac{dT}{dt} = \frac{Q}{MC} - \frac{T}{\tau_h} = \frac{Q}{MC} - au_2 T , \tag{3.39}$$

where

$$\tau_h \approx (au_2)^{-1} , \tag{3.40}$$

$$\delta k = u_1 = u_c + \delta k_t + \delta k_\rho , \tag{3.41}$$

$$\delta k_t \approx c_t T, \tag{3.42}$$

$$\delta k_\rho \approx \frac{c_\rho u_2}{T^{\frac{1}{2}}} , \tag{3.43}$$

u_1 = total reactivity, u_c = control reactivity and u_2 = coolant flow rate = $\dot{w}$. Generally $c_t < 0$ and $c_\rho > 0$. Notice that n has been replaced by Q (power), and C_i must have units of power in (3.37).

Suppose it is desired again to startup the system, from some initial steady-state Q_0, T_0 with $u_2 = u_a$, to some desired terminal steady-state Q_1, T_1 with power constrained and with coolant con-

sumption held to a minimum such that $Q \leq Q_1$. Then the cost function for this problem is u_2 and $(\bar{p},\bar{f})$ is

$$\mathcal{R}(\vec{x};\bar{p}) = I(\vec{x};\bar{p}) + \frac{p_1 Q u_1}{\ell} + (p_9 - a\rho_8 T)\, u_2 \quad , \tag{3.44}$$

where the components of $\bar{x}$ are Q, $C_1,\ldots,C_6$, T and u_2; $I(\vec{x};\bar{p})$ is that part of $\mathcal{R}$ not involving the control explicitly. Again the flow rate u_2 is constrained by (3.3). The constraint on the neutronics control is on total reactivity δk rather than control reactivity. For this reason δk is treated as a control variable in the following discussion. Such reactivity constraint is discussed in Chapter II and appears as

$$|u_1| \leq \gamma\,\beta. \tag{3.45}$$

Then $(\bar{p},\bar{f})$ is maximum for $\vec{u}$ on the constraint boundary of the allowable control set. That is, the optimal reactivity process is $u_1^\circ = \gamma\beta\ \mathrm{sgn}\ p_1$ or the optimal control reactivity is

$$u_c^\circ = \gamma\beta\ \mathrm{sgn}\ p_1 - (\delta k_t + \delta k_\rho) \tag{3.46}$$

[$\delta k_t + \delta k_\rho$ is computed from (3.42) and (3.43).]

and

$$u_2^\circ = \begin{cases} u_a & \text{for } F(\vec{x},\bar{p}) < 0 \\ u_b & \text{for } F(\vec{x},\bar{p}) > 0 \end{cases} , \tag{3.47}$$

where from (3.44)

$$F(\vec{x};\bar{p}) = p_9 - a\rho_8 T \ . \tag{3.48}$$

Meanwhile the Hamiltonian is

$$\mathcal{H}(\vec{x};\bar{p}) = \max_{\vec{u}\in U} \mathcal{R}(\vec{x};\bar{p};\vec{u}) = 0 \quad . \tag{3.49}$$

The costate is defined by the adjoint equation while the trajectory is within the phase constraint boundary. When the trajectory is on the phase constraint boundary, however, the costate is considerably complicated by the presence of vector control. Such problems are discussed in Reference 8, Chapter 6 and briefly treated in Appendix A. In Appendix E it is shown that the necessary costate equations are satisfied by proper selection of $\bar{p}(t_o)$.

It is not necessary, however, to solve the costate equations along with the two-point boundary-value problem in order to arrive at the optimal process. With reactivity coupling the heat-exchange process to the neutron kinetics, equations (3.37) and (3.43) show that either of the control variables could be utilized to change power level. Since there is a constraint on total reactivity, however, no increase in flow rate u_2 would permit a faster change of state than does $u_1 = \gamma\beta$ for startups and $u_1 = -\gamma\beta$ for shutdowns. Hence, the power is changed in minimum time if $|u_1| = \gamma\beta$ and any increase in flow rate u_2 would require the system to consume more coolant. Optimality of this process is not surprising; after the analysis of the previous problems, one would again suspect the optimal process to require a time-optimal power change.

At the constraint surface $Q(t) = Q_1$, it is necessary to maintain steady-state power. Theoretically, this requires that $u_1 = \ell \sum_{i=1}^{6} \dot{C}_i/Q_1$ but again such open-loop control is unstable. A closed-loop dither type of control, however, is found to do the job adequately. In this case, the rod reactivity u_c dithers between $\pm \gamma\beta - (\delta k_t + \delta k_\rho)$ and a rough approximation to the theoretical terminal control. The optimal startup of such a system is given by Figure 3.2. At the desired terminal

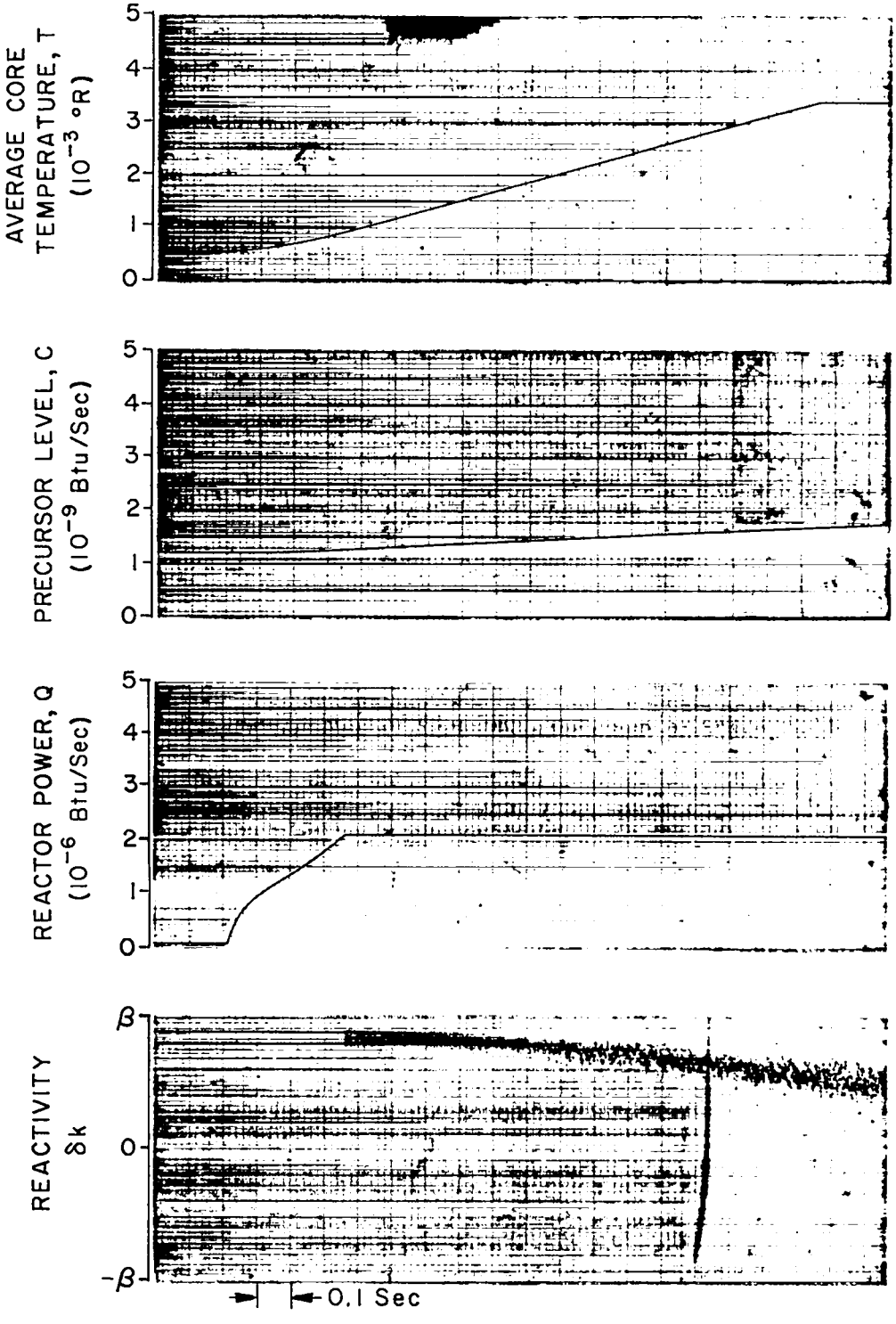

FIGURE 3.2 MINIMAL PROPELLANT CONSUMPTION STARTUP WITH DITHER TERMINAL CONTROL

core temperature, coolant flow rate is increased from $u_2 = u_a = 20$ lb/sec to the required terminal value: $u_2(t_1) = Q_1/MCaT_1 = 130$ lb/sec in order to maintain $\dot{T} = 0$ in equation (3.39). In practice it would be simpler to increase the constraint γ on reactivity (if this can be allowed) at low temperatures and neglect the corrections due to reactivity coupling from the heat exchanger. This is relatively safe for some applications with weight flow rate low because the negative temperature reactivity causes the net total reactivity to steadily decrease as temperature increases. Such a system is really in the suboptimal category but approximates an optimal solution. Figures 3.3 and 3.4 show such a response with $\gamma = 1.5$ and $\gamma = 1.6$. These figures indicate that for the model considered (see Table 1.2), it is not necessary to compensate for the feedback reactivity as long as γ is at least 1.6. If the temperature reactivity were less or the propellant reactivity were more than that used for this system, then the reactivity required to keep the process optimal and yet so simple would be less.

The analog computer simulation used to obtain these data utilized a circuit diagram that is similar to Figure 2.10 with the addition of a six-delay-group neutron kinetics. The heat-exchanger time constant is varied according to equation (3.2).

For most systems the power response is so rapid that any suboptimal power control has little effect on the slower temperature response. Hence, such closed-loop suboptimal systems as discussed in Chapter II are adequate for most minimal coolant processes.

Notice from Figure 3.2 that temperature increases approximately linearly for the interval (t_0, t_1). For small flow rate, (3.39) predicts that $\dot{T} \approx Q_1/MC$ and substantiates the response shown in Figure 3.2.

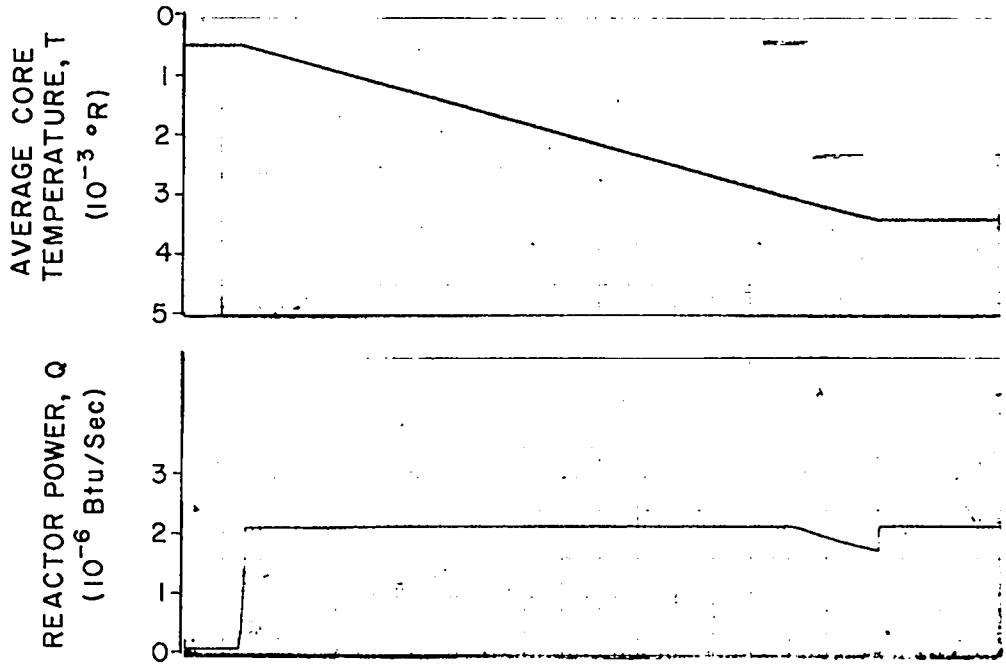

FIGURE 3.3 BANG-BANG CONTROL OF NEUTRONICS-HEAT -EXCHANGE PROCESS WITH $\gamma = 1.5$

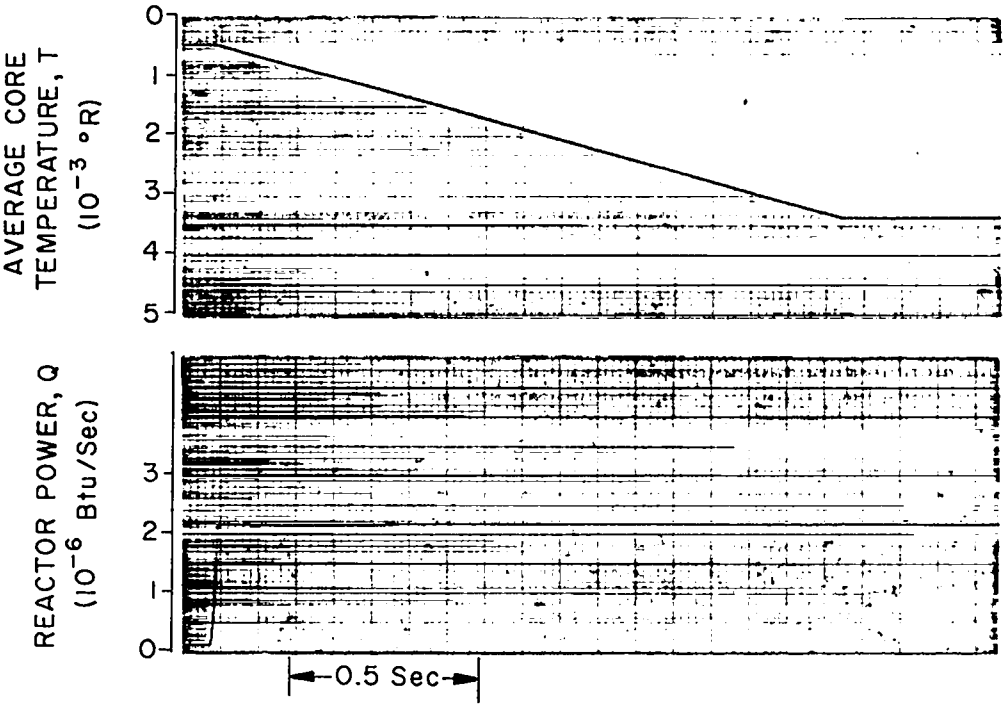

FIGURE 3.4 BANG-BANG CONTROL OF NEUTRONICS-HEAT -EXCHANGE PROCESS WITH $\gamma = 1.6$

Hence, as mentioned in Section 3.1 power magnitude constraint may also be interpreted roughly as a $\dot{T}$ or core thermal-stress constraint for such minimal-coolant processes. This constraint may require that $\dot{T} \leq \alpha_m \approx Q_m/MC$, where Q_m may be less than Q_1.

In addition to power constraint the coolant pumping system may be constrained. Such constraints are treated in the following section.

3.3 Flow system constraints

The coolant may be supplied from a pressurized tank or may be pumped from a low pressure supply tank. With regards to nuclear rockets, the latter is more desirable due to the saving in tank weight and the pump is driven by a gas turbine. The output flow rate of the system is constrained by the velocity of the flow control valve (which is very fast), mechanical stresses and certain regions of performance on the pump map. The following discussion assumes the first two constraints are negligible.

A hypothetical pump performance map is presented in Figure 3.5. This is a plot of pressure rise across the pump (approximately proportional to nozzle entrance pressure) vs pump flow rate. Constant specific-speed lines are parabolic on this map[25]. Temperature lines refer to the nozzle entrance and are approximately linear due to the nozzle equation (1.44). The quantity, specific speed, is defined according to

$$N_s = NQ^{\frac{1}{2}}/H^{\frac{3}{4}}, \tag{3.49}$$

where N = pump speed (rpm), Q = flow rate (gpm) and H = pump pressure head (ft.)[25].

The importance of specific-speed may best be explained by a pump map (See Figure 3.5). Here the flow system is constrained by

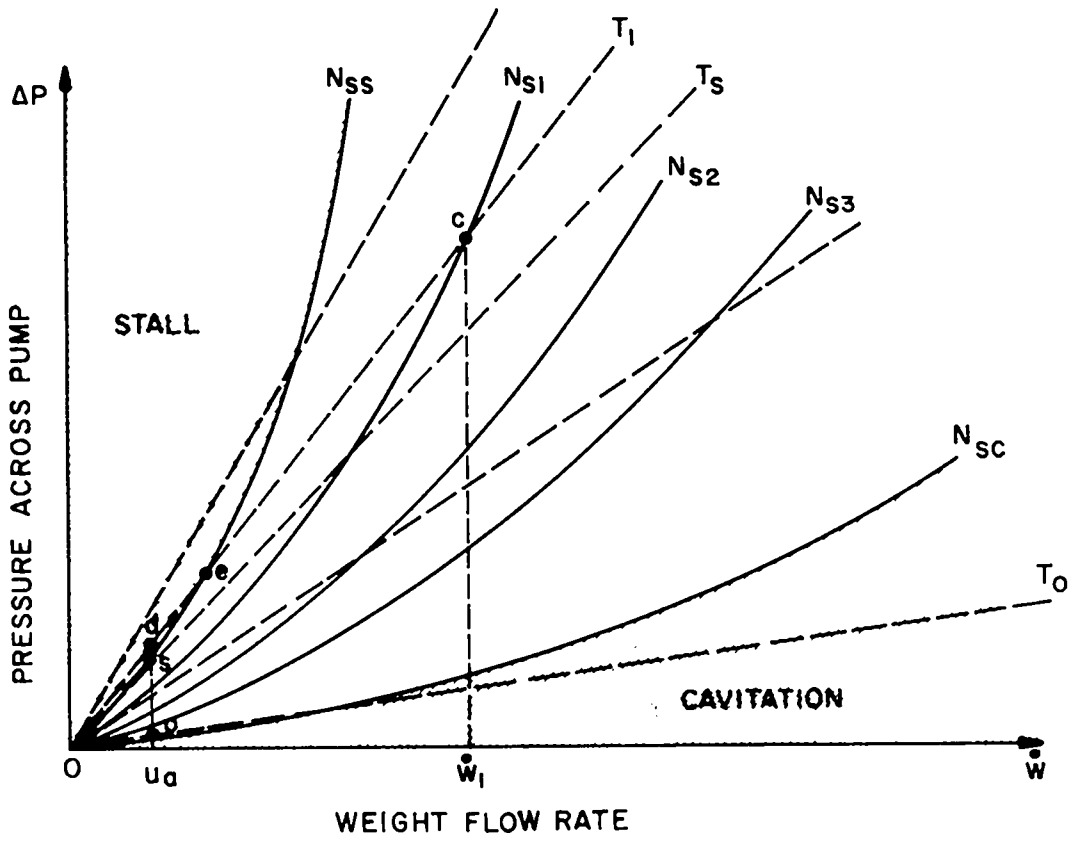

N_S = SPECIFIC-SPEED

T_1 = TERMINAL TEMPERATURE

T_O = INITIAL TEMPERATURE

FIGURE 3.5 HYPOTHETICAL PUMP PERFORMANCE MAP

regions of stall and cavitation. Above some specific speed N_{ss} the pump stalls and below some specific-speed N_{sc} cavitation exists. Operation in either of the regions is not tolerable for any finite time. A typical optimal trajectory o-d-e-c in Figure 3.5, with a bang-bang flow variation, shows a pump constraint violation. For such a case the temperature could only be allowed to increase to T_s. At point s mass flow rate and temperature would have to be increased so as to maintain constant specific-speed N_{ss}. If flow rate were increased at some lower temperature or power, more coolant would be consumed upon reaching the desired terminal temperature. At point e mass flow rate could be stepped to point c.

Suppose the pressure during stall specific-speed operation is approximated by

$$P = b_s \dot{w}^2 \quad , \tag{3.50}$$

where b_s is a constant. Substitution of the nozzle equation (1.44) into (3.50) (with $T \propto T_o$) yields

$$\dot{w} = \frac{c_n' T^{\frac{1}{2}}}{b_s} \quad , \tag{3.51}$$

where c_n' is a constant. Then for $T > T_s$, the optimal trajectory (as discussed in section 3.2) is altered as follows. At $T(t_s) = T_s$ (where $t_a < t_s < t_b$)

$$u_2^o = \frac{c_n' T_s^{\frac{1}{2}}}{b_s} \quad . \tag{3.52}$$

Assume $u_2(t)$ remains so small that temperature increases nearly linearly, i.e., $T \approx \alpha_m (t - t_s) + T_s$, where $\alpha_m = Q_1/MC$. Then it is seen from (3.51) that

$$u_2(t) \approx \frac{c_n'}{b_s} [\alpha_m (t - t_s) + T_s]^{\frac{1}{2}} \tag{3.53}$$

for $t_s < t < t_1$. At the terminal end, $T = T_1$, and $Q = Q_1$; then from (3.39) with $\dot{T} = 0$ recognize that flow rate must be increased to

$$u_2(t) = \frac{Q_1}{MCaT_1} \quad . \tag{3.54}$$

In summary then, the optimal-control process as defined in Section 3.2 should be pieced together continuously with (3.50) to (3.53) if the pump stall constraint must be considered.

It is possible to bypass some of the coolant back to the tank and only send the minimum mass flow rate to the reactor but increased energy is required to pump this bypass flow. In a bleed-cycle or topping-cycle nuclear rocket, the turbine gets this energy from the reactor[20]. In practice such a process requires more coolant than the previous one due to energy losses.

The arguments presented in this section are not rigorous, but the constraint problem is so complicated (involving vector control with a constraint explicitly including both control and phase) that physical arguments are much simpler. Furthermore, the theory developed in Reference 8 and discussed in Appendix A does not apply to optimization problems with constraints which involve both phase and control jointly.

Again in practice, a simple closed-loop suboptimal process would be desirable for most applications. Such closed-loop systems for a nuclear rocket engine are presented in Figures 3.6 and 3.7. There the inputs are limited to meet the necessary constraints that were discussed above. Though the latter control system is simplified by the coupling from propellant reactivity (i.e., an increase in flow rate causes an increase in power), the more complicated system allows the necessary constraints to be applied in a simpler manner. Notice

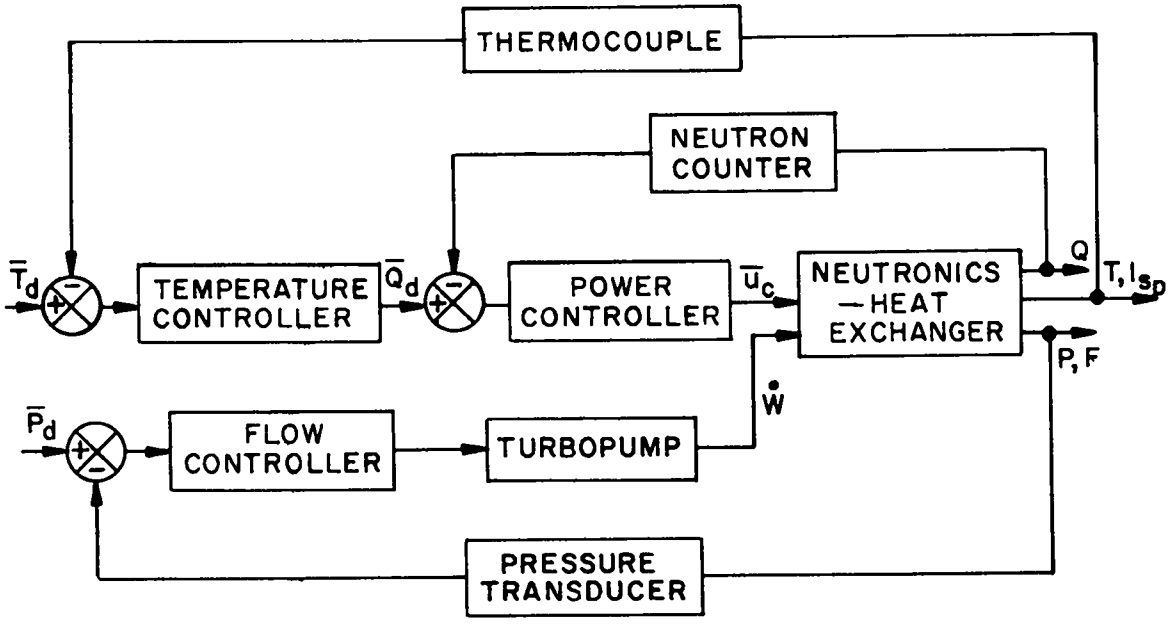

FIGURE 3.6 CLOSED-LOOP NUCLEAR ROCKET ENGINE CONTROL SYSTEM WITH CONSTRAINED DEMANDS

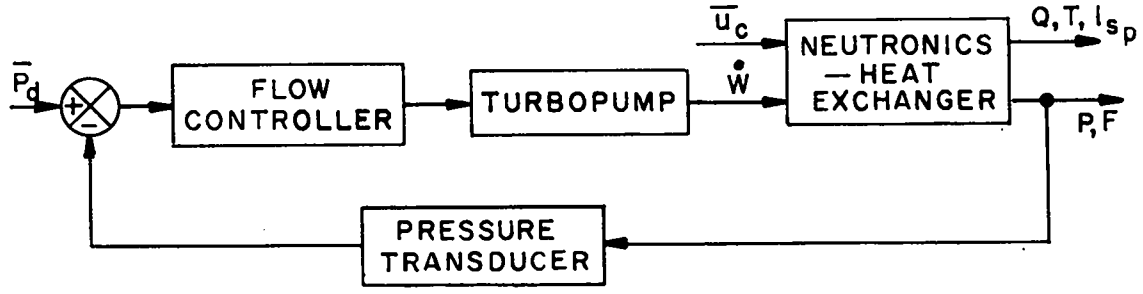

FIGURE 3.7 A SIMPLE TYPE OF CLOSED-LOOP NUCLEAR ROCKET ENGINE CONTROL SYSTEM WITH CONSTRAINED INPUTS

that control reactivity still appears in Figure 3.7 and may be used to bias appropriately the total reactivity.

As mentioned in Chapter 1, specific impulse (or temperature) and thrust (or pressure) are the variables of most interest to a rocket engine. Hence, these are the variables controlled directly in Figure 3.6. Temperature and pressure determine flow rate from the nozzle equation (1.44). Therefore, flow rate can be held approximately constant by programming pressure demand from temperature according to the nozzle equation for constant flow rate. An alternate suboptimal scheme could use a closed $\dot{w}$ loop. Notice from Figures 2.22 and 3.2 that the variation of the suboptimal power trajectory from that of the minimal time case has no noticeable effect on the temperature trajectory.

Chapter IV
CONCLUSIONS

Optimal control of nuclear-reactor processes has been analyzed and synthesized above by means of physical considerations as well as mathematical arguments. Modern techniques of optimal-control theory, along with the state-variable approach and computer analyses, have been applied to this problem.

Although safety limitations of many commercial reactors require more stringent constraints than those given here, the techniques may still be applied to the optimal-control design.

Based on the above study, the following conclusions are of particular value:

1. The time-optimal startup or shutdown of neutron density (with steady-state conditions at the initial state and terminal state) requires no switching in control between end points (see Section 2.1.2). The key to this time-optimal neutronics control is the ability to maintain essentially steady-state neutron density at the desired terminal level while the neutron-percursor densities are not near steady state. The theoretical terminal control, being open loop, is unstable in practice; a closed-loop dither type of control, however, is found to be stable (see Section 2.4). Furthermore, a continuous type of terminal feedback control, although suboptimal, is analyzed in Section 2.5 and found to be satisfactory for most practical purposes. A describing-function analysis indicates the stability limitation of such systems.

2. The minimal propellant consumption control of neutron dynamics direct-cycle heat-exchange processes, such as that of the nuclear

rocket engine, is at least partly a bang-bang process. Though ostensibly a minimal propellant process, this problem leads to a minimal-time control process, as analyzed in Chapter III.

3. Physical constraints on maximum power level, (approximately equivalent to constraints on rate of change of core temperature or core thermal stress) and the coolant flow system performance are discussed above. These constraints, as analyzed in Sections 2.2.5, 3.2 and 3.3, cause the optimal control trajectories to be a connection of those due to bang-bang and continuous types of control.

4.1 Suggestions for further work

The optimal control of more complicated reactor models should be analyzed. In particular, distributed model core heat-exchange processes with thermal-stress constraints should be studied along with optimal reactor processes. Indeed, the optimal process is only as good as the constraints and the model. Vibrations (such as those experienced in nuclear rocket reactor cores) may require consideration of constraints thus far ignored. Furthermore, the stability of these optimally controlled systems could be analyzed by such techniques as Liapunov's direct method. The effects of reactor noise should also be studied.

Bilinear systems (i.e., systems for which the state $\vec{x}$ and control $\vec{u}$ appear linearly but for which products of these linear terms may exist) in general seem to be a fruitful area for future research. The neutron kinetic equations, (1.30) and (1.31), describe a particular bilinear system. Since (with reference to the maximum principle) the bang-bang process is a candidate for the optimal control for a broad class of problems it would be worthwhile to compute the maximum number of possible switchings. It is apparent that there can be more switchings

than the maximum for the system jointly linear in the state and the control. Sufficiency of the maximum principle should be rigorously proved for at least a sub-class of optimization problems relative to the bilinear system.

APPENDIX A

OPTIMAL PROCESSES WITH CONSTRAINED STATE VARIABLES

For many problems, not only the region of admissible control, but also the region of allowed phase values, must be restricted. In these cases, the optimization problem consists of selecting an allowable control whose phase trajectory $\vec{x}$ lies in a given fixed region B of the n-dimensional phase space. $\vec{x}$ also satisfies the equations of state (along with necessary end conditions) and minimizes a performance index J (see equations 1.1 and 1.5).

The object of this formal presentation is to summarize the necessary conditions which are used in this thesis. The reader is referred to Chapter 6 of Reference 8 for detailed theorems and the necessary assumptions.

In addition to the restrictions placed on the allowable control region U in Section 1.2, assume that $\vec{u}(t)$ is composed of piecewise smooth components and furthermore, that the admissible control set satisfies certain "regularity" conditions in a neighborhood of its boundary points. These regularity conditions are defined below.

Let u_1 be an arbitrary boundary point of U which belongs to U and let $q_i(\vec{u})(i=1,\ldots,s)$ be continuously differentiable scalar functions such that U is given by $q_i(\vec{u}_1) = 0$ $(i=1,\ldots,s)$ in the neighborhood of u_1. Furthermore, the vectors $\partial q_i/\partial \vec{u}$ $(i=1,\ldots,s)$ are linearly independent.

Let the closed region B (in the n-dimensional phase space) be smooth and defined by

$$S(\vec{x}) \leq 0.$$

$S(\vec{x})$, also, must have continuous second partial derivatives near the boundary $S(x) = 0$ and the vector $\partial S(\vec{x})/\partial \vec{x}$ must not vanish on the boundary.

As in Chapter I, the system is made to have order n + 1 by letting $\dot{x}_{n+1} = f_{n+1}(\vec{x};\vec{u}) = C(\vec{x};\vec{u})$ with $x_{n+1}(t_0) = 0$ and $x_{n+1}(t_1) = J$. The optimal trajectory must connect $\bar{x}(t_0) = \begin{bmatrix} \vec{x}(t_0) \\ 0 \end{bmatrix}$ with $\bar{x}(t_1) = \begin{bmatrix} \vec{x}(t_1) \\ x_{n+1}(t_1) \end{bmatrix}$ so that $x_{n+1}(t_1)$ takes on the minimum possible value.

Every function which depends on $\vec{x}$ can be considered to be a function of $\bar{x}$; e.g., $S(\vec{x}) = S(\bar{x})$. Hence, let the closed region G in the (n+1)-dimensional phase space be defined by $S(\bar{x}) \leq 0$.

For $S(\bar{x})$ negative, i.e., optimal motions not on the phase constraint boundary, the previous conditions stated by the maximum principle are valid. Necessary conditions for solutions to be optimal on the phase-constraint boundary,

$$S[\vec{x}(t)] \equiv S(\vec{x}) \equiv S(\bar{x}) \equiv 0, \tag{A.1}$$

are discussed below.

Equation (A.1) requires that all the time derivatives $S^{(k)}$ must vanish. Assume that the required $\vec{u}(t)$ may be computed from $\dot{S} = 0$, where

$$\dot{S}(\bar{x};\vec{u}) = \frac{d}{dt} S(\bar{x}) = \left[\frac{\partial S(\bar{x})}{\partial \bar{x}}\right]^T \bar{f}(\vec{x};\vec{u}) = 0. \tag{A.2}$$

Also, assume that the phase trajectory $\bar{x}$ is "regular" with respect to $\vec{u}_1$. That is, for each $\bar{x}$ on the trajectory $\bar{x}$ is regular, where regular means the following conditions are satisfied:

(1) $\dot{S}(\vec{x};\vec{u}_1) = \dot{S}(\bar{x};\vec{u}_1) = 0$,

(2) $\dfrac{\partial \dot{S}(\bar{x};\vec{u}_1)}{\partial \vec{u}} \neq 0$

and

(3) $\dfrac{\partial \dot{S}(\bar{x};\vec{u}_1)}{\partial \vec{u}}$, $\dfrac{\partial q_i(\vec{u}_1)}{\partial \vec{u}}$ $\quad (i = 1, \ldots, s)$

are linearly independent. If $\vec{u}$ [as determined by (A.2)] is an interior point, condition (3) doesn't appear. Let $\omega(\bar{x})$ designate the set of all admissible controls for which $\bar{x}$ is regular. If u_1 is an interior point, $\omega(\bar{x})$ is a point.

With these assumptions, the maximum principle may be extended as follows (see pages 267 and 268 of Reference 8). If $\bar{x}(t)$ is an optimal trajectory of $\dot{x} = \bar{f}(\vec{x};\vec{u})$ for corresponding $\vec{u}(t)$ and $\bar{x}$ is located entirely on the boundary of G, then a continuous $\bar{p}(t)$ and a piecewise smooth $\rho(t)$ exist such that

$$\dot{\bar{x}} = \bar{f}(\vec{x};\vec{u}) = \frac{\partial \mathcal{R}(\vec{x};\bar{p};\vec{u})}{\partial \bar{p}} \quad , \tag{A.3}$$

$$\dot{\bar{p}} = -\frac{\partial \mathcal{R}(\vec{x};\bar{p};\vec{u})}{\partial \bar{x}} + \rho \frac{\partial \dot{S}(\bar{x};\vec{u})}{\partial \bar{x}} \tag{A.4}$$

and

$$\mathcal{H}[\vec{x}(t);\bar{p}(t)] = \max_{\vec{u}\in\omega(\bar{x})} \mathcal{R}[\vec{x}(t);\bar{p}(t);\vec{u}(t)] = 0, \tag{A.5}$$

where as before $\mathcal{R}(\vec{x};\bar{p};\vec{u}) = [\vec{p}, \vec{f}(\vec{x};\vec{u})]$. $\rho(t)$ is determined from (A.5) as a Lagrange multiplier for $\partial \dot{S}(\bar{x};\vec{u})/\partial \vec{u}$ in

$$\frac{\partial \mathcal{R}(\vec{x};\bar{p};\vec{u})}{\partial \vec{u}} = \rho \frac{\partial \dot{S}(\bar{x};\vec{u})}{\partial \vec{u}} + \sum_{j=1}^{s} \nu_j \frac{\partial q_j}{\partial \vec{u}} \, . \tag{A.6}$$

Also, $p_{n+1}(t)$ is a nonpositive constant; $\bar{p}(t_a+)$ is a nonzero vector and is not collinear with $\partial S(\bar{x})/\partial \bar{x}$ and $\dot{\rho}(t)$ is nonpositive. t_a+ is the time at which the trajectory $\bar{x}(t)$ initially is on a phase-constraint boundary.

We now have necessary conditions for optimal trajectories on phase-space constraint boundaries. For interior points the maximum principle as presented previously yields the appropriate necessary conditions. Next consider the necessary conditions such optimal trajectories must have at their junction points (i.e., points where phase trajectories meet phase-constraint boundaries). Consider a junction time t_a such that the trajectory is on a phase-constraint boundary for $t > t_a$ and is not on a phase-constraint boundary for $t < t_a$. Then either

$$\bar{p}(t_a-) = \bar{p}(t_a+) + \mu \frac{\partial S(\bar{x})}{\partial \bar{x}} \Bigg|_{t = t_a} \tag{A.7}$$

or

$$\bar{p}(t_a-) - \mu \frac{\partial S(\bar{x})}{\partial \bar{x}} = 0, \quad \mu \neq 0, \tag{A.8}$$

where μ is some real number (of opposite sign to that of Reference 8). Hence, $\bar{p}(t)$ may be discontinuous at the junction time.

In References 8 and 15, it is noted that an arbitrary jump [proportional to $\partial S(\bar{x})/\partial \bar{x}$] can be added to $\bar{p}$ during (t_a, t_b). This arbitrary jump can be utilized (as is done in Reference 15) so that if the phase leaves the phase-constraint boundary at $t = t_b$, then $\bar{p}(t)$ can be assumed continuous at $t = t_b$. The necessary costate conditions at t_a

and t_b could be interchanged but following the convention of Reference 15, assume this arbitrary jump is utilized to make $\bar{p}(t)$ continuous at the exit corner, $t = t_b$.

Hence,

$$\bar{p}(t_b+) = \bar{p}(t_b-). \tag{A.9}$$

It is shown in Reference 15, also, that $\mathcal{H}(\vec{x};\bar{p};\vec{u})$ is continuous at both entrance corners and exit corners.

Time-optimal neutronic processes with phase-constraint and scalar control are discussed in Chapter II. For these processes u is an interior point of the allowable controls. Hence, from (A.6)

$$\rho = \frac{\partial \mathcal{H}(\vec{x};\bar{p};u)}{\partial u}\left[\frac{\partial \dot{S}(\bar{x};u)}{\partial u}\right]^{-1}. \tag{A.10}$$

Substitution of (A.10) into (A.4) shows that the optimal trajectories on the phase-constraint boundary must satisfy

$$\dot{\bar{p}} = -\frac{\partial \mathcal{H}(\vec{x};\vec{p};u)}{\partial \bar{x}} + \frac{\partial \mathcal{H}(\vec{x};\bar{p};u)}{\partial u}\left[\frac{\partial \dot{S}(\bar{x};u)}{\partial u}\right]^{-1}\left[\frac{\partial \dot{S}(\bar{x};u)}{\partial \bar{x}}\right]. \tag{A.11}$$

Since $\mathcal{H} = \bar{f}^T\bar{p}$,

$$\dot{\bar{p}} = -\left\{\frac{\partial \bar{f}(\vec{x};u)}{\partial \bar{x}} - \frac{\partial \bar{f}(\vec{x};u)}{\partial u}\left[\frac{\partial \dot{S}(\bar{x};u)}{\partial u}\right]^{-1}\left[\frac{\partial \dot{S}(\bar{x};u)}{\partial \bar{x}}\right]^T\right\}^T\bar{p}. \tag{A.12}$$

Thus, for such problems equations (A.4) and (A.6) combine and simplify to yield (A.12).

Appendix B

SOLUTION TO THE SINGLE-PRECURSOR NEUTRON KINETICS AND THE NEUTRONIC ADJOINT SYSTEM FOR CONSTANT REACTIVITY

The solution to the neutronic system (2.28) for $u = \pm \gamma\beta$ may be obtained by conventional means (e.g., see Chapter II of Reference 26). This system may be written in vector form as

$$\dot{\vec{x}} = A\,\vec{x} \quad , \tag{B.1}$$

where $x_1 = n$, $x_2 = C$ and A is a constant matrix defined by:

$$A = \begin{bmatrix} \frac{u-\beta}{\ell} & \lambda \\ \frac{\beta}{\ell} & -\lambda \end{bmatrix} \quad , \text{ for } u(t) \text{ constant} \tag{B.2}$$

The solution to this autonomous system (B.1) for u(t) constant is

$$\vec{x} = e^{A(t-t_o)}\,\vec{x}_o \quad , \tag{B.3}$$

where $\vec{x}_o = \vec{x}\,(t_o)$[27]. The transition matrix $e^{A(t-t_o)}$ is the solution to the matrix equation

$$\dot{X} = A\,X \quad , \tag{B.4}$$

with $X(t_o) = I$, the identity matrix.

Elements of the exponential transition matrix for the neutronic system are as follows:

$$e^{A(t-t_o)} = \left[\frac{c^1_{ij} e^{\rho_1 (t-t_o)} + c^2_{ij} e^{\rho_2 (t-t_o)}}{\rho_2 - \rho_1} \right] \quad , \tag{B.5}$$

where the ij subscript refers to the i, jth element of the matrix and

$$
\begin{aligned}
c^1_{11} &= \rho_2 + \frac{\beta}{\ell}(1 \mp \gamma) \\
c^2_{11} &= -\left[\rho_1 + \frac{\beta}{\ell}(1 \mp \gamma)\right] \\
c^2_{12} &= \lambda = - c^1_{12} \\
c^2_{21} &= \frac{\beta}{\ell} = - c^1_{21} \\
c^1_{22} &= \lambda + \rho_2 \\
c^2_{22} &= - (\lambda + \rho_1) \quad .
\end{aligned}
\tag{B.6}
$$

Here the order of signs is read according to $u = \pm \gamma\beta$.

ρ_1 and ρ_2 are computed by (2.34) or approximated by (2.35).

Hence the solution may be written as follows:

$$
n = \frac{(c^1_{11} n_0 + c^1_{12} C_0) e^{\rho_1 (t-t_0)} + (c^2_{11} n_0 + c^2_{12} C_0) e^{\rho_2 (t-t_0)}}{\rho_2 - \rho_1}
$$

and

$$
C = \frac{(c^1_{21} n_0 + c^1_{22} C_0)\, e^{\rho_1 (t-t_0)} + (c^2_{21} n_0 + c^2_{22} C_0) e^{\rho_2 (t-t_0)}}{\rho_2 - \rho_1} \quad . \tag{B.7}
$$

If $\dot{C}$ is initially zero then $\frac{\beta}{\ell} n_0 = \lambda C_0$ [see (B.1) and (B.2)] and the solution (B.7) may be written as:

$$
n = \frac{(\rho_2 \mp \gamma\beta/\ell) n_0 e^{\rho_1 (t - t_0)} - (\rho_1 \mp \gamma\beta/\ell) n_0 e^{\rho_2 (t - t_0)}}{\rho_2 - \rho_1}
$$

and

$$
C = \frac{\rho_2 C_0 e^{\rho_1 (t - t_0)} - \rho_1 C_0 e^{\rho_2 (t - t_0)}}{\rho_2 - \rho_1} \quad . \tag{B.8}
$$

The solution to the adjoint system $\dot{\vec{p}} = -A^T\vec{p}$ is (see p. 27 of Reference 28.)

$$\vec{p}^T = \vec{p}_o^T \, e^{A(t_o - t)} \tag{B.9}$$

where $\vec{p}_o = \vec{p}\,(t_o)$. Hence, the adjoint solution is given by (B.9) where the exponential matrix is defined by (B.5) and (B.6) but the argument $(t-t_o)$ is reversed in sign. In other words, the adjoint solution is similar to the solution of the original system with time reversed.

Appendix C

PHASE-PLANE EIGENVECTORS

Consider the system $\dot{\vec{x}} = A\vec{x}$. For this system to have a nontrivial solution of the form $\vec{x}(t) = \vec{C}e^{\rho t}$ it is necessary and sufficient that ρ be a root of the characteristic equation:

$$|A - \rho I| = 0 \quad . \tag{C.1}$$

Suppose the system is of order n and there are n real and distinct characteristic roots or eigenvalues. Then there are n principal directions or eigenvectors along which[29]

$$\dot{\vec{x}} = \rho\vec{x} \quad . \tag{C.2}$$

These eigenvectors $\vec{x}^i$ must satisfy the following relation:

$$[A - \rho_i I]\,\vec{x}^i = 0 \quad , \tag{C.3}$$

where $i = 1,\ldots,n$.

Consider the second-order system with A_{ij} components of the A matrix and with real and distinct eigenvalues ρ_1 and ρ_2. The eigenvectors must satisfy

$$\begin{bmatrix} A_{11} - \rho_i & A_{12} \\ A_{21} & A_{22} - \rho_i \end{bmatrix} \begin{bmatrix} x_1^i \\ x_2^i \end{bmatrix} = 0 \tag{C.4}$$

or

$$\begin{aligned} (A_{11} - \rho_i)\, x_1^i + A_{12} x_2^i &= 0 \\ A_{21}\, x_1^i + (A_{22} - \rho_i)\, x_2^i &= 0 \quad . \end{aligned} \tag{C.5}$$

Hence, the tangents of the eigenvectors are

$$\frac{x_2^i}{x_1^i} = \frac{\rho_i - A_{11}}{A_{12}} = \frac{A_{21}}{\rho_i - A_{22}} \qquad (C.6)$$

where $i = 1, 2$.

Appendix D

COMPUTATION OF PHASE-PLANE TRAJECTORIES

Computation of phase-plane trajectories for constant reactivity may be made as follows. The analysis is valid for $x_1 = n$ or $x_1 = C$. The form of solution with $t_o = 0$ is

$$x_1 = c_{1i} e^{\rho_{1i} t} + c_{2i} e^{\rho_{2i} t}$$

and (D.1)

$$x_2 = \dot{x}_1 = \rho_{1i} c_{1i} e^{\rho_{1i} t} + \rho_{2i} c_{2i} e^{\rho_{2i} t} ,$$

where $i = 1$ for $u = \gamma\beta$ and $i = 2$ for $u = -\gamma\beta$.

Then $$\rho_{2i} x_1 - x_2 = c_{1i} (\rho_{2i} - \rho_{1i}) e^{\rho_{1i} t}$$

or

$$\log (\rho_{2i} x_1 - x_2) = \log c_{1i} + \log (\rho_{2i} - \rho_{1i}) + \rho_{1i} t \quad . \qquad (D.2)$$

Similarly

$$\log (\rho_{1i} x_1 - x_2) = \log (-c_{2i}) + \log (\rho_{2i} - \rho_{1i}) + \rho_{2i} t \quad . \qquad (D.3)$$

Eliminate t from (D.2) and (D.3):

$$\log \left[(\rho_{1i} x_1 - x_2)^{\rho_{1i}} (\rho_{2i} x_1 - x_2)^{-\rho_{2i}} \right] = \log \left[(-c_{2i})^{\rho_{1i}} c_{1i}^{-\rho_{2i}} (\rho_{2i} - \rho_{1i})^{\rho_{1i} - \rho_{2i}} \right].$$

Let $x_{1i}(0) = x_{1o}$ and $x_{2i}(0) = x_{2o}$, then

$$c_{1i} = \frac{\rho_{2i} x_{1o} - x_{2o}}{\rho_{2i} - \rho_{1i}} \qquad (D.4)$$

and

$$c_{2i} = \frac{\rho_{1i}x_{1o} - x_{2o}}{\rho_{1i} - \rho_{2i}} \quad . \tag{D.5}$$

Hence,

$$\left[\frac{\rho_{2i}x_1 - x_2}{\rho_{2i}x_{1o} - x_{2o}}\right]^{-\rho_{2i}} = \left[\frac{\rho_{1i}x_1 - x_2}{\rho_{1i}x_{1o} - x_{2o}}\right]^{-\rho_{1i}} \quad . \tag{D.6}$$

Furthermore, $t = t_o = 0$ can apply to any given point for this piecewise autonomous system.

Then compute the trajectories for the phase plane n vs C by substituting the $\dot{C} = x_2$ equation (2.28) into (D.6) with $x_1 = C$.

Hence,

$$\left[\frac{(\rho_{2i}+\lambda)C - \frac{\beta}{\ell}n}{(\rho_{2i}+\lambda)C_o - \frac{\beta}{\ell}n_o}\right]^{-\rho_{2i}} = \left[\frac{(\rho_{1i}+\lambda)C - \frac{\beta}{\ell}n}{(\rho_{1i}+\lambda)C_o - \frac{\beta}{\ell}n_o}\right]^{-\rho_{1i}} \quad , \tag{D.7}$$

where $n(0) = n_o$ and $C(0) = C_o$ but $t = t_o = 0$ can apply to any given point. If n_c, C_o is a given point on the trajectory, then all n and C on this trajectory must satisfy (D.7).

Appendix E

NEUTRONICS HEAT-EXCHANGE SWITCHING PROBLEM FOR OPTIMAL STARTUP WITH $Q \leq Q_1$

It is seen from equation (3.44) that

$$\mathcal{H} = I(\vec{x};\bar{p}) + \frac{p_1 Q u_1}{\ell} + (p_\vartheta - a p_\theta T)u_2 \ . \tag{E.1}$$

Hence, the optimal control is described by

$$u_1^\circ = \delta k^\circ = \gamma\beta \ \text{sgn} \ p_1 \tag{E.2}$$

and

$$u_2^\circ = \begin{cases} u_a & \text{for } F < 0 \\ u_b & \text{for } F > 0 \ , \end{cases} \tag{E.3}$$

where

$$F = p_\vartheta - aTp_\theta \ . \tag{E.4}$$

The costate is defined by the adjoint system for an interval of no phase constraint (i.e., $t < t_a$),

$$\begin{aligned} \dot{p}_1 &= \frac{\beta - u_1}{\ell} p_1 - \sum_{i=1}^{6} \frac{\beta_i}{\ell} p_{i+1} - \frac{p_\theta}{MC} \ , \\ \dot{p}_j &= \lambda_{j-1}(p_j - p_1) \qquad (j = 2,\ldots,7), \\ \dot{p}_\theta &= a u_2 p_\theta \\ \dot{p}_\vartheta &= 0. \end{aligned} \tag{E.5}$$

and

Also, p_ϑ is non-positive .

Equation (E.5) shows that F as given by (E.4) cannot change sign if $p_\theta(t_0)$ is non-negative since aT is positive. Also the behavior of p_1 is only changed slightly (from that of Chapter II) by the addition of a particular solution of slow transient due to $p_\theta(t)$, if $p_\theta(t_0)$ is

selected small enough. Hence, one would expect that $\vec{p}(t_o)$ may again be chosen so that $p_1(t)$ does not change sign.

It is shown below in (E.14) that $p_j(t_a) = 0$ for $j = 2,\ldots, 7$. This is also the terminal condition that yields no zeros for $p_1(t)$ in Chapter II (see Figure 2.12).

While $Q(t) = Q_1$, it is seen from (A.4) that with $t_a < t < t_1$,

$$\dot{\vec{p}} = -\frac{\partial \mathcal{H}}{\partial \vec{x}} + \rho \frac{\partial \dot{S}}{\partial \vec{x}} , \tag{E.6}$$

where $S = Q - Q_1$. Since $\partial \dot{S}/\partial \vec{x} = \begin{bmatrix} (u_1-\beta)/\ell \\ \lambda_1 \\ \vdots \\ \lambda_6 \\ 0 \end{bmatrix}$,

$$\dot{p}_1 = \frac{\beta-u_1}{\ell} p_1 - \sum_{i=1}^{6} \frac{\beta_i}{\ell} p_{i+1} - \frac{p_\varepsilon}{MC} + \frac{(u_1-\beta)}{\ell} \rho ,$$

$$\dot{p}_j = \lambda_{j-1} (p_j - p_1) + \lambda_{j-1} \rho , \tag{E.7}$$

$$(j = 2,\ldots, 7)$$

$$\dot{p}_8 = a u_2 p_8$$

and

$$\dot{p}_9 = 0 .$$

As hypothesized in Chapter III, let $u_1 = \ell \sum_{i=1}^{6} \dot{C}_i/Q_1$ and $u_2 = \dot{w} = u_a$ for the interval (t_a, t_b). Then from (A.6)

$$\frac{\partial \mathcal{H}}{\partial \vec{u}} = \rho \frac{\partial \dot{S}}{\partial \vec{u}} + \nu \frac{\partial q}{\partial \vec{u}} , \tag{E.8}$$

where

$$q = u_a - \dot{w} .$$

Substituting (E.1) into (E.8) one obtains:

$$\frac{p_1 Q}{\ell} = \frac{\rho Q}{\ell} \qquad \text{(E.9)}$$

and

$$F = (p_\theta - a p_s T) = -\nu \quad .$$

Hence, from (E.9)

$$\rho = p_1 \qquad \text{(E.10)}$$

and from (E.7)

$$p_s = p_{sa} \exp\left[a \int_{t_a}^{t} u_2(\sigma)\, d\sigma\right] ,$$

where $p_{sa} = p_s(t_a+)$ is the value of p_s at the point where the trajectory enters the phase constraint boundary. Therefore,

$$F = p_\theta - a p_{sa} T(t) \exp\left[a \int_{t_a}^{t} u_2(\sigma)\, d\sigma\right] . \qquad \text{(E.11)}$$

Then since T and u_2 are positive, the switching function, (E.11), cannot change sign if p_{sa} is non-negative.

The other switching function p_1 is described by

$$\dot{p}_1 = -\sum_{i=1}^{6} \frac{\beta_i}{\ell} p_{i+1} - \frac{p_a}{MC} , \qquad \text{(E.12)}$$

where

$$\dot{p}_j = \lambda_{j-1} p_j , \qquad (j = 2, \ldots, 7)$$

or

$$\dot{p}_1 = -\sum_{i=1}^{6} \frac{\beta_i}{\ell} p_{i+1}(t_a) e^{\lambda_1 (t-t_a)} - \frac{p_{sa}}{MC} \exp\left[a \int_{t_a}^{t} u_2(\sigma)\, d\sigma\right] . \qquad \text{(E.13)}$$

Since the terminal manifold is defined by $T(t_1) = T_1$ and $Q(t_1) = Q_1$, $p_j(t_1) = 0$ (for $j = 2,\ldots,7$). Then

$$p_j(t) = 0 \tag{E.14}$$

and

$$\dot{p}_1 = -\frac{p_8}{MC}$$

or

$$p_1 = p_{1a} - \frac{1}{MC}\int_{t_a}^{t} p_8\ (\sigma)\ d\sigma\ , \tag{E.15}$$

where $t_a < t \leq t_1$ and $p_{1a} = p_1(t_a+)$. Substituting (E.10) into (E.15),

$$p_1 = p_{1a} - \frac{p_{8a}}{MC}\int_{t_a}^{t} \exp\left[a\int_{t_a}^{\sigma} u_2\ (\lambda)\ d\lambda\right] d\sigma. \tag{E.16}$$

From (A.7),

$$p_j(t_a-) = p_j(t_a+) \qquad (j = 2,\ldots,9) \tag{E.17}$$

and

$$p_1(t_a-) = p_1(t_a+) + \mu\ ,$$

where, since there is no constraint exit corner, μ may be set to zero. Hence, by selecting p_{1a} large compared to p_{8a} or p_{1o} large compared to p_{8o}, $p_1(t)$ remains positive. Furthermore, $\dot{\rho}(t) = \dot{p}_1(t)$ is non-positive for $t_a < t < t_1$ and $\bar{p}(t_a)$ is not collinear with $\partial S(\bar{x})/\partial \bar{x}$ (as required).

In summary then the costate system of equations is satisfied by the optimal startup control if: 1) $p_8(t_o)$ is a small non-negative number; 2) p_8 is a negative constant; 3) $p_1(t_o)$ is selected positive and considerably larger than $p_8(t_o)$ so that $p_1(t)$ doesn't change sign;

4) $p_j(t_1) = 0$, $j = 2,\ldots,7$; and 5) the actual initial values of p_1, p_8, and p_9 should be selected so that $\mathcal{H} \equiv 0$.

The actual solution of the costate equation should again progress from the terminal end. By selecting the above conditions (1), (3) and (5) [along with (4) at the terminal end], the costate equations can be solved and there are no switchings in control between end points.

An example startup trajectory with steady-state power and temperature at the end points is presented in Table E.1. Recognize that the switching functions $p_1(t)$ and $F(t) = p_9 - a\ T\ p_8$ are positive and negative respectively, between end points and hence the hypothesized constant control satisfies the maximum principle. These data were obtained from an IBM 7090 computer.

Table E.1 **Optimal reactor startup trajectory with $Q(t) \leq Q_1$**

Input Data:

$u_1 = 0$, $t < 0.1$ sec $= t_o$

$u_1 = 0.9\ \beta$; $t \geq 0.1$, $p_1 > 0$ and $Q < Q_1 = 2.142(10)^6$ Btu/sec

$u_1 = \ell \sum_{i=1}^{6} \dot{C}_i/Q_1$, $Q = Q_1$

$u_2 = u_a = 2$ lb/sec, $T < T_1$ and $F < 0$

$u_2 = Q_1/MCaT_1$, $T = T_1 = 4501.1°$ R

$\mathcal{H} = 0$, $t_o < t < t_1$

$a = 1.153(10)^{-2}$, $T(0) = 500°$ R, $\dot{Q}(0) = \dot{T}(0) = 0 = \dot{C}_i(0)$ $(i = 1, \ldots, 6)$.

$\dot{T}(t_1) = \dot{Q}(t_1) = 0$, other data given by Table 1.2

Time sec	Power 10^{-4} Btu/sec	Temperature 10^{-2} °R	$p_1(t)$ 10^6 sec^2/Btu	$p_6(t)$ 10^4 sec/°R
0	1.3144	5.0000		
t_o = 0.1	1.3144	5.0000	11.946	7.2139
0.2	13.253	5.0651	9.2838	7.2306
0.4	24.889	5.3720	5.6093	7.2640
0.6	42.642	5.9257	3.3932	7.2976
0.8	71.793	6.8790	2.0589	7.3313
1.0	119.91	8.4903	1.2663	7.3652
t_a = 1.24	214.20	11.911	5.0718	7.4101
1.4	214.20	14.868	4.9676	7.4375
1.6	214.20	18.549	4.8368	7.4718
1.8	214.20	22.213	4.7054	7.5064
2.0	214.20	25.860	4.5734	7.5411
2.2	214.20	29.490	4.4408	7.5759
2.4	214.20	33.104	4.3076	7.6110
2.6	214.20	36.701	4.1737	7.6461
2.8	214.20	40.281	4.0393	7.6815
t_1 = 3.08	214.20	45.011	3.8500	7.7751

BIBLIOGRAPHY

1. Mulcahey, T. P., "Time Optimum Control of Nuclear Reactors with Velocity-Limited Control Devices", Proceedings of the 1963 Symposium on Reactor Kinetics and Control, U.S.A.E.C., TID 7662, pp 278-298, April, 1964.

2. Shen, C. N., and Haag, F. G., "Application of Optimum Control to Nuclear Reactor Start-up", I.E.E.E.-PTGNS, Vol. NS-11, No. 2, pp 1-8, April, 1964.

3. Mohler, R. R., "Optimal Control of Nuclear-Reactor Systems", presented at the 1964 national meeting of the American Nuclear Society in Philadelphia. (Summary is published in the ANS Transactions, Vol. 7, No. 1, June, 1964.)

4. Rosztoczy, Z. R., and Weaver, L. E., "Optimum Reactor-Shutdown Program for Minimum Xenon Buildup", presented at the 1964 national meeting of the American Nuclear Society in Philadelphia. (Summary is published in the ANS Transactions, Vol. 7, No. 1, June, 1964.)

5. Kliger, I., "An Adaptive Automatic Control of a Nuclear Reactor for a Minimal Time Response", presented at the 1964 national meeting of the American Nuclear Society in Philadelphia. (Summary is published in the ANS Transactions, Vol. 7, No. 1, June, 1964.)

6. Berkovitz, L. D., "Variation Methods in Problems of Control and Programming", J. Math. Anal. and Appl., Vol. 3, No. 1, pp 145-170, August, 1961.

7. Bliss, G. A., "Lectures on the Calculus of Variations", University of Chicago Press, Chicago, Ill., 1946, and Part II, 1961.

8. Pontryagin, L. S., Boltyanskii, V. G., Gamkrelidze, R. V., and Mishchenko, E. F., "The Mathematical Theory of Optimal Processes", Interscience Publishers, John Wiley and Sons, New York, 1962.

9. Bellman, R. E., "Dynamic Programming", Princeton University Press, Princeton, New Jersey, 1957.

10. Kalman, R. E., "The Theory of Optimal Control and the Calculus of Variations", RIAS Technical Report 61-3.

11. Desoer, C. A., "Pontryagin's Maximum Principle and the Principle of Optimality", Journal of Franklin Institute, Vol. 271, May, 1961.

12. Rozonoer, L. I., "L. S. Pontryagin's Maximum Principle in Optimal System Theory", Parts I - III, Automation and Remote Control, Vol. 20, No. 10, 11, 12, Oct., Nov., Dec., 1959.

13. Berkovitz, L. D., "On Control Problems with Bounded State Variables", J. Math. Anal. and Appl., Vol. 5, No. 3, pp 488-498, December, 1962.

14. Chang, S. S. L., "Optimal Control in Bounded Phase Space", Automatica, Vol. 1, pp 55-67, 1962.

15. Bryson, A. E., Jr., Denham, W. F., and Dreyfus, S. E., "Optimal Programming Problems with Inequality Constraints I: Necessary Conditions for Extremal Solutions", AIAA Journal, Vol. 1, No. 11, pp 2544-2550, November, 1963.

16. Schultz, M. A. "Control of Nuclear Reactors and Power Plants", McGraw-Hill Book Co., New York, 1955.

17. Glasstone, S., "Principles of Nuclear Reactor Engineering", pp 223-243, D. Van Nostrand Co., Princeton, New Jersey, 1955.

18. Keepin, J. R. and Wimett, T. F., "Reactor Kinetic Functions - A New Evaluation", Nucleonics, Vol. 16, No. 10, 1958.

19. Eckert, E.R.G., and Drake, R. M., Jr., "Heat and Mass Transfer", McGraw-Hill Book Co., New York, 1959.

20. Mohler, R. R., and Perry, J. E., Jr., "Nuclear Rocket Engine Control", pp 80-84, Nucleonics, Vol. 19, No. 4, April, 1961.

21. Zucrow, M. J., "Aircraft and Missile Propulsion", John Wiley and Sons, New York, 1958.

22. Johnson, C. D., and Gibson, J. E., "Singular Solutions in Problems of Optimal Control", IEEE-PTGAC, Vol. AC-8, No. 1, pp 4-15, Jan., 1963.

23. Gille, J-C, Pelegrin, M.J., and Decaulne, P., "Feedback Control Systems", McGraw-Hill Book Co., pp 403-421, New York, 1959.

24. Cunningham, W. J., "Introduction to Nonlinear Analysis", McGraw-Hill Book Co., pp 281-282, New York, 1958.

25. Stepanoff, A.J., "Centrifugal and Axial Flow Pumps", John Wiley and Sons, New York, Second Edition, 1957.

26. Kaplan, W., "Ordinary Differential Equations", Addison-Wesley Publishing Co., Reading, Massachusetts, 1961.

27. Kaplan, W., "Operational Methods for Linear Systems", Addison-Wesley Publishing Co., Reading, Massachusetts, 1961.

28. LaSalle, J., and Lefschetz, S., "Stability by Liapunov's Direct Method", Acedemic Press, New York, 1961.

29. Bellman, R., "Introduction to Matrix Analysis", McGraw-Hill Book Co., New York, 1960.